EFFECT OF STRAND DIAMETER ON BOND, TRANSFER AND DEVELOPMENT LENGTH PERFORMANCE OF PRESTRESSING STRANDS

By

GABRIEL DOMINGO ALCARAZ EMMANUELLI

A DISSERTATION PRESENTED TO THE GRADUATE SCHOOL OF
THE UNIVERSITY OF FLORIDA IN PARTIAL FULFILLMENT OF THE
REQUIREMENTS FOR THE DEGREE OF DOCTOR OF PHILOSOPHY

UNIVERSITY OF FLORIDA

2000

Copyright 2000

by

Gabriel Alcaraz

I dedicate this work to my wife, Lissie, for her unconditional support during this adventure, and to my son, Gabby, who unknowingly sacrificed time that otherwise, would have been dedicated to him.

ACKNOWLEDGMENTS

I wish to express my most sincere appreciation to Dr. Fernando Fagundo, P.E., Chairman of my supervisory committee for most part of my graduate studies, for without his support and continuous encouragements this endeavor would not have been possible. I also would like to acknowledge and express my gratitude to the Faculty of the Civil and Coastal Engineering Department, especially to the members of my supervisory committee: Dr. Ronald Cook, P.E., co-Chairman, Dr. John Lybas and Dr. Mike McVay, for their support and advise.

I would also like to thanks, Dr. Milagros Rivera, external member to my supervisory committee, from the Journalism and Communications Department for her support and attention to detail in proof reading the early drafts of this work, the people at the Structures Research Laboratory: Bill Studstill, Danny Brown, Hubert, Javier Quiros, Eladio Castrodad, Valerie Hoffman, Guillermo (Memo) Madriz, Danny Richardson, Erik Sverdlow and Nathan Niebauer, for their help and support during the experimental phases of this project and the ladies at the Civil Engineering Department office, Doretha, Debra, Dona, Nell, Sandra Bivins, Becky and Thelma.

I must acknowledge the generosity of Florida Wire & Cable, Inc in financially supporting this research program, for which I would like to convey my deepest gratitude.

Last, but not least, I must express my gratitude to my wife, Lissie, and son, Gabby, for their unconditional support during this adventure and to my family for their prayers and support.

TABLE OF CONTENTS

ACKNOWLEGMENTS iv

ABSTRACT x

CHAPTER 1 INTRODUCTION

1.1 Introduction 1

1.2 Bond, Transfer and Development Length 3

1.3 Bond Mechanism 4

1.4 Scope 5

1.5 Objectives 6

1.6 Organization of the Thesis 6

CHAPTER 2 BACKGROUND AND LITERATURE REVIEW

2.1 Introduction 8

2.2 FHWA Memorandum 8

2.3 Large Diameter Strands 9

2.4 Transfer and Development Length 11

  2.4.1 Definitions 11

  2.4.2 Transfer Length 11

  2.4.3 Development Length 12

2.5 Bond Mechanisms 13

2.5.1 Adhesion 14
2.5.2 Friction 14
2.5.3 Mechanical Interlocking 15
2.6 Evolution of the current ACI and AASHTO code expressions 16
2.6.1 Evolution of ACI Transfer Length Expressions 17
2.6.2 Evolution of the Development Length Expression 18
2.7 Review of Published Literature 21
2.7.1 Chronological Literature Review 21
2.7.2 Review of Proposed Transfer and Development Length Expressions 33
2.6.3 Variables Identified to Affect Bond, Transfer and Development Length Performance of Prestressing Strands 39
2.7 End Slip - Transfer Length Relationship 51

CHAPTER 3 EXPERIMENTAL PROGRAM

3.1 Introduction 54
3.2 Experimental Phases 54
3.3 Specimen Design 56
3.4 Specimen Nomenclature 58
3.5 Specimen Description 59
3.6 Materials Properties 61
3.6.1 Prestressing Steel 61
3.6.2 Mild Steel 63
3.6.3 Concrete 64
3.7 Specimen Fabrication 64

3.8 Experimental Procedures and Instrumentation 69
3.8.1 Concrete Surface Strain Measurements and Determination of Transfer Length 69
3.8.2 End Slip Measurements and Estimate of Transfer Length 70
3.8.3 Internal Concrete Strains 70
3.8.4 Flexural Test Instrumentation 72
3.8.5 Summary of the Experimental Procedure 73

CHAPTER 4 EXPERIMENTAL RESULTS

4.1 Introduction 76
4.2 Experimental Program 76
4.3 Transfer Length 77
4.3.1 Concrete surface strains 77
4.3.2 Constructing the Strain Profile 79
4.3.3 Estimating the transfer length from strain profiles 80
4.3.4 End-slip based transfer length estimate 84
4.3.5 Measured transfer length 85
4.3.6 Summary of Transfer Length Results 94
4.4 Flexural Bond Test 96
4.4.1 Determination of the Embedment Length 96
4.4.2 Types of Failures 97
4.4.3 Flexural Bond Tests Results: Phase I 99
4.4.4 Flexural Bond Test Results: Phase II 100
4.4.5 Flexural Bond Tests Results: Phase III 101

4.4.6 Flexural Bond Tests Results: Phase IV 104

CHAPTER 5 DISCUSSION OF EXPERIMENTAL RESULTS

5.1 Introduction 113
5.1.1 Dimensional Analysis and Buckingham's Pi-Theorem 113
5.2 Transfer Length Data 115
5.2.1 Transfer Length Database 115
5.2.2 Effect of Method Used to Determine Transfer Length 115
5.2.3 Effect of Concrete Strength at Transfer 118
5.2.4 Effect of the Initial Prestress 121
5.2.5 Effect of Strand Diameter 126
5.2.6 End Slip – Transfer Length Relationship 136
5.3 Development Length 139

CHAPTER 6 TRANSFER LENGTH PREDICTOR EQUATION

6.1 Introduction 145
6.2 Nature of Bond 145
6.3 Transfer Length Predictor Equation 147
6.3.1 Transfer Length Equation Limitation and Assumptions 147
6.3.2 Mechanical Interlocking Bond Strength 150
6.3.3 Frictional Bond Strength 153
6.4 Friction and Mechanical Bond 155
6.5 Transfer Length Predictor Equation 157

6.5.1 Measured Transfer Lengths versus Predicted Transfer Lengths: University of Florida Data 158
6.5.2 Recent Research Projects Database 159
6.5.3 Test for Systematic Errors 160
6.6 Transfer Length Design Equation 170

CHAPTER 7 CONCLUSIONS AND DESIGN RECOMMENDATIONS

7.1 Introduction 172
7.2 Transfer Length 172
7.2.1 Experimental Program 172
7.2.2 Conclusions 173
7.3 Development Length 174
7.3.1 Experimental Program 174
7.3.2 Conclusions 174
7.4 Design Recommendations 175
7.5 Future Research 176

APPENDICES

Concrete Strain Profiles 178
Load Deformation Diagrams 198
MathCAD Templates 236
REFERENCES 244
BIOGRAPHICAL SKETCH 251

Abstract of Dissertation Presented to the Graduate School
of the University of Florida in Partial Fulfillment of the
Requirements for the Degree of Doctor of Philosophy

EFFECT OF STRAND DIAMETER ON BOND, TRANSFER AND DEVELOPMENT LENGTH PERFORMANCE OF PRESTRESSING STRANDS

By

Gabriel Domingo Alcaraz Emmanuelli

August 2000

Chairman: Fernando E Fagundo
Ronald A Cook
Major Department: Civil Engineering

In the 1980s, the producers of prestressing strands introduced a 6/10” diameter seven-wire strand for use in prestressed concrete applications. Recently, strand producers have introduced a 7/10” diameter strand, with almost twice the area and the capacity of the 1/2" diameter strand, the current industry standard.

The applicability of the transfer length equation presented in the ACI and AASHTO codes to these large diameter strands has been questioned. In the 1980s, research conducted at North Carolina State University found current code equations inadequate and unconservative, prompting a memorandum by the Federal Highway Administration imposing a moratorium on the use of 6/10” strand. Several research efforts were initiated in an attempt to improve the state of knowledge regarding bond performance of prestressing strands.

Research efforts at the University of Florida concentrated on the effect of strand diameter on bond performance of prestressing strands. Forty rectangular prismatic specimens were fabricated and tested for transfer length and end-slips at transfer and for development lengths with static loading. The strand sizes and grades tested include: 3/8" Grade 270 and Grade 300, 1/2" Grade 270 and Grade 300, 1/2" special Grade 270 and Grade 290, 6/10" Grade 270 and 7/10" Grade 270.

The transfer lengths of small diameter strands were found to be linearly proportional to the strand diameter. The transfer lengths for large diameter strands did not followed this trend. The transfer length equation presented in current ACI and AASHTO Standards codes was found to predict the mean of the experimentally measured transfer lengths, about 50 strand diameters. The inclusion of 95% of the experimental data required a transfer length of 75 strand diameters.

A transfer length predictor equation that considered the effect of concrete strength, initial prestress, strand surface condition, method of transfer and strand diameter was developed. Transfer lengths estimated with the proposed equation were compared to the transfer lengths measured at the University of Florida and other institutions, ensuring that the equation is representative of a large number of data.

CHAPTER 1

INTRODUCTION

1.1 Introduction

Current American Concrete Institute, ACI 318-99, [4] [1] and American Association of State Highway and Transportation Officials, AASHTO [3] code provisions for transfer and development length for prestressing strands are essentially identical. These expressions were developed in the 1960s, based on best-fit type analysis of data obtained from research using clean Grade 250 Stress-Relieved strand that ranged from ¼" to ½" in diameter [30, 34]. The current industry standard is Grade 270, Low Relaxation strand.

Grade 270, Low Relaxation, strand allows for higher initial and effective prestress. Its higher Grade, allows for the initial prestress in the strand to be increased in proportion to the increase in breaking strength. Yet, because of its reduced relaxation[2] characteristics, the increase in effective prestress is not proportional to the increase in breaking strength. Hence, the effective prestress attained with a Low Relaxation strand is higher than that achieved with a Stress-Relieved strand of the same Grade, or breaking strength. Currently, Grade 300, Low Relaxation, strands are being tested for introduction to the industry.

---

[1] Number in parenthesis refers to the Reference number.

[2] Relaxation is the loss of stress in a stressed material held at a constant length. The relaxation loss for low-relaxation strand is about 25% of the loss for stress-relieved strand [56].

As early as the mid-1970s, when the Low-Relaxation strands were introduced, the adequacy of ACI and AASHTO code provisions for transfer and development length was questioned [50, 80]. In the 1980s, concerns regarding the ACI and AASHTO code provisions were raised once again when strand producers began to manufacture a strand 6/10" in diameter. The applicability of current code expressions to this strand was questioned. Research conducted at North Carolina State University found development lengths substantially longer than those computed by current code expressions [16-18], not only for the new 6/10" strand, but for the smaller diameter strands also. These findings led to a memorandum from the Federal Highway Administration, imposing severe restrictions on the prestressed concrete industry [13, 14, 16-18].

Several research efforts were initiated as a result of the FHWA memorandum. The goal of these efforts was to improve the state of knowledge regarding the bond performance of prestressing strands.

Research conducted at the University of Florida has focused on the effect of the strand diameter on the bond, transfer and development length performance prestressing strands. The suitability of large-diameter tendons to prestressed concrete applications will form part of the investigation.

The term " large-diameter strand" has been re-interpreted through the years. In 1950s, 1/2" diameter strands were considered "large-diameter strand" [77]. In the 1990s, researchers referred to 1/2" and 6/10" strands as "large-diameter strand" [70]. For the purpose of this study, "large diameter strand" refers to strands 6/10" and 7/10" in diameter.

The move toward larger diameter strands is the result of the development of, economically viable, high strength concrete. The efficient use of these high strength concretes requires the prestressing force applied to the section to be increased. The prestressing force can be increased by either increasing the number of strands in the section or by increasing the force per strand.

The space required to accommodate additional strands is limited. Bigger sections that provided more space where strands could be accommodated had to be developed. The increase in prestressing force per strand can be achieved by increasing the cross-sectional area of individual strands, increasing the strand breaking strength or a combination of both.

1.2 Bond, Transfer and Development Length

In prestressed concrete applications, the strands are stressed before the concrete is poured. Once the concrete has achieved a minimum prescribed strength, typically 3,500 psi, the strands are released. The prestress force is then transferred from the steel to the concrete at the ends of the members through bond. The stress build up is gradual, from zero at the ends to the effective prestress level. The distance over which the build up of stresses occurs is called the transfer length, L_t.

As external loads are applied, the difference in bending moments at two adjacent sections causes the stresses in the strands to increase. While the concrete member, i.e. beam or girder, is un-cracked, the stress increase in the strand is negligible. After cracking, the stresses in the strand increase abruptly. These additional stresses are called flexural bond stresses. The flexural bond length, L_{fb}, is the additional bonded length of strand required to equilibrate the flexural bond stresses at the limit state.

The Development Length is the total length of bonded strand required to transfer the strand's design limit state force to the concrete. This required bonded length is the summation of the transfer and the flexural bond lengths.

1.3 Bond Mechanism

As mentioned before, the forces in the strands are transferred to the concrete through bond mechanism. Three bond mechanisms have been identified: adhesion, friction and mechanical interlocking.

Adhesion is the result of a chemical reaction at the strand-concrete interface. This mechanism is lost and cannot be regained once relative movement occurs at the concrete-strand interface. This mechanism is not present in the transfer zone.

Friction is the result of the contact between the concrete and strand. This force is proportional to the normal force and a friction coefficient. As the strand is tensioned the diameter is reduced due to Poisson's effect[3]. When de-tensioned, the strand tries to return to it original diameter. The surrounding concrete resists the strand's attempt to regain its original size, resulting in an increase in normal force and friction forces. As the strand's stresses are transferred to the concrete, the normal and friction forces are reduced, resulting in a wedging action in the ends of the beams. The improved anchorage due to the swelling in the strand, or wedging action, is also known as Hoyer's Effect. Hoyer's effect is considered a major component in the anchorage of prestressing strands.

---

[3] A deformable body, when subjected to an axial load, not only elongates but it also contracts laterally. In the 1800s, the French scientist S.D. Poisson found these deformations to be proportional within the elastic range. The ratio of the strains caused by these deformations is constant. The constant is known as the ***Poisson's ratio.***

Concrete shrinkage and steel relaxation also contribute to the generation of normal forces.

Up to this point, the bond phenomena of wires and strands are identical. Strands differ from wire in its ability to develop additional bond strength after slippage occurs. This additional bond mechanism, known as mechanical interlocking, is due to the helical shape of the strand. The concrete is poured in fluid form and fills the interstices of the strand. The interstices are the narrow valleys or crevices between individual wires. The hardened concrete matches the strand surface. As the strand tries to slip without twisting, the outer wires of the strand react against the matching deformations in the concrete, resisting movement.

1.4 Scope

The experimental program of this research effort is limited to rectangular sections reinforced with 3/8", 3/8" indented, 1/2", 1/2"special, 6/10" and 7/10" diameter Grade 270 uncoated strands. Also, Grade 300 and Grade 290 uncoated strands are being studied to a limited degree. The strands will be used in "as received" surface condition and detensioned by flame cutting. The section's size, cover-to-strand diameter ratio and confinement steel are to be proportioned such that the section stresses, i.e. the level of prestress and extreme fiber stresses, are similar for all sections.

The concrete mix to be used will be similar to industry standards with design strength at 28 days of 6000 psi. The strands are to be detensioned within a limiting range of concrete strengths of 3500 psi to 4300 psi. The specimens are to be tested in flexure after curing for 28 days.

The collected data will be compared and analyzed in light of available published data related to uncoated 7-wire Grade 270 strands. A transfer length design equation and design recommendations will be formulated, based on the understanding of the strand's transfer length behavior acquired from the analysis of the data.

1.5 Objectives

The main objective of this research is to study the effect of strand diameter on the bond performance of prestressing strands. The applicability of large-diameter strands to prestressing applications and the relation between the transfer and development length to the strand draw-in at transfer will also be studied.

An attempt will be made to develop a rational design-oriented model to predict the strand development length. Modified truss analogies will be used to better understand the state of stresses in the anchorage region in developing the rational approach.

1.6 Organization of the Dissertation

This dissertation consists of seven (7) chapters. A state-of-the art is presented on Chapter 2. This state-of-the art includes a brief history of the development of current transfer and development length code expressions followed by a literature review. The literature review is presented in three forms. First, a brief description of previous research projects and their conclusions is presented. Followed by a discussion of several proposed transfer and development expressions found in the literature review. Then, the effect of various parameters, identified as affecting strand bond, transfer and development length performance, such as concrete strength, strand diameter, release method and strand surface condition, is explored.

Chapter 3 presents the experimental program. Specimens are described and properties of the materials used are presented. Experimental practices, instrumentation setups and a step-by-step procedure are also presented and discussed.

Chapter 4 presents the data obtained from the experimental program. Data reduction procedures are discussed and results are presented in table format. The results are discussed in Chapter 5. The results are also discussed in light of data obtained from the literature.

Chapter 6 presents the development of a design transfer length equation and a comparative study of the proposed equation with other equations presented in the literature. Conclusions and design recommendations are presented in Chapter 7, followed by a list of references.

Appendix I presents the Strain Profile charts, from which transfer lengths were estimated. Appendix II presents the Load Deflection charts obtained during the flexural bond test. Appendix III presents a sample of a MathCAD template prepared for the estimation of prestress losses and the section's nominal capacity.

CHAPTER 2

BACKGROUND AND LITERATURE REVIEW

2.1 Introduction

Current ACI [4] and AASHTO [3] code provisions for transfer and development length for prestressing strands are essentially identical. These expressions were developed in the 1960s, based on data obtained from research using clean Grade 250 Stress-Relieved strand that ranged from ¼” to ½” in diameter [30, 34]. The current industry standard is 1/2" Grade 270 Low Relaxation strand, which allows for higher initial and effective prestressing stresses. Large diameter strands, 6/10” and 7/10”, already have been introduced to the industry. Higher Grade strands, Grade 300, are being tested for introduction to the industry.

2.2 FHWA Memorandum

In the 1980s, strand producers began to manufacture 6/10” diameter strand. Serious concerns were raised on the applicability of current code expressions to this strand. Research conducted at North Carolina State University found development lengths substantially longer than those computed by current code expressions (14-16), not only for the new 6/10” strand, but for the smaller diameter strands as well. These findings led to a memorandum from the Federal Highway Administration, which imposed a moratorium on the use of the 6/10” strand. In addition, the FHWA memorandum imposed a four-strand diameter center-to-center spacing of the strands and required the development length estimated for uncoated strands to be 60% longer than the development length computed using the AASHTO expression. The development length for blanketed[1] strands was to be twice the length estimated per AASTHO development length equation [12, 13, 14-17 & 40-42].

Several research efforts were initiated as a result of the FHWA memorandum. The goal of these efforts was to improve the state of knowledge of prestressing strands bond performance in general. Some of the variables that have been studied are: the effect of the concrete cross section, strand surface condition, strand size, strand spacing and the effect of concrete strength.

2.3 Large Diameter Strands

Research conducted at the University of Florida focused on the effect of the strand diameter on the bond, transfer and development length performance of prestressing strands. The suitability of large-diameter tendons to prestressed concrete applications, also formed part of this investigation. The effect of the initial stress in the strand at transfer was studied on a limited basis.

The term " large-diameter strand" has been re-interpreted through the years. In 1956 Thorsen [77] published his paper " Use of Large Tendons in Pre-Tensioned Concrete" in which he referred to 1/2" strands as large-diameter strand. Most recently in 1993, Russell and Burns referred to 1/2" and 6/10" strands as large-diameter strands [69].

---

[1] Blanketed strands are also known as de-bonded or partially de-bonded strands. The de-bonding is achieved by applying grease to the strand, or with a de-bonding a device, such as a plastic duct. De-bonded strands are typically used at the end of the girders to reduce the prestress levels at those sections.

For the purpose of our discussion large-diameter strands refers to 6/10” and 7/10” diameter strands.

The move toward larger diameter strands is the result of the development of high strength concrete. Economically viable concrete mixes with compressive strengths in the 10,000-psi to 15,000-psi range are readily available. These High Performance Concretes, HPC, allow engineers to bridge longer spans with a given section. These would not be possible with regular strength concrete, RSC.

To take advantage of higher strength concretes in an efficient manner, the level of prestress on the section must be increased. The increase in the level of prestressing, can be achieved be either increasing the number of strands in the section or by increasing the force in each strand.

The space required to accommodate additional strands is limited. Sections, such as the Texas U-beam and the Florida Department of Transportation Bulb-T, have been developed to allow for more space where the strands can be accommodated.

On the other hand, the increase in force in the individual strands can be achieved by increasing the cross-sectional area of the strand or increasing the breaking strength of the strand. The strand producers responded, first, with the development of the 6/10” diameter strand and recently with the 7/10” diameter strand, which has almost twice the cross-sectional area of a 1/2" strand. Most recently, Grade 300 strands have been tested for introduction to the industry.

2.4 Transfer and Development Length

2.4.1 Definitions

In prestressed concrete applications the strands are stressed before the concrete is poured. Once the concrete has achieved a minimum prescribed strength, typically 3,500 psi, the strands are released. The prestress force is then transferred from the steel to the concrete at the ends of the members through bond. The stress build up is gradual from zero at the ends to the effective prestress level, over a distance called the transfer length, L_t. As external loads are applied, the difference in bending moments at two adjacent sections causes the stresses in the strands to increase. While the concrete member is un-cracked, the stress increase in the strand is negligible. After cracking, the stresses in the strand increase abruptly [70]. These additional stresses are called flexural bond stresses. The flexural bond length, L_{fb}, is the additional bonded length of strand required to equilibrate the flexural bond stresses at the limit state.

The development length is the total length of bonded strand required to transfer the strand's design limit state force to the concrete. This required bonded length is the summation of the transfer and the flexural bond lengths.

2.4.2 Transfer Length

Transfer length normally will not control the design or the structural performance of prestressed elements. It is a structural requirement only to the effect that the prestressing force must be transferred to maintain structural integrity. Its exact value is not necessary to design or build safe pretensioned structures [70].

While the importance of having an exact value for the transfer length should not be overestimated, the transfer length is very important for the structure's serviceability behavior. In the transfer region the prestress is not fully effective. As a result, the propensity to cracking is greater in the transfer zone than on the regions where the prestress is fully effective.

The ACI and AASHTO design codes suggest a transfer length of 50 strand diameters for shear strength computations and suggest the assumption that the prestress is transferred linearly from zero to a maximum at the end of the transfer length. These assumptions allow designers to estimate the shear strength contribution of the concrete cross-section at sections where the prestress is not fully effective.

It should be noted that the codes shear design philosophy does not consider a reduction in the concrete shear strength contribution due to a loss of strand anchorage. On the other hand, research has shown that the occurrence of diagonal shear cracks within the transfer zone leads to anchorage failure [72].

2.4.3 Development Length

ACI and AASHTO codes only require that the development length be verified for the maximum bending moment section. The ACI and AASHTO codes do not recognize the effect of the horizontal component of shear stresses on the strand's stresses, nor the effect of diagonal shear cracking on the strand's anchorage zone on the strand's ability to develop.

ACI Building Code Commentary Section 12.0 says that the reduction factor, ϕ, is not used in the development length equations because a safety factor for overloading already has been incorporated. ACI's development length expression for deformed bars results in development lengths 15% longer than those predicted by experimental results. This factor of safety, inherent in the estimation of the development length of mild reinforcement bars, is not included in the expressions for prestressing strands [13, 14]

Strand development seldom controls the design of prestressed concrete elements. The exceptions are cantilever, deep and short span beams. Typically for slender elements[2] the embedded length[3] of strand is sufficient to ensure proper development of the strands even in the event of crack formation in the transfer region, localized bond failures or poor bond performance.

In the case of cantilevers and deep-short beams it is not necessarily so. In these type of structures, the embedded length of strand may not be sufficient to preclude bond failure in case any of the above-mentioned events occurs. In addition, the effect of the horizontal shear components becomes critical in short-deep beams. The propensity for the formation of diagonal shear cracking within the transfer zone also increases for this type of element.

2.5 Bond Mechanisms

As mentioned before, the forces in the strands are transferred to the concrete through bond mechanisms. Three bond mechanisms have been identified: adhesion, friction and mechanical interlocking.

---

[2] Slender elements are elements with length to depth ratio in excess of 2.5.

[3] The embedded length is the length of bonded strand available for the development of anchorage.

2.5.1 Adhesion

Adhesion is the result of a chemical reaction at the strand-concrete interface. Once a critical a bond stress is exceeded and relative displacement at the concrete-strand interface occurs, this mechanism is lost and cannot be regained. In the transfer zone, there is relative displacement along the concrete strand interface [24], thus this bond mechanism cannot be present in the transfer zone.

2.5.2 Friction

Friction is the result of the contact between the concrete and strand. The friction force is proportional to the normal force and acts opposite to the displacement. As the strand is tensioned, the diameter is reduced due to Poisson's effect. When de-tensioned, the strand tries to return to it original diameter. The surrounding concrete will resist the strands attempt to regain its original size resulting in an increase in the normal force, consequently an increase in friction forces. As the strand's longitudinal stresses are transferred to the concrete, the normal and friction forces are reduced, resulting in a wedging action in the ends of the beams.

The improved anchorage due to the swelling in the strand, or wedging action, is known as Hoyer's Effect. Hoyer's effect is considered a major component in the anchorage of prestressing strands. Concrete shrinkage and steel relaxation also contribute to the generation of normal forces. Figure 2.1 depicts Hoyer's effect.

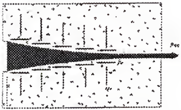

Figure 2-1 Hoyer's Effect .
Source: Russell and Paulsgrove [72]

2.5.3 Mechanical Interlocking

Bond phenomena of wires and strands are identical, up to this point. Strands differ from wire in their ability to develop additional bond strength after slippage occurs [58,59]. This additional bond mechanism, known as mechanical interlocking, is due to the helical shape of the strand. The concrete is poured in fluid form and fills the interstices of the strand. The interstices are the narrow valleys or crevices between individual wires. The hardened concrete matches the strand surface. As the strand tries to slip without twisting, the outer wires of the strand react against the matching deformations in the concrete, resisting movement.

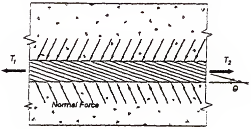

Figure 2-2 Mechanical Interlocking.
Source: Russell and Paulsgrove [72]

2.6 Evolution of the Current ACI and AASHTO Code Expressions

The following section describes the evolution of the ACI and AASHTO code expression for transfer and development length. In 1993, Tabatai and Dickson [76] published a paper titled *The History of the Pretensioning Strand Development Length Equation*, a study commissioned by the Federal Highway Administration. The information provided in this section is based on that publication.

The American Concrete Institute and AASHTO provisions for transfer and development length are identical. Current development length provisions are presented in Section 12.9 of the ACI 318-99 [4]. This provision states that: Three and seven-wire pretensioning strand shall be bonded beyond the critical section for development length, in inches, not less than Equation 2.1.

$$L_d = (f_{ps} - \tfrac{2}{3} f_{se})\, d_b \qquad \text{Equation 2.1}$$

where, L_d is the development length, (in.)

f_{ps} is the strand stress at the limit state, (ksi)

f_{se} is the strand effective stress, (ksi), and

d_b is the strands nominal diameter, (in.)

With regard to transfer length, neither ACI 318-99 nor AASHTO Standards, have explicit provisions for a minimum or maximum length over which the prestress must become effective. The ACI 318-99 Commentary provides an expression to estimate transfer length by re-writing Equation 1 as the sum of transfer length and flexural bond length, see Equation 2.2.

$$L_d = \frac{f_{se}}{3} d_b + (f_{ps} - f_{se})\, d_b \qquad \text{Equation 2.2}$$

ACI 318-99 Section 11.4.3 and AASHTO 9.20.2.4 suggests that a transfer length of fifty strands diameter ($50d_b$) and a linear distribution be assumed for shear design consideration.

2.6.1 Evolution of the ACI Transfer Length Expression

ACI transfer length provisions, derived by Alan Mattock, are based on tests conducted in the 1950s and early 1960s with clean Grade 250 Stress Relieved Strands [30, 34]. In deriving an expression to predict transfer length, Mattock noted that the average transfer bond strength of 400 psi reported by Hanson and Kaar seemed reasonable [76]. With this information and the equilibrium equation for prestressing steel force and bond force, a transfer length expression, Equation 2.3, was obtained from the following derivation.

$$U_t \Sigma_o L_t = A_{ps} f_{se}$$

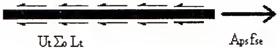

$$U_t = 400\text{psi}$$

$$\Sigma_o = \frac{4}{3} \pi d_b$$

$$A_{ps} = 0.725 \pi \left(\frac{d_b}{2}\right)^2$$

$$L_t = \frac{A_{ps} f_{se}}{U_t \Sigma_o}$$

$$\therefore \; L_t = \frac{f_{se} d_b}{2.94} \quad \longrightarrow \quad Lt = \frac{f_{se} d_b}{3}$$

$$L_t = \frac{f_{se}}{3} d_b \qquad \text{Equation 2.3}$$

In the above derivation, it should be noted that a 4/3 factor is used to relate the strands surface area, Σ_o, to the perimeter of a circle with the same nominal diameter. This factor remains constant for every strand size and grade of steel. Similarly, a factor of 0.725 is used to relate the strands nominal area, A_{ps}, to the area of a circle of the same nominal diameter. This factor changes for the different strand sizes and grades of steel. For example this factor of 0.725 is specific for a ½" Grade 250 strand. The factor for a ½" Grade 270 strand is about 7% larger, 0.779 [13, 14, 76].

Regarding ACI 318-99 Section 11.4.3 provision for transfer length it should be noted that the effective prestress in Hanson and Kaar's tests never exceeded 150 ksi. Evaluating Equation 2.3 for this level of effective prestress resulted in a simplified expression for transfer length in the form of $50d_b$. As such, this expressions applicability should be limited to a maximum level of prestress of 150 ksi. [30, 76] If the derivation above is done for a ½", Grade 270, strand and is evaluated for an effective prestress of 168 ksi (See Example 4.7.1 of the PCI Design Manual [60]), the simplified expression for transfer length would be $61.3d_b$ instead of $50d_b$, or 22.6% longer.

2.6.2 Evolution of the Development Length Expression

The equation to predict the strand's development length was also developed by Alan Mattock and is also based on data from Hanson and Kaar's work in the late 1950s

[30]. The development length expression was developed following a best-fit linear approach. See Figure 2.3 [76].

Mattock originally recommended Equation 2.4 as an estimate of the development length. Eventually, Equation 2.5 was presented to the ACI Committee on Bond. Equations 2.4 and 2.5 are presented in the notation used on the AASHTO code.

$$L = (1.11 f^*_{su} - 0.77 f_{se}) D \qquad \text{Equation 2.4}$$

$$f^*_{su} \leq f_{se} + 0.9 \left[\frac{L - L_t}{D} \right] \qquad \text{Equation 2.5}$$

where, f^*_{su} is the strand's stress at flexural capacity, (ksi) (f_{ps} in ACI notation)

D is the strand diameter, (in.) (d_b in ACI notation)

L is the development length, (in.) (L_d in ACI notation) and

f_{se} is the effective prestress, (ksi) and

L_t is the transfer length (in.)

After discussion in the ACI Committee 323 (bond), Equation 2.1 was adopted in ACI Section 12.9.1 in 1963. AASHTO later adopted the same expression in 1972 as AASHTO Equation 9-32 [76].

Solving Equation 2.5 for the development length, Equation 2.6, we can compare the original expression presented to the ACI with the adopted expression, Equation 2.1, in the form presented in the ACI Commentary.

$$L = Lt + 1.11 (f^*_{su} - f_{se}) D \qquad \text{Equation 2.6}$$

From simple inspection of Equation 2.5 and Equation 2.6 it could be observed that the flexural bond length for the adopted expression is 11% shorter than that recommended from a linear best-fit of the data. It should be emphasized that these expressions are based on a linear best fit and not an envelope of the data. This 11% reduction in flexural bond length causes four (4) specimens with long embedment (i.e. $L_b/d_b>80$) length to fail either by general bond or ultimate bond slip at stresses lower than those predicted by the adopted expression, See Figure 2.3.

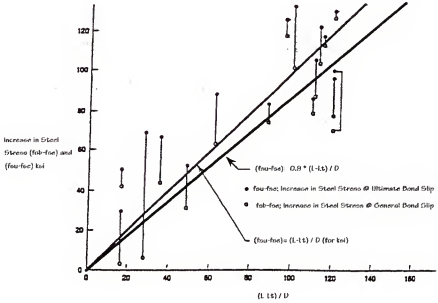

Figure 2-3 Comparison of Hanson and Karr's data to the proposed and adopted Development Length Equations. Source: Buckner [13,14]

As adopted 62.5% of the specimens, same data on which the expressions are based, will experience general bond failure. Seventy percent (70%) of the specimens with long embedment experienced general bond failure. Ultimate bond failure will occur in 31.2% of all the specimens and 50% of the specimens with long embedment length. [13, 14]

2.7 Review of Published Literature

An extensive review of the published literature was conducted as part of these research efforts. The following section attempts to provide a foundation for the reader on the experimental evolution of prestressing strand bond research. The section is divided into three parts.

The first part is a chronological review of the literature, beginning with the first paper published in the United States on the subject, by Jack Janney. Followed by a review of the equations that have been proposed for estimating transfer and development length, as a result of experimental research efforts and third parties re-analyzes of the available data. The third part consists of a summary of the effect of several variables on bond, transfer and development length of prestressing strands.

2.7.1 Chronological Literature Review

Janney [32]. Janney published the first report on development length of prestressing strands in the United States. The research program studied the effect of the wire diameter, the surface condition of the wires and strand and the strength of the concrete on bond. The investigation consisted of two parts; the first part studied the transfer bond and the second studied flexural bond.

Transfer length was determined from concrete surface strains measured along prisms. The prisms, 72" and 96" long, had a 2" by 2" cross-section. The wires/strand were cleaned with carbon tetrachloride and acetone. The wire diameters included in the study were 0.100", 0.162", 0.197" and 0.276". A 5/16"strand was also studied. The surface conditions considered were clean, oiled and rusted. Concrete strength at 21 days was 4,500 psi. One specimen was fabricated with a concrete strength of 6,500 psi. The initial stress in the wires/strand was 120 ksi. The prestressing force was gradually transferred.

Eleven (11) specimens were fabricated and tested for flexural bond portion of the study. The specimens consisted of 6'-6" long beams with a 6" by 10" cross-section. The wires surface conditions were either clean or rusted. The prestress in the wires varied; one specimen had the wires prestressed to 60 ksi and 165 ksi, each. Seven specimens were prestressed to 120 ksi. The wires on the remaining two specimens were not prestressed. The reinforcement ratio varied between 0.137 and 0.199. The specimens were loaded, with a center-point-load, with a 6' span. Electrical strain gauges were attached to the wires.

Janney found a moderate increase in transfer length with increases in wire diameter, slight decrease in transfer length associated with an increase of concrete strength and a marked improvement on transfer and development length for the rusted wires. In the flexural bond tests, Janney found the formation of a flexural bond stress wave that propagated toward the supports.

As the specimens were loaded and the concrete section cracked the stress in the strand increased abruptly. As loading continued, the stress in the strand increased until a limiting bond strength value was reached. At this point some slippage between wire and concrete occurred at the region around the crack, reducing the bond stress in the crack region and increasing the bond stress at the adjoining regions. This process continues, creating a flexural bond stress wave moving away from the point of loading. Whenever the flexural bond stress wave overlapped the transfer length, bond failures were observed.

Critical Note:

The strands/wires used in this research program were cleaned with carbon tetrachloride, a solvent. Recent research has shown strands cleaned with this substance to have bond performance similar to that of weathered/rusted strands[66-67].

Hanson and Karr [30]. Hanson and Karr investigated the effect of concrete strength and strand diameter and surface condition on the flexural bond in prestensioned concrete beams. The strands studied were seven-wire Grade 250 stress relieved strands. The actual breaking strength of the strand was about 270 ksi, although the manufacturers guaranteed 250 ksi. The strand diameters investigated were 1/4", 3/8" and 1/2". The strands were cleaned with carbon tetrachloride. The concrete strengths investigated were 3,700 psi, 5,420 psi and 7,230 psi. The effective prestress in the strands ranged between 113 ksi and 148 ksi. Strain gages were attached to the strands.

Like Janney before them, Hanson and Karr observed very small strain in the strand prior to cracking of the concrete section followed by an abrupt increase after cracking. A flexural bond stress wave progressed toward the ends as the loading increased. They hypothesized that bond/anchorage failure occurred when this high bond stress wave overlapped the transfer zone.

Hanson and Kaar, also, found a reduction in strain even as the load increased, indicating bond slip. The slip destroyed the adhesion bond and developed mechanical interlocking. The authors concluded that specimens reinforced with strands were able to develop additional strength after the strand had slipped due to mechanical interlocking.

Karr, LaFraugh and Mass [31]. Karr, LaFraugh and Mass investigated the effect of concrete strength on transfer length. The same concrete mix was used for all specimens. The concrete strengths were determined by the age of the specimen at transfer, 1, 2, 3, 9 and 22 days. The concrete strengths at transfer were 1,660 psi, 2,500 psi, 3,330 psi, 4,170 psi and 5,000 psi. The strands, 1/4", 3/8", 1/2" and 6/10" in diameter, were prestressed to 175 ksi. The prestressing force was transferred by flame-cut. The transfer lengths were estimated from concrete surface strain measurements.

Karr et al. concluded that concrete strength had little influence on transfer length for strands up to 1/2" in diameter. They found a marked reduction in the transfer length for 6/10" strands with higher concrete strength. The reduction in transfer length was attributed to the 6/10" strand being slightly rusted.

In addition, the authors found the transfer length measured on the cut end to be 20% longer than those measured on the free end. Transfer length, for all strand diameter, increased 6% over a year.

Over and Au [58,59]. Over and Au investigated the effect of strand diameter on transfer length. The specimens, 60" and 80" long prisms with 3" by 3" cross-section, were reinforced with strands 1/4", 3/8" and 1/2" in diameter and a 1/4" diameter wire. The transfer of the prestressing force was done through gradual release.

Over and Au found that, at transfer, the average stress in the concrete is proportional to the stress in the strand up to a point. Then the stress in the strand decreases at a faster rate compared to the rate of change in the stresses in the concrete. For specimens reinforced with strand, the stress in the concrete continued to increase. The concrete stress, for specimens reinforced with wire, diminished. This indicates that the strand, unlike the wires, is able to develop additional bond stresses after slip.

Based on this observation the authors concluded that a multi-wire strand required a smaller transfer length than a wire with the same area.

Bandaliance and VanHorn [8]. Bandaliance and VanHorn bond performance research formed part of an extensive prestressed concrete research program at Lehigh University in the late 1950s and mid 1960s. The specimens were beams with a 7 ½" by 12" cross-section and their length varied from 8 ft to 23 ft. Each was reinforced with four (4) 1/2" diameter Grade 270 strands. Three (3) strands were placed near the bottom with 1½" cover. The fourth strand was placed 2" from the top. Three-eighth of an inch, #3's, Grade 50 deformed bars spaced at 6" on center provided shear reinforcement. The strands were pre-tensioned to 70% f_{pu}, or about 189,000 psi. The concrete strength averaged 4000 psi at transfer and 6000 psi at flexural test. After several tests a slab was added to increase the stresses in the steel at failure.

Electrical strain gages were mounted on the bottom strands. Strains on the concrete surface were measured with a Whittemore gage. Strand slip was measured with dial gages.

Results were compared with Hanson and Kaar's results. The Grade 270 strands tested at Lehigh appeared to have higher bond stresses prior to slip than the Grade 250 strands tested by Hanson and Kaar.

Bond slip failures were observed when the cracks propagated into the transfer zone. They concluded that if the stress in the strand within the transfer region exceeded the stress due to initial prestress, less the creep and shrinkage losses, bond failure would occur.

Hanson [31]. Hanson studied the effect of surface roughness on bond performance. The fourteen (14) beams were reinforced with strands 7/16" or 1/2" in diameter. The 7/16" diameter strands were tested for four (4) surface conditions; as received, partially rusted, rusted and deformed (dimpled). The half (1/2") inch strands were tested for two (2) conditions: as received and dimpled.

Hanson found the transfer lengths on the flame cut end were, on average, 4" longer than on the free end. For the range of transfer length reported this represents an increase of 20%. Holmberg & Lingren reported reductions of 20% on the transfer length for gradually released strands over flame-cut strands.

Transfer length for rusted and dimpled strands improved by 30% over those measured for as received strands.

Stoker and Sozen [75]. The project conducted by Stoker and Sozen consisted of 486 pull-out specimens with short embedment length (1"). The objective was to study the bond slip behavior and the effects of variables such as strand/wire size, lateral confining pressure, time effects and concrete's consistency, curing method, age and settlement. From the data obtained from the experimental program they attempted to develop an hypothesis on the nature of bond and compare this hypothesis to the applicability of the simple pull-out results to the design of prestressed concrete members. The pull-out data based computations were compared to results from five (5) beams. Only transfer length was studied.

The authors found the effect of concrete strength on bond to be small but well defined. For concrete strengths in a 2300 psi to 7600 psi range and using a 4000 psi concrete strength as a benchmark, the effect of concrete strength on bond strength was estimated to be 10% per every 1000 psi change in concrete strength. Bond strength was found to be more sensitive to variables that affect shrinkage of the concrete than concrete strength, i.e. high slump and dry curing increases the bond strength while low slump and moist curing reduces it. The authors concluded that concrete shrinkage increases the contact pressure between the strand and the concrete, which increases the bond strength.

The unit bond force increased with strand diameter. The nominal bond force, the ratio of the pullout force to the theoretical surface area, showed a slight trend of reducing with increases in strand diameter. This trend was determined to have no statistical significance.

On tests where a lateral confining pressure was applied the authors found an increase in bond strength. A reduction in bond strength of 10% - 15% was found for long-term loading.

Bond strength is reduced as the depth of the concrete below the strand increases. Bond strength was reduced to 60% of the maximum bond strength for strands with ten (10) inches of concrete below them. For concrete depth exceeding ten (10) inches there was no further reduction on the bond strength. If the concrete was not vibrated the bond strength was reduced by 30%. Measured transfer length for top strands were 28% than transfer length for bottom stands on companion beams.

The authors were able to predict transfer length and end slip from data obtained from simple pull-out tests. The embedment length of one (1) inch reduced the required pullout force, limiting the tensile stress on the strand to about 15,000 ksi, limiting the influence of "Negative Hoyer's effect" on the tests.

Mayfield, Davies and Kong [52]. Mayfield et al. compared the bond performance of Dyform strand with standard seven-wire strand. The Dyform strand, also a seven-wire strand, has an increased area of steel to area of voids ratio. The strand is compacted to a given area, yielding a smoother profile and lower coefficient of friction. This characteristic makes Dyform suitable for post-tensioning applications.

Mayfield et al. found the Dyform strand to have a longer transfer length than the standard strand. The flexural bond behavior was similar for both strands, although the few bond failures observed were observed on specimens reinforced with the Dyform strand.

Martin and Scott [50]. Martin and Scott did not perform experimental work for their publication. The authors found the transfer and development length code provisions to be inadequate and did not provide for the design of members with spans shorter than the development length. Martin and Scott re-evaluated Hanson and Karr's data and proposed a bi-linear design equation.

Anderson and Anderson [5]. Anderson and Anderson investigated the effect of strand slip at transfer, end-slip or draw-in, on the flexural strength of pretensioned hollow core slabs. A theoretical value of the end-slip was back-computed using a theoretical relationship between the end-slip and transfer length, and the transfer length estimated with the ACI 318 model. The measured end-slips were compared to this theoretical value. All the slabs, twenty-six (26), with end-slip smaller than this theoretical value were able to develop strand stresses in excess of the strand tension limitation criteria of the ACI 318-71 code. Of the ten slabs with poor bond, i.e. end-slips longer than the computed theoretical value, only three developed their flexural capacity. The remaining seven failed in bond.

Zia and Mostafa [80]. Zia and Mostafa performed an extensive review of the available literature. They concluded that the transfer length was directly proportional to the stress in the strand and the strand diameter, while inversely proportional to the concrete strength at transfer. Based on these conclusions they proposed a new transfer and development length equation that accounted for the concrete strength at transfer.

Brooks, Gerstle and Logan [9]. Brooks et al. tested eleven (11) hollow core slabs, ten of which had end-slips considered excessive. The purpose of the research program was to investigate the influence of excessive strand slip at transfer on the slabs flexural capacity.

The only specimen with acceptable end-slips, that is end-slip shorter than the computed theoretical value, developed flexural capacity at an embedment length of 71.25 inches. Two specimens with excessive end-slips, with embedment lengths of 119 inches and 141 inches, respectively, developed high flexural capacity. These embedment lengths are approximately 150% and 175% the development lengths estimated per ACI 318. The remaining seven (7) specimens failed in bond. These tests indicated that excessively long transfer lengths, indicated by long end-slips at transfer, lead to premature bond failures.

Cousins, Johnston and Zia [16-18]. The purpose of Cousins et al. research was to investigate the bond performance of epoxy-coated prestressing strands. This research program was initiated in 1986. Uncoated strands were tested as benchmark for the epoxy-coated strand results. Research results indicated that the ACI and AASHTO provisions for transfer and development length are inadequate. The reported average transfer length for ½" and 6/10" strand was 50 inches and 57 inches, respectively. Required embedment lengths were 1.9 times the estimated development lengths per ACI 318. These findings prompted the FHWA Memorandum imposing a moratorium on the use of 6/10" strand, as well as other restrictions on smaller diameter strands.

FHWA Memorandum [13-14]. In October of 1988 the Federal Highway Administration issued a memorandum placing the following restrictions on the use of seven-wire strands on bridge applications:

1. The use of 6/10" strand is prohibited for pretensioning applications.
2. Four (4) strand diameter minimum center to center spacing.
3. Increase the development length computed per AASHTO Equation 9-32 by 60%.
4. The development length requirements for de-bonded strands remained in-place, i.e. twice the development length estimated with Equation 9-32.

As a result, of this memorandum several research projects were initiated to improve the state of knowledge of prestressing strands bond behavior and their transfer and development length performance.

Deatherage and Burdette [19]. Deatherage and Burdette fabricated and tested 20 AASHTO type girders. The beams were reinforced with 1/2", 1/2" special, 9/16" and 6/10" diameter strands. A set of four (4) beams was fabricated for each strand size with a 2" concrete cover. An additional set of four (4) beams was fabricated with 1.75" concrete cover. The concrete strength at transfer was 4,000 psi. The strands were released by flame-cut. The transfer length was estimated from concrete surface strains. The specimens were loaded with a single point load.

Deatherage and Burdette found the transfer length to be proportional to the strand diameters for strands up to 9/16" in diameter. The 6/10" strand did not follow this trend.

The authors concluded that:

1. The use of 6/10' strand should not be restricted.
2. The transfer length should be related to the concrete strength at transfer, instead of the 28-day concrete strength.
3. The reduction in strand spacing did not appear to affect bond performance.
4. The development length estimated from ACI equations should be increased by 50%.

Russell and Burns [68-71]. Russell and Burns conducted an extensive research program at the University of Texas-Austin. Transfer and development lengths were measured on 1/2" and 6/10" strands. The study included the effect of variations in strand spacing, specimens shape and size, strand confinement and partial de-bonding of the strands.

Russell and Burns concluded that: "... to prevent anchorage failures, beams should be designed so that no concrete cracks will propagate through the the transfer zone of the pretensioned strand... If cracks propagate through the anchorage zone of a strand, or immediately adjacent to the transfer zone, failure of the strand [anchorage] is imminent". Results indicated that the previous statement stands true for any kind of application, size of strand and for partially-debonded or fully bonded strands.

With respect to transfer length, the authors found an exponential relationship between the transfer length and the diameter of the strand. A linearly proportional design equation was proposed.

Mitchell, Cook, Tham and Khan [55]. Mitchell et al. tested twenty-two (22) prestressed concrete beams to investigate the effect of high performance concrete on transfer and development length. Concrete strengths, at transfer, ranged between 3,050 psi to 7,250 psi. At flexural bond test, the concrete strengths were within a 4,500 psi to 12,900 psi range. The prestressing force was gradually released.

The authors found the transfer and flexural bond to decrease with an increase in concrete strength. It should be noted that the low end of the concrete strengths studied by Mitchell et al. coincide with the high end of concrete strengths on Karr, LaFraugh and Mass research. Modifications to the ACI and AASHTO equation were proposed to account for the concrete strength.

Buckner [13-14]. FHWA commissioned Buckner to attempt to reconcile the myriad of design recommendations proposed by a similar number of research programs initiated in response to the 1988 FHWA memorandum that severely restricted the use of prestressed concrete [13, 14]. Buckner presents an extensive literature review and reanalyzes the experimental data from those research programs in his attempt to rationalize their differences.

The author proposed an equation that modifies the current ACI equation flexural bond length by a correction factor. This correction factor is function of the strain in the strand at the limit state. The transfer length equation is also modified. The transfer length is related to the initial prestress instead of the effective prestress.

Den Uijl [21]. Den Uijl investigated the effect of High Performance Concrete (HPC) on bond performance of prestressing strands. The research program consisted of a series of 13 prisms prestressed with one or two strands. The diameters studied were 3/8" (9.3mm) and 1/2" (12.5mm). Concrete strengths were 40Mpa (5.8 ksi) and 70Mpa (10.15 ksi) at transfer. Two concrete mixes were used: gravel concrete and limestone concrete.

The author found improved bond performance for High Performance Concretes, over regular strength concrete specimens with cube strengths at transfer similar to those of HPC specimens. The authors attribute this finding to the improved tensile properties of HPC. Transfer lengths measured on gravel high-performance gravel concrete specimens were about half of those measured on normal-strength concrete. Transfer lengths measured on high-performance limestone concrete specimens were shorter than those measured on normal-strength limestone concrete, but the difference was not as marked as with gravel concrete.

2.7.2 Review of Proposed Transfer and Development Length Expressions

With the advent of Grade 270 Low-Relaxation strands in the early 1970s researchers began to question the applicability of the adopted expressions [50]. The higher breaking strength of the Grade 270 strands allowed for higher initial prestress. The effective prestress achieved with the Grade 270 low Relaxation strand is also higher, yet, not in proportion to the increase in the strand's breaking strength. The Low-Relaxation characteristics of the new strands reduced the steel relaxation losses to one-fourth the losses experienced by the Stress-Relieved strands. This allows the Low-Relaxation strands to maintain a higher effective prestress than a Stress-Relieved strand of the same Grade. In addition to allowing a higher initial and effective force per unit area, the new Grade 270 Low-Relaxation strands cross sectional area is larger than that of the Grade 250 strand with the same nominal diameter, yet the surface area remained the same.

Hanson and Kaar's [30] strand was cleaned with carbon tetrachloride, a solvent, and gradually released. Recent research found that these two variables could independently improve bond performance by up to 20% [30, 66-72].

Hanson and Kaar's [30], and other early research projects, data was re-evaluated and new expressions were proposed. Martin and Scott [30] developed an equation based on a bi-linear best-fit curve of their data. Zia and Mostafa [65] also re-evaluated Hanson and Kaar's [30] data and developed an expression for transfer and development length, Equation 2.7. This expression is presented in Arthur Nilson's *Prestressed Concrete Design* textbook as an alternative to the code expressions [57].

$$L_t = 1.5\left[\frac{f_{si}}{f'_{ci}}\right]d_b - 4.6 + 1.25\left(f_{ps} - f_{se}\right)d_b \qquad \text{Equation 2.7}$$

In 1986 researchers at North Carolina State University obtained development lengths for uncoated prestressing strands significantly longer than those predicted by Equation 2.4 [16-18]. This prompted a Federal Highway Administration, FHWA, memorandum that severely restricted the use of prestressing strands. This memorandum disallowed the use of 0.6"strand, imposed a center to center spacing of four strand diameters and increased the development length of uncoated strands by 60% and 100%, for fully bonded and blanketed strands respectively [13-19].

This memorandum resulted in the initiation of several research projects to improve the state of knowledge of prestressing strands bond behavior and their transfer and development length performance. The following expressions for transfer and development length are the result of these research efforts:

As a result, of research efforts conducted at the Florida Department of Transportation on full-scale AASHTO girders expressions for transfer and development length were presented, Equation 2.8. [74]

$$L_d = \left(\frac{\frac{f_{si}\, d_b}{3} + \left(f_{ps} - f_{se}\right) d_b}{k_b\, \mu_{ave}} \right) \qquad \text{Equation 2.8}$$

where, f_{ps} is the strand's stress at the limit state (ksi)

f_{si} is the initial prestress (ksi),

d_b is the strand's nominal diameter (in.),

k_b is 250 psi and μ_{ave} is a dimensionless constant that assumes a value of 8, 4 or 2 for piles embedded on pile caps, slender elements and deep elements (shear span/depth < 3) respectively.

McGill University [55] focused their research efforts on the effect of high strength concrete on bond performance. An expression was presented that modifies the current code expressions for concrete compressive strength. See Equation 2.9.

$$L_d = \frac{f_{si}}{3}\, d_b \sqrt{\frac{3}{f'_{ci}}} + (f_{ps} - f_{se})\, d_b \sqrt{\frac{4.5}{f'_c}} \qquad \text{Equation 2.9}$$

where, f'_{ci} is the concrete strength at the time of detensioning (ksi),

f'_c is the concrete strength at service (ksi)

The Eurocode expression for transfer length considers the concrete strength at transfer as well as the ratio of cross-sectional area to the perimeter of a circle with the same nominal diameter. Three corrections factors are introduced to account for method of strand release, strand surface condition and stress condition in the vicinity of the strand [13, 14]

$$L_t = \alpha_8 \alpha_9 \alpha_{10} \left[\frac{A_{ps}}{\pi\, d_b} \right] \left[\frac{f_{si}}{f'_{ci}} \right] \qquad \text{Equation 2.10}$$

where, A_{ps} is the strands nominal area, and

α_8, α_9, α_{10} are coefficients that account for release method, stress condition around strand and strand surface condition.

A comprehensive research project, conducted at the University of Texas-Austin presented a strand development criterion that eliminates the concept of development length [68-71]. They concluded that inhibiting cracks from forming in the transfer region ensures the development of the flexural capacity of the section. Since strand stresses increase dramatically at cracks, the formation of cracks within the transfer region would drastically increase the stress in the strand, nullifying Hoyer's effect and resulting in a loss of anchorage.

Janney observed this behavior in the 1950s [34]. He noted that as the specimens were loaded no considerable increase in steel stress was observed until after the section had cracked. After the section cracked the steel stresses increased dramatically. These stresses moved, as waves, toward the ends of the specimen as the load increased.

Whenever this stress wave overlapped the transfer region bond failure was observed [8, 34]

The researchers at the University of Texas at Austin, and later at the University of Oklahoma, recognized that cracks could be in the form of flexural cracks or diagonal shear cracks and recommended the use of end blocks to minimize the possibility of diagonal shear cracks in the transfer zone. A development length expression based on the concept of inhibiting cracks within the transfer zone is presented. Figure 2.4 shows a graphical representation of the proposed relation, Equation 2.11 [68-71].

$$L_d = \frac{M_n}{M_{cr}} L_t \qquad \text{Equation 2.11}$$

where, M_n is the section's flexural strength,

M_{cr} is the section's cracking moment, and,

L_t is the transfer length.

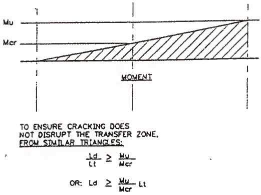
Mu
Mcr
MOMENT
TO ENSURE CRACKING DOES
NOT DISRUPT THE TRANSFER ZONE.
FROM SIMILAR TRIANGLES:
$\frac{Ld}{Lt} \geq \frac{Mu}{Mcr}$
OR: $Ld \geq \frac{Mu}{Mcr} Lt$

Figure 2-3 Graphical Representation of Equation 2.11
Source: Russell and Burns [70]

Equation 2.11 considers the formation of flexural cracks only. In addition is similar in form and function to the expression presented by Brooks, Gerstle and Logan [9] equating the development length to the transfer length times the ratio of the stress in the strand at the limit state to the effective prestress. For the estimate of the transfer length, Russell and Burns [68-71] proposed Equation 2.12.

$$L_t = \frac{f_{se}}{2} * d_b \qquad \text{Equation 2.12}$$

Equation 2.11 was modified on a report published by Russell and Paulsgrove [71], when the researchers realized that an additional length was required to prevent the crack from propagating into the transfer region, adding a mechanical interlocking length, Lmi. See Equation 2.13.

$$L_d = \frac{M_n}{M_{cr}}\left(L_t + L_{mi}\right) \qquad \text{Equation 2.13}$$

where, L_{mi} is the mechanical interlocking length.

The mechanical interlocking length is taken as the least of the beams effective depth or the spacing of the shear reinforcement. An explanation for the source of this additional length is not offered on the publication, yet appears to be derived from a truss analogy.

As stated before, the FHWA memorandum resulted in the initiation of a number of research efforts, which resulted in an equal number of design recommendations. In an attempt to reconcile the differences in results and design recommendations from the various research projects, FHWA conducted a review of the available data [13, 14]. In this review, performed by Buckner, the author contends that bond failures are not due to the formation of cracks in the transfer zone, but due to the strains in the strand

For example, if the section has an effective prestress, f_{ps}, of 150 ksi and a maximum stress, f_{ps}, of 230 ksi this stress increase of 80 ksi represents an increase in strain from 0.0053 to 0.0081, a 52% increase. On the contrary if the effective prestress is 185 ksi that same 80-ksi stress increase represents a strain increase from 0.0065 to 0.015, a 130% strain increase. These stress levels are achieved on bridge girder where the deck acts composite with the girder. Buckner has pointed out that with few exceptions these kind of stresses have not been achieved in current research projects.

Buckner proposed the following modification to the current development length expression, see Equation 2.14;

$$L_d = \frac{f_{si}\, d_b}{3} + \lambda\,(f_{ps} - f_{se})\, d_b \qquad \text{Equation 2.14}$$

where, $\lambda = 0.6 + 40\,\varepsilon_{ps} < 2$, and

ε_{ps} is the strand strain at the limit state

2.7.3 Variables Identified to Affect Bond, Transfer and Development Length Performance of Prestressing Strands

This section discusses the variables identified as affecting strand's bond, transfer and development length performance. This variables are: method of measurement of the transfer length, concrete compressive strength at transfer, specimen age, confinement of the concrete surrounding the strand, End-slip or draw-in, detensioning method, strand size, spacing and surface condition, pull-out force, position of the reinforcement in the cross-section and type of loading.

2.7.3.1 Measurement of Transfer Length

The prestressing force is transferred to the concrete by bond mechanisms. This force is assumed to transfer linearly from zero at the end of the beam to a maximum at the end of the transfer region. Beyond the transfer region, strains are remains constant.

Most research projects have measured the transfer length by measuring deformations on the concrete surface. These deformations are converted to strains and plotted versus distance along the specimen, constructing a strain profile. There are several approaches to the determination of the transfer length. At this point the various research projects depart from one another in their determination of the measured transfer length.

Russell and Rose [66,67], at University of Oklahoma, OU, and Russell and Burns [68-71], at University of Texas-Austin, UTA, used a smoothing technique to plot their data points. Transfer length is defined as the distance from the end of the beam to the intercept of the line connecting the data points in the increasing portion of the graph and a line equal to 95% the average of the plateau region data points.

Another approach is the slope-intercept method, based on the bi-linear idealization of the strain profile. Transfer length is defined as the intercept of the line that describes the linearly increasing portion of the strain profile with a horizontal line representing the plateau region. Research at the University of Florida have used this approach defining the horizontal line as 95% the average of the data points in the constant strain region [25-27].

Finite element models have shown that, due to shear lag, the transfer length measured at the surface of the concrete with 2 inches cover are 10% longer than the actual transfer length [13, 14]. After comparing various research projects results and transfer length measurement techniques, Buckner concluded that the 95% average maximum strain technique produced results similar to those obtained by the Finite Element Model.

Transfer lengths, at the University of Florida, were estimated following both methodologies. In general, the 95% Average Maximum Strain methodology with smoothing technique, used by Russell, yielded transfer lengths 5% to 10% longer than the transfer lengths estimated the slope-intercept method with plateau at 95% of the average maximum strain used at University of Florida. This difference could be considered negligible when compared to the 20% scatter found within methodologies.

2.7.3.2 Concrete Compressive Strength at Transfer, f'ci:

Early research projects reported that the concrete's compressive strength at transfer, f'_{ci}, has no effect on the strands performance. The compressive strengths in Karr et al. study ranged from 2,000 psi to 5,000 psi [36]. It should be noted that the concrete strength at transfer was controlled by the age of the specimen at transfer. The roles played by variables such as concrete shrinkage and steel relaxation must be considered. The authors did not mention such considerations.

Research at the University of Illinois in the late 1960s and early 1970 found that the bond strength increased at a rate of 10% for every 1000-psi increase in concrete strength [75].

Recent projects at McGill University, where concrete compressive strength at transfers, f'ci, ranged from around 3,000 psi to over 7,000 psi have shown that it does have an effect on the strands performance [55]. McGill University's researchers have proposed the following transfer length expression, Equation 2.15, which indicates an inversely proportional relation between the transfer length and the concrete strength.

$$L_t = \frac{f_{se}}{3} * \sqrt{\frac{3}{f'ci}} * d_b \qquad \text{Equation 2.15}$$

Note that Equation 2.15 is the transfer length portion of Equation 2.9 presented in the previous section. It could be argued that the range of concrete strengths studied in the research program conducted by Mitchell, Cook, Khan and Tham at McGill University (43) are not realistic for practical applications due to the economics of the prestressed concrete industry. The competitiveness of the industry demands quick turnarounds and repetitive use of forms and space. Industry standards have chosen 3,500-psi concrete strength as the target strength for detensioning of the strands [60]. Within this range research by Kaar, LaFraugh and Mass showed no, or little, effect on transfer length. For practical purposes the effect of concrete strength could be neglected. AASHTO 1.6.18 sets the minimum compressive concrete strength at transfer to 4,000 psi. Likewise, ACI sets 3,000 psi as the minimum compressive strength at transfer for 3/8" strand or smaller and 3500 psi for larger strands.

On the other hand, acknowledgeable designers can take advantage of the improved bond performance of higher concrete strength by specifying the design concrete strength at transfer in the contract documents.

2.7.3.3 Mechanical Interlocking

Mechanical interlocking is a bond mechanism mobilized when the strand tries to slip without twisting. If the strand is allowed to rotate, the strand will twist, i.e. effectively un-screwing itself, through the concrete and the mechanical interlocking is ineffective.

The magnitude of the mechanical interlocking contribution to bond is not clear. Stocker and Sozen [75] performed a series of pullout tests where the strand was restrained from twisting and compared the results to those from tests where the strand was allowed to twist. They expected an increase in pullout force, but little difference was found between the pullout force for specimens where twist was restrained and those where twisting was allowed. These results led to discounting the bond stresses due to mechanical interlocking.

Russell and Burns [68-71] found the mechanical interlocking to be a major contributor to the flexural bond. They pointed to evenly dispersed crack patterns as evidence of the mechanical interlocking. They explained that test setup used by Stocker and Sozen allowed for longer "Free Strand"[4] than those found in actual pretensioned beams. The test setup, used by Stoker and Sozen, restrained the strand several inches from the point where the strand entered the concrete. Consequently, the torsional restraint was reduced rendering the mechanical interlocking ineffective. According to Russell and Burns the actual "Free Strand" in pretensioned concrete members is exactly the width of the crack.

---

[4] Distance between points where the twisting is restrained

2.7.3.4 Specimen Age

Transfer length does not significantly vary with the age of the specimen at the time the transfer length is measured. One of the few advantages of measuring transfer length on an older specimen is that the strain profile is less erratic.

However, specimen age at the time the strands are detensioned do affect the transfer length. In his report to the FHWA [13, 14], Buckner found a correlation between transfer length and an apparent concrete's Modulus of Elasticity, Equation 2.16.

$$L_t = \frac{f_{se} * d_b}{E_c} \qquad \text{Equation 2.16}$$

where E_c is the apparent Modulus of Elasticity, back computed from measured strains.

Buckner then simplified this equation for a compressive strength, f'_{ci} equal to 3,500 psi and normal weight concrete. He reasoned that 3,500-psi is the industry's target concrete strength for detensioning the strands. The above equation was simplified and became, Equation 2.17,

$$L_t = \frac{f_{si}\, d_b}{3} \qquad \text{Equation 2.17}$$

where, f_{si} is the initial strand stress.

First presented by the researchers at the Florida Department of Transportation, Equation 2.17, represents the mean of their measured transfer lengths [74]. Equation 2.17 is the transfer length portion of the expression they proposed for estimating the development length, Equation 2.8. The proposed expression, Equation 2.17, with it's simplifications and assumptions, seems reasonable since the economics of the industry demands a quick turn around in the casting yard. The Precast/Prestressed Concrete Institute (PCI) requires a minimum concrete's compressive strength of 3,500 psi for the detensioning of the strands in their Plant Certification Program. In addition, PCI requires a minimum curing period of 28 days [60].

2.7.3.5 Confinement pressure

Stoker and Sozen [75] applied external confining (tri-axial) pressure on specimens as they performed short-embedment pull-out test. They found an improvement in bond performance with an increase in pressure.

2.7.3.6 Concrete Slump

Stoker and Sozen [75] found an improvement in bond performance with an increase in slump. They rationalized that the higher slump concrete would have more shrinkage than the less fluid concrete. The confinement pressure on the strand increased as a result of the shrinkage. As mentioned above the bond performance improves with increases in confining pressures.

2.7.3.7 Specimen Size

Tests at the University of Texas–Austin [68-71], have shown that the effect of flame cutting the strands diminishes with the specimen size. Their explanation for this phenomena is that as the specimen size increases the section has more mass to absorb the energy released by the strand, since the strands are released one at a time.

2.7.3.8 Aggregate Type

Den Uijl [21] found the transfer length performance of strands embedded in Gravel High Performance Concrete to be two times better than in regular strength gravel concrete. For limestone concrete, the strands embedded in HPC performed better than in regular strength concrete, yet, this improvement was not as marked as with gravel concrete.

2.7.3.9 Concrete Confinement

Hanson [30] found a 15% reduction in transfer length for strands with confinement steel over those where confinement steel was omitted. Russell and Burns [68-71], research project at UTA found that the presence of confining steel does not affect the overall performance of prestressing strands.

Meanwhile, a research project conducted at the Florida DOT showed that what Russell and Burns stated is true unless the section has cracked at the transfer stage [74]. If the section cracked during the prestressing strand release then the presence of confining steel ensured the integrity of the section at the ultimate stage [13, 14].

Den Uijl [21] found the confinement capacity of high performance concrete, compared to that of regular strength concrete with the same cube strength at transfer, to be more efficient, resulting in smaller required effective cover to prevent the formation splitting cracks. The presence of transverse reinforcement resulted have a favorable influence on anchorage capacity

2.7.3.10 End-slip

End slip measurements have shown strong correlation to the strands transfer length performance. End slips are measured under the same conditions in which the prestressing force in the strand is being transferred to the concrete, i.e. concrete strength, specimen age, confinement, etc. The measurement is simple and inexpensive.

Several equations have been developed to relate the end-slip to the transfer length. These expressions are developed from the integration of the difference between the steel strain and concrete strain over the transfer zone. The expression frequently seen in the American literature is based on the assumed linear distribution of the strains. This assumption yields Equation 2.18.

$$L_t = 2L_{es}\left(\frac{E_{ps}}{f_{si}}\right) \qquad \text{Equation 2.18}$$

Where L_{es} is the end-slip or draw-in[5]

The FIP and European researchers have developed the following expression where the strain distribution is assumed parabolic, Equation 2.19. [6,7,9-11,13,14]

$$L_t = 3L_{es}\left(\frac{E_{ps}}{f_{si}}\right) \qquad \text{Equation 2.19}$$

The relationship between end slip and transfer length is explored in more detail in Section 2.8 and Chapter 4.

---

[5] The end-slip is the length of strand drawn into concrete section when the prestressing strands are released from the bulkheads.

2.7.3.11 Transfer Method: Flame Cut versus Gradual Release.

Kaar, LaFraugh and Mass (29) found that transfer lengths were 20% longer on the flame-cut sides than on the free ends. Holmberg & Lingren reported reductions of 20% on the transfer length for gradually released strands over flame-cut strands.

2.7.3.12 Strand size

The expressions presented in the ACI 318-99 Commentary and Section 11.4.3 of ACI 318-99 assumes that the transfer length is linearly proportional to the strands diameter. This assumption held true for strands up to 0.52 and 9/16" in diameter. Detherage et al. found that 0.6" strands did not followed this trend [19]. They found that although the transfer length had increased for the 0.6" strand the increase was not proportional to the increase in strand diameter.

Russell and Burns, although the equation proposed assumes a linear relationship between transfer length and strand diameter, found this relationship to follow an exponential curve [70]. McGill University's research team found that the transfer and development length are directly proportional to the strands diameter [1,2].

2.7.3.13 Strand spacing

Tests at the University of Texas Austin [70], Florida Department of Transportation [74] and the University of Tennessee-Knoxville [19] showed that strands spaced at 3.5 d_b performed similar to strands spaced at AASHTO required spacing of $4d_b$. In his report to FHWA, Buckner [13,14] suggested relaxing the four strand diameters ($4d_b$) spacing restriction imposed on the FHWA Memorandum.

2.7.3.14 Strand Surface Condition

Research projects at Oklahoma University [66, 67] have demonstrated that weathering the strand surface can improve bond performance by up to 60%. Hanson [31] found that rust improved the strands bond performance by up to 53% and 30% on average over cleaned strands.

Buckner in his project for the Federal Highway Administration found that the coefficient of friction is too erratic to be used as a predictor of the bond performance [13, 14].

Hanson and Kaar cleaned the strands used in their project with carbon tetrachloride. Recent tests have shown that strands cleaned with carbon tetrachloride behave similar to strands exposed to moist environment for four (4) days. Current design provisions are based on the results of Hanson and Kaar's project.

2.7.3.15 Pullout force

It has been proposed that only strands with pullout exceeding the benchmarks established by Moustafa's pull-out tests in 1974 and 1992 at CTC be used for research projects [45]. The simple pull-out test do not reproduce the Hoyer's effect, resulting from the swelling of the strand at transfer. Hoyer's effect and the frictional forces associated with it are considered an important component of the bond performance phenomena.

Cousins, Badeaux and Moustafa (12) attempted a tensioned pullout test at Louisiana State University. This test simulates Hoyer's effect by pre-tensioning the strands, then casting a concrete block around it. The concrete block is then pushed from the strand. They found variations similar to those found with the simple pullout tests

(Moustafa's). They suggest the need for more research to investigate the relationship between their test method and transfer length results. Research at Oklahoma University attempted to find such relationship and found the test to be too erratic and difficult to perform.

Moustafa's pull-out test results are limited to qualitatively describe the bond performance of prestressing strands. Tests showed that strands with pull-out tests exceeding 38,000 pounds have good bond performance. Similar tests performed at Oklahoma University showed that strands with high (~32 kips) pull-out forces exhibited good bond performance. The differences in the benchmark load, from 38 kips to 32 kips, were attributed to the difference in rate of loading [66, 67].

Recently, in an attempt to standardize a simple pull-out test, tests were conducted at three (3) locations, Stresscon Corporation, Florida Wire and Cable, Inc. and Oklahoma University. All three sites tested the same set of strand samples under similar conditions. These tests showed agreement in the qualitative results between sites. Two of the three sites pull-out forces agreed within two or three thousand pounds. The average pull-out force of the third site lagged the first two by more than 9,000 pounds.

Preliminary results at the University of Florida with 3/8" strand showed no difference in pull-out for strands with smooth and indented wires. The measured transfer length for the strands with smooth wires was, on average, 50% longer than those measured for indented wire strands.

2.7.3.16 Strand Position

No research program has evaluated the strand's performance with 12" or more of concrete underneath the strand. Researchers at University of Tennessee Knoxville reported measured end slips ranging from 1.5 to 5.1 times those measured on the bottom strands of the same specimen [19]. The average value was 2.6.

2.7.3.17 Load Type: Cyclic Loading versus Static Loading

The University Texas at Austin reported little deterioration of the flexural bond occurring under cyclic loading at service load (i.e. load that causes an extreme tension fiber stress of $6\sqrt{f`_c}$) [70]. They observed that slip occurred during periodic overloads (160 to 180% of the service load), but then stabilized. They concluded that the slip was due to the overloads, not due to the distress caused by the cyclic loading. Bond fatigue is not a concern in the performance of prestressing strands. The overall behavior under cyclic loading was similar to that of the companion specimens loaded under static load.

2.8 End Slip - Transfer Length Relationship

The region where the strains are increasing is called the transfer region. The length over which the strains are increasing, i.e. the prestress is being transferred from the strand to the concrete, is called the transfer length, L_t. Researchers have argued that the strain variations follow a parabolic profile [6,7,10-12,28], yet others have simplified it to a linear profile [66-72]. Others have observed the strain variation to consist of a concave region followed by a linear portion and finally a convex portion [1,2]. The plateau region is where the prestressing force has already been transferred to the concrete. The areas outside this plot, and bounded by the vertical axis and the maximum strain, the shaded area in Figure 2.5, is the end slip.

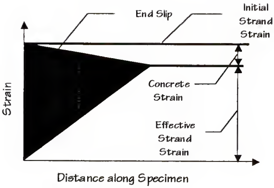

Figure 2-4 Graphical representation of the End-Slip.

This relation is summarized in Equation 2.20, where ε_{pi} is the initial prestressing strain and ε_s (x) and ε_c (x) are the steel and concrete strain as a function of the distance from the end of the beam.

$$L_{es} = \int_0^{L_t} \varepsilon_{pi} - (\varepsilon_s(x) + \varepsilon_c(x))dx \qquad \text{Equation 2.20}$$

The exact expressions describing the variation of the steel and concrete strains along the transfer zone are not known; yet the shape of them will suffice. Realizing that Equation 2.20 is no more than the shaded area in Figure 2, this expression can be reduced to Equation 2.21 or Equation 2.22. Note that Equation 2.21 and Equation 2.22 are equal for initial prestressing in the elastic range.

$$L_{es} = \frac{1}{\lambda} * \varepsilon_{pi} * L_t \qquad \text{Equation 2.21}$$

$$L_{es} = \frac{1}{\lambda} * \frac{E_{ps}}{f_{pi}} * L_t \qquad \text{Equation 2.22}$$

Where λ describe the assumed shape of the strain variation. The parameter λ can assume a value of 2, 3 or 4.6 depending on the assumed strain profile, linear, parabolic or elliptic, respectively. Solving Equation 2.21 for the transfer length, L_t, an expression for transfer length is obtained, Equation 2.23.

$$L_t = \lambda * \frac{L_{es}}{\varepsilon_{pi}} \qquad \text{Equation 2.23}$$

Currently two slip theory based transfer length expressions are generally accepted. In the United States, the generally accepted expression assumes a linear profile, Equation 2.18. One proposed by the International Federation of Concrete, FIP, assumes a parabolic strain profile, Equation 2.19.

$$L_t = 2 * \frac{L_{es}}{\varepsilon_{pi}} \qquad \text{Equation 2.18}$$

$$L_t = 3 * \frac{L_{es}}{\varepsilon_{pi}} \qquad \text{Equation 2.19}$$

These expressions have been consistently proven by research work done in various laboratories. Equation 2.18 coincides with the average of the available data. Polish researchers have found λ to be 2.86 and through simulations it was found that the actual value of λ lies between 2.4 and 2.7 with an average of 2.56(den Uijl).

CHAPTER 3

EXPERIMENTAL PROGRAM

3.1 Introduction

Research efforts to investigate bond transfer and development length performance of prestressing strands at the University of Florida were initiated in December 1996. The main thrust of these efforts were focused toward improving the state of knowledge on the effect of the diameter of prestressing strands, i.e. strand size, on transfer length and flexural bond performance. To a lesser extent, the effect of the stress in the strand prior to transfer was also investigated.

A research program was designed to mimic current prestressed concrete industry standards. Forty (40) specimens were fabricated and tested. With the exception of series UF13 and UF14, which were fabricated at Gate Concrete Products Jacksonville, Florida, all the specimens were fabricated and tested at the Structures Research Laboratory, Department of Civil Engineering, University of Florida. The fabrication and testing of these specimens was done in four (4) phases.

3.2 Experimental Phases

The first phase of this research program, series UF 1, studied bond, transfer and development length performance 1/2" Grade 270 strand and its adequacy for prestressing applications. This phase consisted of six flexural test specimens reinforced with prestressing strands from a single coil of strand. The six specimens were fabricated simultaneously in a single concrete placement. Phase I was completed in May 1996.

The second phase, Phase II, consisting of series UF 2 through UF 7, investigated the effect of various manufacturing processes on the bond, transfer and development length performance of 1/2" Grade 270 prestressing strands. Two flexural test beam specimens and a simple pull out specimen were fabricated and tested for each series.

The bond performance of strands produced following two different manufacturing processes were compared in each of these series. That is each specimen within a series was reinforced with strands from different strand coils.

The samples of strands were provided to the research team in a blind manner, that is the research team was provided only with the strand serial number, allowing the sponsors to keep track of the strands. For this reason, the research team had no knowledge whether or not strands in different coils were actually the same strand or strands produced at different production lines, but following similar production processes. The changes in manufacturing processes, or the extent to which the manufacturing processes were varied, were not provided to the research team.

A simple pull out specimen consisted of twelve strands, four (4) samples from each of the strands being tested, plus four (4) control strand samples. Phase 2 began on September 1997 and concluded in February 1998.

Phase III consisted of series UF 8 through UF 14. The principal variable studied was the effect of the strand's diameter on bond transfer and development length performance of Grade 270 prestressing strands. The strand sizes studied included: 3/8", 3/8" indented, 1/2" special, 6/10" and 7/10". Specimens for Phase III were scaled with respect to the diameter of the strands with which they were reinforced to achieve cover to strand diameter ratio, extreme fiber stresses at transfer, confinement steel and strand stress at the limit state similar to those of the specimens used in Phases I and II. Specimen dimensions are presented on Table 3.1

Each of the seven series of Phase III consisted of two flexural test beams and a simple pull out block. Series UF 8 through UF 12 were fabricated at the Structures Research Laboratory. Series UF 13, reinforced with 6/10"strand, and UF 14, reinforced with 7/10" strand, were fabricated simultaneously at Gate Concrete Products, Jacksonville Florida. This phase ran from December 1998 to September 1999.

Phase IV, completed in December 1999, studied the effect of higher strength strands and strand diameter. Phase IV consisted of series UF 15 through UF 18, each series consisting of two flexural test beams. The specimen cross-sections were similar to those used in Phase III. See Table 3.1.

The strands studied were Grade 290 and Grade 300, i.e. a guaranteed breaking strength of 290 ksi and 300 ksi. The initial prestress level, although still seventy-five percent (75%) of the breaking strength, were approximately 217 ksi and 225 ksi, respectively.

3.3 Specimen Design

The specimens were designed to provide worst-case conditions for transfer and flexural bond tests. In addition, the specimens, the materials used for their fabrication and their fabrication were to conform to current prestressed concrete industry standards.

The concrete mix used mimicked that used in the industry. The strands were provided with a four-strand diameters concrete cover. The prestressing strands were tensioned to 75% of the guaranteed ultimate strength and detensioned by flame-cutting. Detensioning of the strand was done after the concrete had achieved a minimum compressive strength of 3,500 psi. A maximum compressive strength of the concrete of 4300 psi was observed for detensioning. Detensioning typically occurred within 24 hours after placing the concrete. On Phase III and Phase IV, specimens were allowed to cure for at least 28 days before performing flexural bond tests.

An under-reinforced[1] section was selected to ensure a high level of deformations in the strand at flexural capacity. The compressive stresses in the extreme fiber of the concrete section were not to exceed ACI allowable stresses at transfer. Top mild reinforcement was provided to resist tensile stresses developed at transfer of the prestressing force. The mild reinforcement, in conjunction with an under-reinforced section, ensured large deformations in the strand at the limit state.

The design of the specimens reinforced with 1/2" Grade 270 strands followed the design philosophy presented by researchers at the University of Oklahoma [69]. By standardizing the design of the specimens, thereby removing it as a variable, allowed a more direct comparison of the published results, by the researchers at Oklahoma University, to those obtained at the University of Florida. Specimens reinforced with different diameter strands were scaled based on the 1/2" strand specimen.

---

[1] An under-reinforced section is a section that achieves yielding in the reinforcing (tension) steel prior to the crushing (compression) of the concrete at failure.

3.4 Specimen Nomenclature

The specimens were labeled with an identification code. Information such as the strand diameter and strand grade is provided by this code. In addition the series and casting bed in which the specimen was fabricated is provided.

A typical identification code would be UF "SS" - "CB" - "Db" - "GD", where "UF" identifies the research institution, the University of Florida and "SS" and "CB" refer to the series and casting bed number, respectively. Strand information is provided on the last two characters, "Db", the strand diameter expressed as a fraction, and "GD", the Grade of the strand.

A lower case character following the strand diameter character provides additional information about the strand. A "3/8i" indicates 3/8" indented strand and an "1/2s" indicates a 1/2" special strand. For example, specimen UF 8-1-3/8i-270 was casted on the eighth series (8), on the casting bed number one (1) and is reinforced with a three-eighth of an inch (3/8") Grade 270 strand with indented outer wires.

The ends of the specimens are further identified as "Cut", or "Cut End", and "Free", or "Free End". The ends closest to the point were the strand was flame-cut were identified as "Cut". The opposite end was identified as "Free". Whenever the strands were flame-cut at one end of the prestressing bed, the end of the beam, on the casting bed next to the casting bed where the actual "Cut End" occurred, closest to the actual cut was also named "Cut End". Figure 3.1 presents a schematic of the prestressing beds and the labeling of the specimen associated to the cut sequence.

Case I: Flame Cut at One End

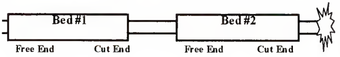

Case II: Flame Cut Between Specimens

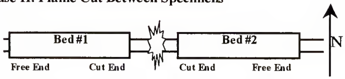

Figure 3-1 Schematic of Prestressing Beds and Cut Sequence

3.5 Specimen Description

The specimens were prismatic beams with a rectangular cross-section. Each beam was reinforced with two (2) prestressing strands in the bottom of the cross-section and two (2) mild steel deformed, reinforcing bars on the compression zone of the cross-section. Closed U-shaped stirrups were provided as shear reinforcement. All the specimens were fabricated with normal weight concrete. A schematic of the specimens cross-section is presented in Figure 3.2.

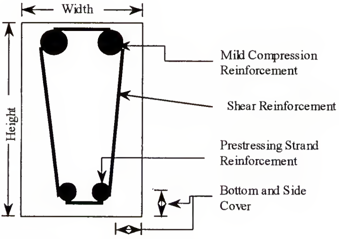
Width
Height
Mild Compression Reinforcement
Shear Reinforcement
Prestressing Strand Reinforcement
Bottom and Side Cover

Figure 3-2 Schematic of the specimen cross-section

The specimens were scaled such that cover to strand diameter ratio, stresses in the extreme concrete fibers at release and stresses in the strand at the limit state were comparable to those on the specimens used on Phases I and II of these research program. Table 3.1 summarizes the pertinent information for each specimen, such as dimensions and reinforcement schedule.

Table 3-1 Summary of Specimen Description

Series	Dimensions	Reinforcement		
		Prestress	Compression	Shear
UF 1	6" x 12" x 17'	1/2" - 270	2#6	#2 @ 6"
UF 2	6" x 12" x 17'	1/2" - 270	2#6	#2 @ 6"
UF 3	6" x 12" x 17'	1/2" - 270	2#6	#2 @ 6"
UF 4	6" x 12" x 17'	1/2" - 270	2#6	#2 @ 6"
UF 5	6" x 12" x 17'	1/2" - 270	2#6	#2 @ 6"
UF 6	6" x 12" x 17'	1/2" - 270	2#6	#2 @ 6"
UF 7	6" x 12" x 17'	1/2" - 270	2#6	#2 @ 6"
UF 8	4 ½" x 9" x 17'	3/8" - 270	2#4	#2 @
UF 9	4 ½" x 9" x 17'	3/8" - 270	2#4	#2 @
UF 10	4 ½" x 9" x 17'	3/8" - 270	2#4	#2 @
UF 11	6" x 12" x 17'	1/2"s - 270	2#6	#2 @ 6"
UF 12	6" x 10 1/2" x 17'	3/8" - 270	2#4	#2 @
UF 13	7 1/8" x 14 1/4" x 24'	6/10" - 270	2#8	#3 @ 9"
UF 14	8 1/4" x 16 5/8" x 24'	7/10" - 270	2#8	#3 @ 6"
UF 15	6" x 10 1/2" x 17'	3/8" - 270	2#4	#2 @ 9"
UF 16	6" x 12" x 17'	1/2" - 300	2#6	#2 @ 6"
UF 17	6" x 10 1/2" x 17'	3/8" - 300	2#4	#2 @ 9"
UF 18	6" x 12" x 17'	1/2"s - 290	2#6	#2 @ 9"

The prestressing strands were placed at four (4) times the strand diameter from the bottom of the cross-section. With the exception series UF12, UF15 and UF17, a side concrete cover of four-strand diameters was provided for the strands. For series UF12, UF15 and UF17 a two-inch (2") side cover was provided. The shear reinforcement on specimen UF18 was mistakenly spaced a 9" on center, instead of 6" on center.

A three-fourth of an inch (3/4") clear cover[2] was provided for the mild reinforcement. This distance is measured from the outermost surface of the stirrups to the edge of the concrete section. The stirrups were supported on the longitudinal reinforcement bars. The scaling of the shear reinforcement was done based on the confinement, or amount of steel in the longitudinal cross-section, not shear strength. Additional shear reinforcement was provided at the ends of the specimens for a distance approximately equal to twice the effective depth of the beam, or specimen. This additional reinforcement, twice of that provided along the specimen, was provided to prevent the formation of cracks along the strand and bursting cracks at transfer in the specimens.

3.6 Materials Properties

3.6.1 Prestressing Steel

The prestressing steel used conformed to the specifications put forth by the American Society of Testing and Measurements, ASTM A 416/A 416M – 94a, *Standard Specification for Steel Strand, Uncoated Seven-Wire for Prestressed Concrete.* The strands used were seven-wire strands in as-received condition. Most of the strands were classified as having surface condition type 1 or type 2, according to Sason's Surface Condition Chart [73]. Type 1 surface condition is the surface condition of a strand as it comes out of the production line, See Appendix I for Sason's Surface Condition Chart. The strand used in series UF14, 7/10" Grade 270, was slightly rusted but it was not pitted, thus it was classified as surface condition type 3, in accordance with Sason's surface condition chart.

---

[2] Clear cover is the shortest distance from the edge of the concrete section to the outermost surface of the reinforcing bar, or strand. Cover is the distance from the edge of the concrete section to the center of gravity of the outermost bar or strand.

The strands studied were 3/8" and 1/2", both Grade 270 and Grade 300, 1/2" special, Grade 270 and 290, 6/10" and 7/10", both Grade 270. Table 3.2 summarizes this information.

Table 3-2 Summary of Prestressing Strand Properties

Strand ID	Grade	Nominal Area (in^2)	Actual Area (in^2)	Load @ 1% (kip)	Breaking Load (kip)	Elongation (%)	Young's Modulus (ksi)
3/8"	270	.085	0.085	21.85	24.00	6.25	29700
	300		0.084	24.27	26.99	5.32	29400
3/8"i	270	.085	.088	22.20	24.60	4.95	28000
1/2"	270	.153	.149	40.76	43.74[3]	5.21	28800
	300		.155	42.53	46.93	5.21	29300
1/2" Special	270	.167	.163	42.00	46.06	4.47	28700
	290		.165	42.92	46.60	5.83	28900
6/10"	270	.217	.218	55.42	60.81	5.00	27700
7/10"	270	.294	.297	75.05	83.53	6.13	27900

For computation purposes, the stress-strain relationships presented in the Prestressed/Precast Concrete Institute Design Handbook were used to estimate the stresses in the strand. See Equation 3.1

---

[3] Values for the 1/2" Grade 270 strands are the average of samples from the eight (8) coils used.

$$f_{ps} = 270 - \frac{0.04}{\varepsilon_{ps} - 0.007} \qquad \text{Equation 3.1}$$

For the higher-grade strands, i.e. Grade 290 and Grade 300, the expression proposed by Prestressed/Precast Concrete Institute was modified to account for the higher guaranteed strength. The PCI expression was modified by a factor equal to the ratio of the grade of the strand to the grade of the strand for which the expression is intended. Equation 3.2 describes the stress-strain relationship for the Grade 300 strand.

$$f_{ps} = 270\left(\frac{300}{270}\right) - \frac{0.04\left(\frac{300}{270}\right)}{\varepsilon_{ps} - 0.007\left(\frac{300}{270}\right)} \qquad \text{Equation 3.2}$$

where f_{ps} is the stress in the strand, and

ε_{ps} is the strain in the strand.

3.6.2 Mild Steel

Compression reinforcement consisted of two (2) deformed reinforcing Grade 60 bars in accordance with ASTM A 615. Shear reinforcement consisted of #2 smooth wire and #3 deformed bars, bent into a closed U-shaped stirrup. The #2 smooth wire stirrups were bent at the Florida Department of Transportation, Materials Laboratory, Waldo Road, Gainesville Florida. The #3 stirrups were provided by SMI Steel, Whitehouse (Jacksonville), Florida. The reinforcement schedule is presented in Table 3.1.

3.6.3 Concrete

The concrete mix was designed to mimic current prestressed concrete industry standards. The design slump ranged between 4 1/2" and 7 1/2". The design compressive strength for the mix used is 6200 psi and 7900 psi at 7 days and 28 days, respectively. Typical values for the measured slump ranged between 3" and 4 1/2".

The concrete strength twenty-four (24) hours after casting ranged between 3500 psi and 4300 psi. The 28-day compressive strengths ranged between 7200 psi and 9000 psi. A summary of the concrete mix is presented on Table 3.3

Table 3-3 Summary of Concrete Mix

Material	Description	Unit	Quantity
Cement	AASHTO M-85 Type II	lb.	686.0
Water		lb.	287.8
Aggregate	Crushed Limestone	lb.	1720.0
	Silica Sand	lb.	912.0
Admixtures	MBVR-S Master Builders	oz.	10.0
	Fly Ash - ASTM C-618 Class F	lb.	154.0
	Pozzolith 100XR MB	oz.	45.0
	Pozzolith 440-N MB	oz.	69.0

3.7 Specimen Fabrication

The specimens for series UF1 through UF12 and series UF15 through UF18 were fabricated at the Structures Research Laboratory, Department of Civil Engineering, University of Florida, Gainesville, Florida. Series UF13 and UF14 were cast simultaneously at Gate Concrete Products, Jacksonville Florida.

For series UF1, UF2, UF8, UF9, UF10, UF13 and UF14, forms were fabricated with 3/4" plywood sheets. Two-by-six (2" x 6") whalers were provided for lateral rigidity. For series UF3 through UF7, series UF11and UF12, and series UF15 through UF18, steel forms were used. The steel forms consisted of two (2), twelve (12") inch high rolled channel sections, as sides, attached to a two-feet high wide flange section. The wide flanged section was bolted to the Laboratory's reaction floor.

Threaded rods with lock nuts spaced eighteen inches (18") apart on the plywood forms, and three feet (3') apart on the steel forms, were used to maintain the required dimensions and shape. After oiling the forms, the reinforcement cages were placed inside the forms, supported on the threaded rods. The reinforcement was secured in place with wire-ties and the prestressing strand threaded through the reinforcement cage. Extreme care was taken not to contaminate the strand with form oil or any other substance.

The prestressing strands were tensioned with a 60 Ton jack actuated by manual pump. The strands were initially stressed to 25% - 30% of the target prestress level. At this point, the alignment of the forms was verified and corrected, if needed.

The strands were stressed incrementally, one at a time, to 75% of the Guaranteed Ultimate Strength, or 202.5 ksi, 217.5 ksi and 225 ksi, for Grade 270, Grade 290 and Grade 300 strands, respectively. The sitting in the clamping devices, chucks, were measured at each increment. The force on each strand was measured with a 200 kip load cell at the jacking end and verified with elongation measurements. The sitting losses were compensated by overstressing the strand by an elongation equal to the measured sitting of the chuck in the previous stressing step. When possible, a 50 kip load cell was provided on the dead end of the prestressing bed to verify the loads on the strand.

The concrete was produced by a local ready-mix producer and delivered to the Structures Laboratory in a Mixer truck. Upon arrival to the Laboratory, a slump test in accordance with ASTM C 143 was performed. The concrete was transferred to a cone-shaped concrete bucket and maneuvered over the forms with an overhead crane. The concrete was placed in removable plywood chutes/skirts placed on the forms and vibrated with a two-inch (2") electrically driven pencil-vibrator. Anchor points were inserted about 18" from the ends of the specimens. The top surface was screeded with a piece of two-by-four lumber and finished with steel trowels. After the concrete on the surface had set, the specimens were covered with plastic sheeting. Twenty-four (24) six by twelve inches (6"x 12") standard cylinders were casted on each casting series for the monitoring of the concrete's compressive strength.

The forms were removed approximately 16 hours after casting. The specimens were wetted and excess form release agent removed from the surface of the specimen. Plexiglas plates were attached at the ends of the specimens to provide a smooth surface for the displacement measuring instrumentation probes. Displacement measuring instrumentation was clamped to the strands. Demountable Mechanical strain gauges (DEMEC) target points were glued to the surface of the specimen at the level of the strand at regular intervals.

The prestressing force was released after the concrete had achieved a compressive strength between 3500 psi and 4300 psi. The prestressing strands were annealed[4] over an 18" length of strand and flame-cut. Excess strand was cut with a radial saw, leaving 10" to 14" protruding from the face of the specimen. Table 3.4 summarizes concrete strength at transfer and at flexural testing as well as the initial, effective and limit state stresses in the strands.

---

[4] Annealing is a process of gradually heating the strand. This process reduces the magnitude of the impact when the strand breaks.

Table 3-4.a Summary of Concrete Strength and Strand Stress (Phase I)

Specimen ID	Concrete Strength (psi)		Strand Stress (ksi)		
	@ Transfer	@ Flexural Test	Initial f_{pi}	Effective f_{pe}	Limit f_{ps}
UF 1-1-1/2-270	3450	5450	203.3	182.3	266.6
UF 1-2-1/2-270	3930	5550	208.2	187.7	266.7
UF 1-3-1/2-270	4280	5660	207.5	187.6	266.7
UF 1-4-1/2-270	3450	5450	203.3	182.3	266.6
UF 1-5-1/2-270	3930	5550	208.2	187.7	266.6
UF 1-6-1/2-270	4280	5660	207.5	187.6	266.6

Table 3-4b. Summary of Concrete Strength and Strand Stress (Phase II)

Specimen ID	Concrete Strength (psi)		Strand Stress (ksi)		
	@ Transfer	@ Flexural Test	Initial f_{pi}	Effective f_{pe}	Limit f_{ps}
UF 2-1-1/2-270	3850	5800/7180[5]	202.0	181.9/180.0	266.8/267.1
UF 2-2-1/2-270	3850	5800/7180	202.0	181.9/180.0	266.8/267.1
UF 3-1-1/2-270	4360	5800/7105	201.0	183.9/180.0	266.7/267.2
UF 3-2-1/2-270	4360	5800/7105	201.0	183.9/180.0	266.7/267.2
UF 4-1-1/2-270	3840	5530	204.3	183.9	266.7
UF 4-2-1/2-270	3840	5530	204.3	183.9	266.7

---

[5] The flexural tests on the ends these specimens were performed on different dates. The cut ends were tested three days after casting. The free ends were tested a week later. The concrete strength, effective prestress and prestress at the limit state are presented at the time the ends were tested in the following format: Cut End/Free End.

Specimen ID	Concrete Strength (psi)		Strand Stress (ksi)		
	@ Transfer	@ Flexural Test	Initial f_{pi}	Effective f_{pe}	Limit f_{ps}
UF 5-1-1/2-270	3470	5100	204.3	183.2	266.5
UF 5-2-1/2-270	3470	5100	204.3	183.2	266.5
UF 6-1-1/2-270	3930	5800	203.4	183.4	266.8
UF 6-2-1/2-270	3930	5800	203.4	183.4	266.8
UF 7-1-1/2-270	3780	5075	208.5	187.6	266.6
UF 7-2-1/2-270	3780	5075	208.5	187.6	266.6

Table 3-5c. Summary of Concrete Strength and Strand Stress (Phase III)

Specimen ID	Concrete Strength (psi)		Strand Stress (ksi)		
	@ Transfer	@ Flexural Test	Initial f_{pi}	Effective f_{pe}	Limit f_{ps}
UF 8-1-3/8i-270	3865	8100	198.8	174.1	266.6
UF 8-2-1/2-270	3865	8100	198.8	174.1	266.6
UF 9-1-3/8i-270	4110	8185	201.2	178.0	266.7
UF 9-2-3/8-270	4110	8185	201.2	178.0	266.7
UF 10-1-3/8i-270	3900	8085	201.8	178.6	266.7
UF 10-2-3/8-270	3900	8085	201.8	178.6	266.7
UF 11-1-1/2s-270	3755	8100	205.4	179.0	267.0
UF 11-2-1/2s-270	3755	8100	205.4	179.0	267.0
UF 12-1-3/8i-270	4075	7020	201.8	186.3	267.5
UF 12-2-3/8-270	4075	7020	201.8	186.3	267.5
UF 13-1-6/10-270	3750	9380	199.3	176.5	267.9
UF 13-2-6/10-270	3750	9380	199.3	176.5	267.9
UF 14-1-7/10-270	3750	9550	195.1	172.6	267.8
UF 14-2-7/10-270	3750	9550	195.1	172.6	267.8

Table 3-6d. Summary of Concrete Strength and Strand Stress (Phase IV)

Specimen ID	Concrete Strength (psi)		Strand Stress (ksi)		
	@ Transfer	@ Flexural Test	Initial f_{pi}	Effective f_{pe}	Limit f_{ps}
UF 15-1-3/8-270	3550	8100	202.3	186.6	267.8
UF 15-2-3/8-270	3550	8680	202.3	186.0	267.9
UF 16-1-1/2-300	4100	6850	224.8	197.6	296.1
UF 16-2-1/2-300	4100	6630	224.8	197.7	296.1
UF 17-1-3/8-300	3650	5350	225.3	207.4	296.6
UF 17-2-3/8-300	3650	5350	225.3	207.4	296.6
UF 18-1-1/2s-	4020	6175	218.4	189.1	285.7
UF 18-2-1/2s-	4020	6175	218.4	189.1	285.7

3.8 Experimental Procedures and Instrumentation

3.8.1 Concrete Surface Strain Measurements and Determination of Transfer Length

The transfer lengths were determined from deformations measured with a digital Whittemore-Type Demountable Mechanical (DEMEC) Strain Gage, precise to 0.00005", along each beam at the strand's level. DEMEC target points, stainless steel discs ⅜" in diameter with a hole milled in the center, were attached to the specimen's sides at the level of the strand along the specimen.

The target points were, typically, spaced three-inches (3") on center, with the first target point three-inches (3") from the end of the specimen. The gage length, the distance over which the deformation is being measured, was six-inches (6"). For series UF8 through UF10, and UF12 the target points were spaced two-inches (2") on center with a gage length of four-inches (4"). For series UF14, the target points were attached at 4" on center with the first target point 2" from the end, with a gage length of eight-inches (8").

The concrete surface strain were computed from the deformation measurements and corrected for the strain induced by the weight of the specimen acting on the cambered specimen. Concrete surface strains were plotted and the transfer length estimated using the slope-intercept method with the intercept at 95% of the maximum average strain and the 95% Average Maximum Strain Method, as described in Reference [43] and Reference [70]. A brief description of these two methods is presented in Chapter 4. Figure 3.3 shows a schematic of the instrumentation setup.

3.8.2 End Slip Measurements and Estimate of Transfer Length

End slips were measured with Linear Voltage Differential Transducers, LVDTs, and dial gauges accurate to 0.001". The instruments were mounted on an aluminum block clamped to the to the protruding portion of the strands. A plexiglass plate, at the end face of each specimen, provided a smooth surface for the instruments probes to rest against. Figure 3.3 shows an schematic of the instrumentation setup.

Using Equation 2.18, a reliable, yet inexpensive estimate of the transfer length is obtained from these measurements. The transfer lengths estimated by the procedures described on Chapter 4 were compared to this estimate of the transfer length.

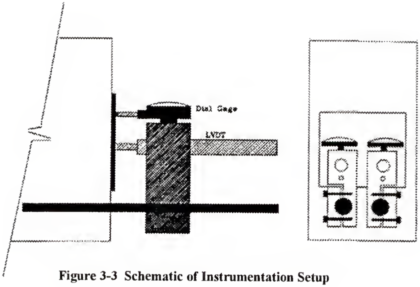

Figure 3-3 Schematic of Instrumentation Setup

3.8.3 Internal Concrete Strains

The free ends of each specimen of series UF12 through UF14 was instrumented with electronic strain gages. The strain gages were attached to Fiber Reinforced Polymers (FRP) reinforcing bars. Slots were milled to mid-depth of each bar. Five (5) Vishay Measurements Group, Inc. CEA-06-500UW-120 strain gages were attached to each bar. The strain gages were attached at 10”, 20” 50”, 60” and 70” from one end of the bar. The strain gages were waterproofed and coated. Lead wires were run through the slots and the bars sealed with silicone.

The physical-mechanical properties of the FRP bars are presented on Table 3.7. Strains were recorded with a Vishay Micro-Measurements Strain Indicator, both at transfer and during flexural test.

Table 3.7 Summary of the Physical-Mechanical Properties of the FRP Bars

Bar Size	Cross Sectional Area (in^2)	Nominal Diameter (in)	Tensile Strength (ksi)	Modulus of Elasticity ($*10^3$ ksi)
#4	0.2245	0.50"	100	5.92

3.8.4 Flexural Test Instrumentation

The specimens were tested in flexure in a two-point load configuration using a manually activated 60-Ton jack. The loads were measured with a 200 kip load cell. The vertical displacements were measured by two LVDT's placed under the resultant load. Vertical displacement, end-slips and load were plotted as the test progressed and recorded on a personal computer through a Data Acquisition System.

The two-point-loads loading configuration was intended to produce a constant moment region, neglecting the effect of the weight of the specimen. For the flexural tests of Phase I and most of the specimens of Phase II, the span was fixed at one-hundred-forty-four-inches (144"), effectively negating the constant moment region for the specimens tested at short embedment length. The remaining specimens on Phase II were tested symmetrically or with one-point-load configuration in an attempt to force the critical section to concur with the embedment length. The specimens of Phase III and Phase IV were tested symmetrically and the span was changed accordingly. Figure 3.4 depicts a schematic of the Flexural Bond Test setup.

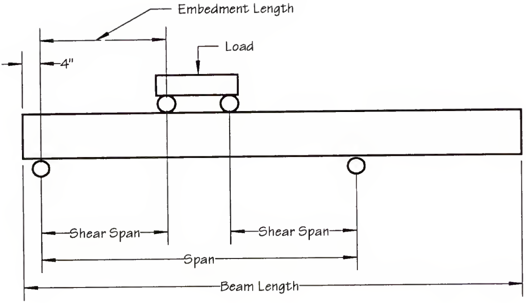

Figure 3-4 Schematic of Flexural Bond Test Setup

End-slips were measured at transfer and during the flexural test with dial gages and LVDT's, each precise to 0.001". The instruments were attached to aluminum clamping devices secured to the strand. A Plexiglas plate was attached to the end of the specimen to provide a flat smooth surface for the instruments.

3.8.5 Summary of the Experimental Procedure

The experimental program of each series was comprised of three (3) parts: specimen fabrication (Steps 1 through 6), detensioning and transfer length measurement (Steps 7 through 11) and flexural test (Steps 12 through 18). Following is an outline of this experimental program.

1. Assemble forms and reinforcement cages.
2. Thread strands through the reinforcement cage. Tension to 25% - 30% of desired initial stress level, 50 ksi.
3. Level and align forms.

4. Tension strand to within 500 psi of 75% of f_{pu}.
5. Perform slump test. Cast specimens and companion cylinders.
6. Cover with plastic sheeting. Allow concrete to set.
7. Remove forms. Wash-off excess oil from sides of the specimens.
8. Attach instrumentation. Glue DEMEC target points along the specimen at strand level.
9. Cure concrete until concrete compressive strength reaches predetermined concrete strength window, 3500 psi to 4300 psi.
10. Record initial readings of glued DEMEC target points.
11. Flame-cut strand. Record end-slip and final DEMEC target point's readings.
12. Allow concrete to cure. Monitor concrete strength. Compute transfer length. Estimate loading configuration.
13. Perform flexural test once the concrete strength has reached 5000 psi or the specimen has cured for 28 days.
14. Center beam on the loading frame and set beams on simple supports. Set spreader beam on simple support twenty-four-inches (24") apart on top of the specimen. Mount jack and swivel base on spreader beam. Install instrumentation.
15. Manually actuate the hydraulic jack until a load of fifty percent (50%) of the estimated breaking load or 75% of the cracking load, the smaller of the two, is achieved. Continue loading in five percent (5%) increments until cracking. Mark cracks as they form on the sides of the specimen.

16. Load until failure occurs. Record maximum load and displacement. Record whether slip occurred or not. Record crack width.
17. Classify failure as flexural, bond, bond/shear, shear or flexural with slip.

CHAPTER 4

EXPERIMENTAL RESULTS

4.1 Introduction

As previously stated, the main objective of this research program was to study the effect of prestressing strand size on its bond performance. To that end, an extensive research program was carried out to measure the transfer length and the flexural bond behavior of a variety of strand diameters. The results of this extensive research program are presented in this chapter.

Supporting and intermediate data are presented in the Appendices. The Concrete Surface Strain Profiles are presented in Appendix I. Load Deflection curves of the Flexural Bond Test are presented in Appendix II. A sample of the MathCAD template used for the computation of prestress losses and the sections nominal capacity is presented in Appendix III.

4.2 Experimental Program

The experimental program consisted of four phases, each consisting of two parts, measurement of transfer length and flexural bond test. In the first two phases, Phase I and Phase II, the strands used were 1/2" in diameter Grade 270 - Low Relaxation. Since this strand, 1/2" Grade 270 – Low Relaxation, is the current industry standard, these first two phases served to set a benchmark to which the following phases were compared.

These phases also allowed the research team to acquire a thorough understanding of the experimental procedures and the nature of bond research.

The effect of strand size, or diameter, was investigated in Phase III. The strand diameters studied were 3/8", 1/2" special, 6/10" and 7/10". Phase IV dealt with the effect of initial prestress level on transfer length and bond performance in general. The following strands were investigated: 3/8" Grade 270 and Grade 300, 1/2" Grade 300 and 1/2" special Grade 290. All the strands were Low Relaxation strands.

4.3 Transfer Length

4.3.1 Concrete Surface Strains

Attaching any instrumentation, or measuring device, to the strand destroys the bond mechanism at the location where the instrumentation is being attached and a certain influence zone, not yet quantified, in the vicinity of that location. In order to avoid, or minimize, the interference of the instrumentation with the strands natural behavior of bond, transfer lengths were measured by means of concrete surface strain measurements. Parameters such as initial prestress, concrete compressive strength and strand draw-in, or end-slip, were also measured to attempt a quantification of their effect on the transfer length of the strands.

Concrete surface strains were measured using Detachable Mechanical (DEMEC) strain gauges. Target points, stainless steel discs with a hole milled in their center, were attached to the concrete with super glue gel. The instrument and target points are presented on Figure 4-1.

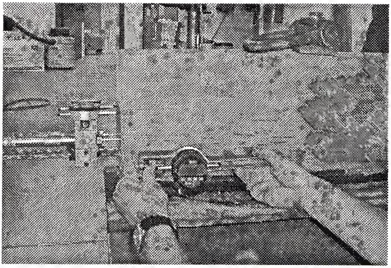

Figure 4-1 Picture of the Demountable Mechanical strain gauge and target points.

The distance between target points were measured before and after the release of the prestressing strands. The average strain in the surface of the concrete between target points was computed using Equation 4.1.

$$\text{Average Concrete Strain} = \frac{\text{Spacing}_{\text{Before Release}} - \text{Spacing}_{\text{After Release}}}{\text{Spacing}_{\text{Before Release}}} \qquad \textbf{Equation 4.1}$$

The average concrete strains were corrected for the strains due to the self-weight of the specimens. Such correction was deemed necessary because the distance between the DEMEC target points, measured before the prestressing force was transferred ($\text{Spacing}_{\text{Before Release}}$), was measured on a specimen fully supported, that is, laying flat. After transfer the specimen was no longer fully supported. Due to the moments induced by the prestress force, the specimen cambered, i.e. bowed up. Due to this camber, the specimen was effectively on simple supports. Thus, the measured distance between

DEMEC target points after transfer of the prestressing force (Spacing $_{\text{After Release}}$), not only included the effect of the prestressing force being transferred but that of the specimens self-weight acting on simple supports as well.

The strains induced by the self-weight were computed and added to the measured concrete surface strains[1]. The computed strains due to self-weight were, typically, an order of magnitude smaller than the measured concrete surface strains.

4.3.2 Constructing the Strain Profile

The strain profiles were constructed using the moving average of three (3) consecutive concrete surface strains. This smoothing technique is similar to the procedure described in Reference 41 and Reference 70. Equation 4.2 summarizes this technique.

$$\text{Strain}_i = \frac{\text{Strain}_{i-1} + \text{Strain}_i + \text{Strain}_{i+1}}{3} \qquad \textbf{Equation 4.2}$$

The measured concrete surface strains are the average strain over the gage length, that is, the distance over which the deformations were measured. The strains, measured and "smoothed", are assumed to occur at the mid-point of this distance. The "smoothed" concrete strains are plotted versus their assigned location along the length of the specimen. The strain profile for specimen UF 1-3-1/2-270 is presented on Figure 4-2.

---

[1] The net result of the operation was the addition of the strain. The actual operation consisted of the subtraction of a tensile (+) strain from a compressive (-) strain.

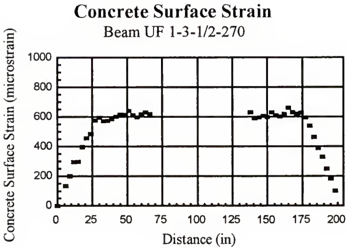

Figure 4-2 Strain Profile for Specimen UF 1-3-1/2-270

4.3.3 Estimating the Transfer Length from Strain Profiles

Transfer lengths were estimated following one of three procedures. The first two procedures, the 95% Average Maximum Strain Method, as described by Reference 41 and Reference 70, and the Slope Intercept Method, are based on the evaluation of the concrete surface strain profiles. The strain profiles, as mentioned above, are constructed by plotting the "smoothed " concrete surface strains versus their location along the specimen. The following sections describe each method.

The third estimate of the transfer length being reported is computed from the draw-in, or end slip, measurement, using Equation 4.6. Reporting the end-slip based transfer length estimate is deemed important because end-slip measurements have been proposed as an indicator of bond performance for the prestressed concrete industry [45]. The correlation between bond and end-slip measurements will be further discussed in Chapter 5.

4.3.3.1 95% Average Maximum Strain Method.

Developed at the University of Texas [70], and recently endorsed by the Federal Highway Administration as the preferred method to estimate transfer length, this method is considered to yield an upper-bound value of the transfer length [41]. The procedure is as follow: The strain profile, a chart of the "smoothed" concrete surface strain versus its location along the specimen, is constructed. The numerical average of the strains for the data points contained within the plateau region is computed. As mentioned before, this plateau region is the region where the prestress force is fully effective following the transfer zone. The transfer length is determined by the intersection of the 95% Average Maximum Strain with the strain profile. To be more precise, the transfer length was determined by linear interpolation of the strain that describes the plateau region, the 95% Average Maximum Strain, between the two points on the strain profile that bound this value.

Reference 41 and Reference 70 describe this procedure in a graphical manner as:

> " 1) Plot the "smoothed' strain profile.
>
> 2) Determine the "Average Maximum Strain" for the specimen by computing the numerical average of all the strains contained within the strain plateau of the fully effective prestress force.
>
> 3) Take 95% of the "Average Maximum Strain" and construct a line corresponding to this value.
>
> 4) Transfer length is determined by the intersection of the 95% line with the "smoothed" strain profile. "
>
> Source: Reference 70

Proponents of the 95% Average Maximum Strain Method have mentioned as one of the advantages of this method, that it removes "arbitrary interpretations" of the data from the estimation of the transfer length. Dale Buckner showed, through Finite Element

Modeling, that the transfer length was best estimated using the 95% Average Maximum Strain method. Explaining that this method appeared to compensate for the shear lag between the stress in the strand and those measured at the concrete surface [13,14].

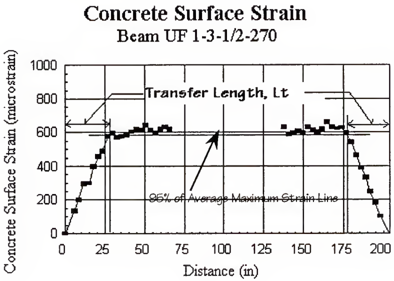

Figure 4-3 Graphical Representation of the 95% Average Maximum Strain method

4.3.3.2 The Slope Intercept Method.

The slope intercept method is based on the bi-linear idealization of the strain profile. This idealization assumes that the strain profile consist of a linearly increasing portion followed by a plateau region. The linearly increasing portion is described by the equation of a straight-line, $y = mx + b$. A horizontal line describes the plateau region. The transfer length is determined as the intercept of these two lines.

The procedure is as follows: The "smoothed' strain profile is plotted. The 95% of the numerical average of the plateau region is computed. The slope, m, of the linearly increasing portion of the strain profile is obtained from a linear regression, with the intercept set at the origin ($b = 0$), performed on the points within the linearly increasing portion of the strain profile using an electronic spreadsheet. Transfer length is determined as the intercept of the line described by this linear regression and horizontal line describing the 95% of the average of the maximum strains. Equation 4.3 summarizes this procedure.

$$L_t = \frac{95\%\ \text{Average Maximum Strain}}{\text{Slope, m}} \qquad \textbf{Equation 4.3}$$

Recently, researchers have suggested that the development length is a linearly proportional function of the transfer length [9,72]. Investigating the validity of this theory required a lower bound value of the transfer length. Since the transfer length estimates obtained using the Slope-Intercept Method with 95% Plateau could be considered a lower bound value of the true transfer length, these estimates were used in the determination of the embedment length used during the flexural bond test.

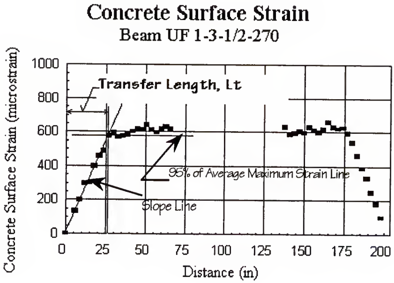

Figure 4-4 Graphical Representation of the Slope Intercept Method

4.3.4 End-slip Based Transfer Length Estimate

The end-slip, or draw-in, is the amount the strand slips into the concrete, at the ends of the specimen when the prestressing force is transferred. Slip theory can be used to relate transfer length, L_t to the end slip, L_{es}. It assumes that there is relative movement between the strand and the concrete, slippage, throughout the transfer region. The area outside the strain profile and bounded by the vertical axis and the maximum strain is the end slip. Equation 4.4 describes this area.

$$L_{es} = \frac{1}{\lambda} * \varepsilon_{pi} * L_t \qquad \textbf{Equation 4.4}$$

Where λ is a constant that depends on the function that describes the change in strains along the specimen, i.e. the shape of the strain profile. The constant λ can take a value of 2, 3 or 4.6 depending on the assumed shape of the strain profile, linear, parabolic or elliptic, respectively. European researchers have found the value of λ to be approximately 2.6 [20].

Equation 4.4 is solved for the transfer length, L_t, and an expression for transfer length as a function of the end-slip is obtained, Equation 4.7. Currently, two slip theory based transfer length expressions are generally accepted. In the United States, generally, a linear variation of the strains is assumed, Equation 4.8. The International Federation of Concrete, FIP, expression assumes a parabolic strain profile, Equation 4.9.

$$\mathrm{Lt} = \lambda * \frac{\mathrm{Les}}{\varepsilon \mathrm{pi}} \qquad \textbf{Equation 4.5}$$

$$Lt = 2 * \frac{Les}{\varepsilon pi}$$ **Equation 4.6**

$$Lt = 3 * \frac{Les}{\varepsilon pi}$$ **Equation 4.9**

4.3.5 Measured Transfer Length

The measured transfer lengths are presented on Table 4.1a through Table 4.1d. Each table presents the measure transfer length of a particular phase on the research program. All transfer lengths were estimated following the procedures described earlier in this section. The values for transfer length obtained following each of these three methods are presented.

4.3.5.1 Phase I - series UF1

The measured transfer lengths obtained on series UF1 are presented on Table 4-1a. Six specimens were cast on a single concrete placement. All the specimens were reinforced with strand from a single coil (strand package). The strands transfer length ranged between 19.2" and 31.8", when estimated using the Slope-Intercept Method, with a 26.9" mean and a 10.7% coefficient of variation[2]. The average of the transfer lengths estimated following the 95% Average Maximum Strain method and based on end-slip measurements were 28.8" and 22.1", respectively, with 11.4% and 9.9% coefficients of variation.

---

[2] Coefficient of Variation is the ratio of the Standard Deviation to the Mean expressed as a decimal. For clarity, the COV is presented as a percentage.

Table 4-1a Measured Transfer Length (Phase I)

Specimen ID	End	Transfer Length (in.)			
		95% SIM[3]	End Slip		95% AMS[4]
UF 1-1-1/2-270	Cut End	28.3	0.090	25.3	30.3
	Free End	27.7	0.084	23.6	33.1
UF 1-2-1/2-270	Cut End	26.2	0.081	22.3	28.3
	Free End	19.2	0.086	23.4	20.2
UF 1-3-1/2-270	Cut End	27.0	0.070	19.3	26.9
	Free End	26.9	0.066	18.2	29.5
UF 1-4-1/2-270	Cut End	31.8	---	---	31.4
	Free End	28.0	0.081	22.8	31.2
UF 1-5-1/2-270	Cut End	26.0	---	---	30.1
	Free End	26.0	0.077	21.2	30.1
UF 1-6-1/2-270	Cut End	26.1	---	---	26.4
	Free End	27.9	0.082	22.6	28.5

4.3.5.2 Phase II - series UF2 through UF7

Table 4-1b presents the transfer lengths measured in series UF2 through UF7. Six two-specimen series were casted. Each specimen of each series used a different strand. Florida Wire and Cable, Inc. provided all the strands. However each strand was produced at a different production plant, used different lubricating agents during production or followed a different cleaning procedure to remove lubricating agents. Due to blind sampling some of the strands within a series were produced following similar production procedures at different production lines, as is the case of series UF6. The strands used on series UF6 were re-tested on series UF7. The measured transfer lengths, using the slope intercept method, were in the 14.2" to 27.9" range. The average was 22.4" with a coefficient of variation of 16.6%. The end-slip based estimate of the transfer length averaged 17.2" with a 26% coefficient of variation. An average transfer length of 24.2" with a coefficient of variation of 19.4% was obtained when the 95% Average Maximum Strain method was followed.

---

[3] SIM stands for Slope Intercept Method

[4] AMS stands for Average Maximum Strain method

Table 4-1b Measured Transfer Length (Phase II)

Specimen ID	End	Transfer Length (in.)			
		95% SIM	End Slip		95% AMS
UF 2-1-1/2-270	Cut End	23.2	---	---	24.1
	Free End	21.4	0.068	19.3	23.7
UF 2-2-1/2-270	Cut End	17.3	0.033	9.34	---
	Free End	16.5	0.053	15.0	---
UF 3-1-1/2-270	Cut End	14.2	---	---	13.8
	Free End	17.6	0.042	11.8	18.0
UF 3-2-1/2-270	Cut End	19.0	---	---	17.1
	Free End	21.5	0.056	16.0	24.0
UF 4-1-1/2-270	Cut End	19.3	0.050	14.0	20.3
	Free End	18.6	0.082	23.1	18.2
UF 4-2-1/2-270	Cut End	27.9	---	---	31.5
	Free End	25.9	0.071	19.8	32.5
UF 5-1-1/2-270	Cut End	26.9	0.046	12.9	26.2
	Free End	24.1	0.089	24.9	27.9
UF 5-2-1/2-270	Cut End	21.8	0.049	13.9	26.8
	Free End	23.6	0.046	12.7	20.7
UF 6-1-1/2-270	Cut End	23.6	---	---	26.3
	Free End	23.9	0.065	18.1	26.0
UF 6-2-1/2-270	Cut End	23.2	0.074	20.8	29.0
	Free End	27.0	0.068	19.2	28.3
UF 7-1-1/2-270	Cut End	24.9	---	---	24.1
	Free End	26.5	0.068	18.7	27.2
UF 7-2-1/2-270	Cut End	25.9	---	---	26.2
	Free End	22.9	2.085	23.2	25.5

4.3.5.3 Phase III - series UF8 through UF14

Table 4-1c presents the transfer lengths measured on Phase III, series UF8 through UF14. Seven (7) two-specimen series were casted. Specimens on series UF8, UF9, UF10 and UF12 were reinforced with 3/8" diameter strand. The strand in all four (4) series came from the same batch, but each specimen within a series contained a different strand. The strand used on the specimens casted on bed #1 had indentations on the outer wires. The specimens on bed #2 were reinforced with smooth wire strands. Specimens within series UF10, UF13 and UF14 were identical. Series UF10 was reinforced with 1/2" “special” diameter strand, UF13 with 6/10" diameter strand and UF14 with 7/10" diameter strand. All the strands used in this phase were Grade 270 Low Relaxation strands.

The 3/8" Indented Wire Strand. The 3/8" Indented Wire Strand had an average transfer length of 14.9" with a coefficient of variation of 25.5%, when the transfer length is estimated following the slope intercept method and the transfer lengths measured on series UF12 are included. The transfer length measured on the Free End of specimen UF 12-1-3/8-270 was almost twice as long as those measured on series UF8, UF9 and UF10. The measured transfer length on the Free End of specimen UF12-1-3/8-270 was 23.9" versus approximately 13" for that measured on series UF8, UF9 and UF10.

The specimens of series UF12 were slightly different from those on series UF8, UF9 and UF10 in that they had an instrumented FRP reinforcement bars embedded on the Free End. The instrumented rod is believed to have affected the bond behavior on that end. The transfer length measured by the strain gauges on the FRP bar was 13.3", similar in magnitude to those measured on series UF8, UF9 and UF10. These specimens had a larger cross section than those on UF8, UF9 and UF10, see Table 3.1.

The measured transfer length averaged 12.7" with a 7.2% coefficient of variation, when the value of the transfer length measured on the Free End of specimen UF12-1-3/8-270 is not included. The average transfer length is 12.6" with a 7.7% coefficient of variation, if transfer lengths measured on specimen UF12-1-3/8-270 are not included, which suggest that apparently the specimen cross sectional area does not affect the transfer length. The estimated transfer lengths were in the 11.8" to 14.2" range.

Neglecting series UF12, the transfer lengths estimated from end-slip measurements averaged 16.7" with a 26.8% coefficient of variation. Similarly, following the 95% AMS method, the estimated transfer length averaged 13.4" with a coefficient of variation of 7.8%. If transfer lengths measured on series UF12 were included the average is 15.5" and the coefficient of variation 33.5%.

The 3/8" Smooth Wire Strand The 3/8" Smooth Wire Strand had an average transfer length of 18.2" with a coefficient of variation of 22.3%. These transfer lengths, estimated with the Slope-Intercept method, were in the 15" to 24" range. The behavior observed in specimen UF12-1-3/8-270 was also observed in specimen UF12-2-3/8-270, thus transfer lengths from this specimen are omitted from this discussion. The end-slip based transfer length average 18.4" with a 7.8 coefficient of variation. Transfer lengths estimated using the 95% AMS method averaged 17.9 with a coefficient of variation of 22.5%.

The 1/2" "special" Strand The 1/2" "special" Strand had an average transfer length of 26.0" with a coefficient of variation of 23.7%. Transfer length estimated from end-slip measurements averaged 25.5" with a coefficient of variation of 27.6%, while those obtained following the 95% AMS method averaged 27.5" with a 13.8% coefficient of variation.

The 6/10" Strand The 6/10" Strand measured transfer lengths averaged 23.3" with a 13.5% coefficient of variation. The transfer length estimated using strains measured by strain gauges on FRP reinforcing bars on the Free End averaged 23.85" with a coefficient of variation of 23.4%. End-slip based transfer length estimates averaged 19.25" with 21.4% coefficient of variation. 95% AMS method transfer lengths averaged 23.2" and had a coefficient of variation of 8.5%.

The 7/10" Strand The 7/10" Strand had a transfer length averaging 21.15" and a 24% coefficient of variation. The transfer length estimated from strain gauges on the Free End of specimen UF14-2-7/10-270 was 18". Transfer lengths computed from end-slip measurements averaged 15.5 with coefficient of variation of 12.3%. Using the 95% AMS approach the transfer length averaged 23.7" with a 15.3% coefficient of variation.

Transfer lengths for the strains measured with electric resistance strain gauges are not being reported for the 95% Average Maximum Strain method because the strain gauges were attached to the FRP reinforcing bar at 10", 20", 50", 60" and 70". The setup of the strain gauges on the FRP bar allowed for the strain gauges to be used on the transfer length and flexural bond test portions of these phases, but limited the order of the strain variation on the transfer length to a straight line. The setup was sufficient for the Slope-Intercept method since it provides the strain variation in the transfer zone and the plateau region where the prestressing force is effective. Trying to apply the 95% AMS method to the data would yield un-realistically long transfer lengths, since there is no data point in the vicinity of the “true” transfer length. The value of the transfer length obtained from the strain gauges on specimen UF14-1-7/10-270, 43”, was considered for similar reasons.

Table 4-1c Measured Transfer Length (Phase III)

Specimen ID	End	Transfer Length (in.)			
		95% SIM	End Slip		95% AMS
UF 8-1-3/8i-270	Cut End	---	---	---	---
	Free End	12.9	---	---	13.1
UF 8-2-1/2-270	Cut End	21.0	.064	18.4	20.6
	Free End	16.0	0.057	16.5	15.5
UF 9-1-3/8i-270	Cut End	12.2	---	---	13.5
	Free End	12.0	0.048	13.5	11.8
UF 9-2-3/8-270	Cut End	---	---	---	---
	Free End	15.2	0.067	19.1	14.3
UF 10-1-3/8i-270	Cut End	11.8	---	---	14.1
	Free End	14.2	0.070	19.8	14.5
UF 10-2-3/8-270	Cut End	24.0	---	---	23.7
	Free End	15.0	0.070	19.7	15.5
UF 11-1-1/2s-270	Cut End	---	0.105	29.3	---
	Free End	21.6	0.111	30.9	24.8
UF 11-2-1/2s-270	Cut End	---	0.055	15.3	---
	Free End	30.3	0.095	26.6	30.2
UF 12-1-3/8i-270	Cut End	---	0.062	17.7	---
	Free End	18.5	0.064	18.1	20.5
	Stran Gauge[5]	13.3	N/A	N/A	21.4
UF 12-2-3/8-270	Cut End	---	---	---	---
	Free End	14.6	0.049	13.8	16.8
	Strain Gauge	11.3	N/A	N/A	---
UF 13-1-6/10-270	Cut End	32.6	0.064	18.3	30.8

---

[5] No value for the 95% Average Maximum Strain method is presented because the spacing of the electric resistance strain gages did not provide for proper definition of the strain profile.

Specimen ID	End	Transfer Length (in.)			
		95% SIM	End Slip		95% AMS
	Free End	20.1	0.055	15.7	21.1
	Strain Gauge	27.8	N/A	N/A	---
UF 13-2-6/10-270	Cut End	26.4	0.063	17.9	25.0
	Free End	23.6	0.063	18.2	23.5
	Strain Gauge	19.9	N/A	N/A	---
UF 14-1-7/10-270	Cut End	---	0.086	25.2	---
	Free End	28.7	0.047	13.9	27.8
	Strain Gauge	43.0	N/A	N/A	---
UF 14-2-7/10-270	Cut End	19.6	0.051	14.9	22.2
	Free End	18.3	0.060	17.6	21.0
	Strain Gauge	18.0	N/A	N/A	---

4.3.5.4 Phase IV - series UF15 through UF18

Four (4) two-specimen series were cast. Each specimen studied a specific strand diameter-Grade combination. Series UF15 studied a 3/8” Grade 270 strand. Series UF16 and UF17 investigated Grade 300 strands, 1/2" and 3/8” respectively. A Grade 290, 1/2" “special” strand was investigated on series UF18. All the strands were Low Relaxation and provided by Florida Wire and Cable, Inc.

The 3/8” Grade 270 Strand The 3/8” Grade 270 Strand had an average transfer length, estimated with the slope-intercept method, of 13.9” with a 17.3% coefficient of variation. These transfer lengths ranged between 12.2” and 15.6”. End Slip based transfer estimates averaged 16.8” with a 5.1% coefficient of variation. Transfer lengths averaged 16.2” when the 95% AMS method was used to analyze the strain profile. The corresponding coefficient of variation was 17.9%.

The 1/2" Grade 300 Strand The 1/2" Grade 300 Strand had transfer lengths averaging 33.1” with a 4.1% coefficient of variation. The transfer lengths were in a 31.9” to 34.6" range. Average transfer lengths corresponding to the end-slip and 95% AMS method estimates were 30.1" and 34.0", respectively. Their respective coefficients of variation were 14.0% and 4.0%.

The 3/8" Grade 300 Strand The 3/8" Grade 300 Strand had transfer lengths in the 14.5" to 21.1" range. Their average was 19.0" with a coefficient of variation of 15.8%. The average of the transfer lengths computed from end-slip measurements was 21.8" with a coefficient of variation of 13.6%. An average of 18.7" with a coefficient of variation of 20.4% was obtained when the 95% AMS method was used to estimate the transfer length.

The 1/2" "special" Grade 290 Strand The 1/2" "special" Grade 290 Strand had measured transfer lengths, averaging 28.3" with a 7.6% coefficient of variation, in the 25.4" to 30.2" range. End-slip based estimates of the transfer length averaged 27.9" with a corresponding coefficient of variation of 13.2%. Transfer lengths estimated following the 95% AMS methodology averaged 31.6" and had a coefficient of variation of 18.3%. If the transfer length value measured on the cut end of specimen UF18-1-1/2s-290 is neglected, then the average transfer length estimated per 95% AMS is 28.8 with a coefficient of variation of 6.1%.

Table 4-1d Measured Transfer Length (Phase IV)

Specimen ID	End	Transfer Length (in.)			
		95% SIM	End Slip		95% AMS
UF 15-1-3/8-270	Cut End	---	---	---	---
	Free End	---	0.057	16.2	---
UF 15-2-3/8-270	Cut End	15.6	---	---	18.2
	Free End	12.2	0.062	17.4	14.1

Specimen ID	End	Transfer Length (in.)			
		95% SIM	End Slip		95% AMS
UF 16-1-1/2-300	Cut End	---	---	---	---
	Free End	32.9	0.101	25.7	34.7
UF 16-2-1/2-300	Cut End	31.9	0.112	30.5	32.4
	Free End	34.6	0.134	34.1	34.8
UF 17-1-3/8-300	Cut End	20.6	---	---	19.0
	Free End	14.5	0.078	19.7	13.7
UF 17-2-3/8-300	Cut End	19.7	---	---	19.1
	Free End	21.1	0.094	23.9	23.0
UF 18-1-1/2s-290	Cut End	27.8	---	---	40.0
	Free End	29.6	0.096	25.3	28.6
UF 18-2-1/2s-290	Cut End	30.2	---	---	30.7
	Free End	25.4	0.116	30.5	27.2

4.3.6 Summary of Transfer Length Results

Table 4-2 presents a summary of the transfer length results. The coefficient of variation [COV], computed as the sample standard deviation divided by the mean, is also presented on Table 4-2. The range of values presented for each strand is based on the transfer lengths estimated using the slope-intercept method.

Table 4-2 Summary of transfer Length Results

Strand	Average transfer length [COV] (in.)			Range (in)
	Slope Intercept	95% AMS	End Slip	
3/8" Grade 270 Phase III	17.6 (22.1%)	17.7 (20.5%)	17.5 (13.8%)	15.0 – 23.7
3/8" Grade 270 Phase IV	13.9 (17.3%)	16.2 (17.9%)	16.8 (5.2%)	12.2 – 15.6

Strand	Average transfer length [COV] (in.)			Range (in)
	Slope Intercept	95% AMS	End Slip	
3/8” smooth Grade 270 ALL	16.1 (24.9%)	17.6 (18.3%)	16.9 (13.5%)	12.2 – 23.7
3/8” Grade 300	19.0 (16.0%)	18.7 (20.4%)	21.8 (13.5%)	14.5 – 21.1
3/8” indented Grade 270	13.7 (7.2%)	13.4 (7.8%)	16.7 (26.8%)	11.8 – 14.2
1/2" Grade 270 Phase I	26.8 (10.7%)	28.8 (11.5%)	22.1 (9.9%)	19.2 – 31.8
1/2" Grade 270 Phase II	22.6 (18.8%)	24.4 (19.3%)	17.2 (25.9%)	14.2 – 27.9
1/2" Grade 270 Phase I & II	24.0 (20.6%)	25.4 (21.7%)	18.9 (21.2%)	14.2 – 31.8
1/2" Grade 300	33.1 (4.1%)	34.0 (4.0%)	30.1 (14.0%)	31.9 – 34.6
1/2" special Grade 270	26.0 (23.7%)	27.5 (13.8%)	25.5 (27.6%)	21.6 – 30.3
1/2" special Grade 290	28.3 (7.6%)	31.6 (6.1%)	27.9 (13.2%)	31.9 – 34.6
6/10” Grade 270	25.7 (13.5%)	25.1 (8.5%)	17.5 (21.4%)	20.1- 27.8
7/10” Grade 270	22.2 (24.0%)	23.7 (15.3%)	17.9 (12.3%)	18.3 – 28.7

4.4 Flexural Bond Test

Flexural tests were performed on each end of the specimens to determine the development length of the strands. The development length is the distance, closest to the end of the specimen, where a section's flexural capacity can be achieved.

Experimentally, the development length is determined by varying the embedment length on a series of flexural bond tests. In a trial and error process, the development length is said to exist in a range bounded by the shortest embedment length where full flexural capacity was achieved and the longest embedment length where slippage occurred prior to achieving the sections flexural capacity.

4.4.1 Determination of the Embedment Length

Determining the lengths of embedment for the first specimen of each series followed a set criterion. The embedment length for the first test of series UF1 through UF7 were determined following the crack inhibiting criteria proposed by researchers at Oklahoma University. Following the 1998 Convention of Precast/Prestressed Concrete Institute in Atlanta Georgia, this criterion was changed to 80% of the development length computed using the ACI expression. During the Prestressing Strand Committee meeting at that Convention, Dr. Maher Tadros, from the University of Nebraska, suggested the performance of flexural bond test following this criteria as a bond performance acceptance test in the absence on a simple bond performance acceptance test.

Considering the failure mode of each previous test on a series, the embedment length in subsequent tests was determined. These embedment lengths were selected in an attempt to determine the range where the development length exists. If the specimen achieved flexural capacity with no strand slippage at certain embedment length, the development length was determined to be shorter or equal than the embedment provided. In instances where the computed nominal flexural capacity[6] of the specimen was not achieved numerically, but sufficient ductility was demonstrated, i.e. displacement to span ratio in excess of 1%, it was determined that the specimen had achieved flexural capacity. If strand slippage was observed, at any load level whether flexural capacity was attained or not, the development length was determined to be longer than the embedment provided.

4.4.2 Types of Failures

The specimens were classified into one of five predetermined types of failure. These were flexural, flexural with slip, shear, shear/bond and bond failure.

Failures where the computed flexural capacity was achieved, crushing of the concrete was observed and no slippage was recorded were classified as flexural[7]. Specimens that did not achieved the computed flexural capacity, but concrete

---

[6] The nominal capacity of each specimen was computed using a MathCAD template. The prestress losses computation was based on the procedure outline in Reference 56. The nominal capacity was computed by Stress-strain compatibility. The stress in the strand was computed using Equation 3.2.

[7] The sections capacity was controlled by the concrete crushing or anchorage failures. No flexural reinforcement breakages were observed. The strain in the strands at the limit state was in the order of 2%, or $f_{ps} \approx 267$ ksi. The minimum guaranteed breaking strain is 3.5%, but typically strands break at strains in the order of 5%.

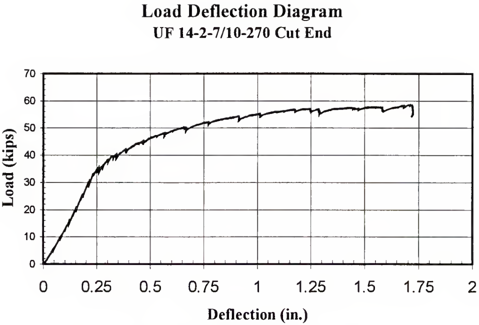

Figure 4-5 Typical Load Displacement Chart (Flexural Failure)

compression crushing was identified and demonstrated a ductile behavior[8], with no strand slippage were also classified as flexural failures. Figure 4.5 depicts a typical Load Deflection Chart for a specimen that achieved flexural failure.

Flexural/Slip failures were specimens that exhibited certain degree of ductility, achieved the computed flexural capacity and/or concrete crushing was observed, but some slippage was recorded.

Shear and bond failures are closely related. The shear and shear/bond types of failure were undesirable, explosive type of failures, see Figure 4.6. The shear carrying capacity of the concrete section is lost once shear failure occurs and the stress in the longitudinal reinforcement increases. The sudden increase in stresses on the strand leads to bond failure. On the other hand, loss of anchorage causes a reduction in the concrete's shear capacity. Whenever it was not possible to determine whether shear failure or loss of anchorage had triggered the failure, the failure was classified as shear/bond. In some instances, where strut-tie behavior was observed or no slippage was recorded until after the shear failure occurred, the failures were classified as shear.

---

[8] Ductile behaviors were characterized by a marked reduction of stiffness. As a result of the reduced stiffness, the specimen will deflect without an increase in load, identified by the "flattening" of the Load-Deflection charts. See Figure 4.3.

Bond failures did not necessarily lead to shear failures. Failures that did not demonstrated sufficient ductility or load carrying capacity to be classified as Flexural/Slip were classified as bond.

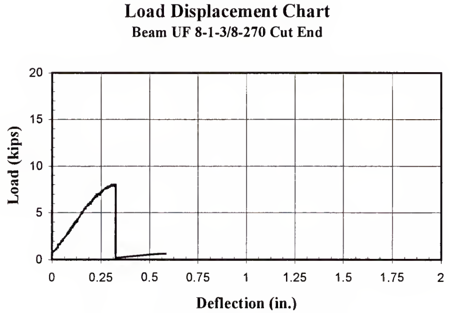

Figure 4-6 Typical Load Deflection Chart
(Shear Failure)

4.4.3 Flexural Bond Tests Results: Phase I

Flexural bond test results for the specimens on Phase I are presented on Table 4-3.a. The strand, 1/2" Grade 270 Low Relaxation, was able to achieve flexural capacity at an embedment of 56", or 70.3% of the development length estimated using the ACI expression. As to the exact value of the transfer length no conclusion can be drawn since no lower bound failure, that is a failure that exhibited some strand slippage or bond degradation, occurred in this series of tests.

4.4.4 Flexural Bond Test Results: Phase II

Flexural Bond tests results for the specimens on Phase II are summarized on Table 4-3.b. Flexural capacity was achieved with embedment as short as 26" as was the case for the cut end of specimen UF3-1-1/2-270.

The strand used on Specimen UF3-2-1/2-270 was re-tested on specimen UF4-2-1/2-270. Specimen UF4-2-1/2-270 developed its computed flexural capacity at embedment length of 40" with some strand slippage. Yet, bond failure was observed at an embedment length of 46" on specimen UF3-2-1/2-270 free end, when a shear/torsion[9] crack formed from the support to the point load at 18 kips, of 74% of the estimated capacity.

On the specimens of series UF5, where the cut ends were tested with embedment lengths of 40' and 34", and flexural capacity were achieved. The free ends of these specimens were tested symmetrically. The span lengths were reduced while the embedment lengths were maintained constant. Bond and shear failures were observed on the free ends.

---

[9] The specimen was, apparently, improperly loaded causing some torsion. The shear/torsion crack appeared to spiral around the specimen.

Similar behavior was observed on series UF6. The cut end tests were able to develop higher loads than the free ends, while the embedment lengths were kept constant at 38". The cut ends, tested on a two-point load configuration, developed flexural capacity. Some slippage in the strand was recorded, so they were classified as Flexural/Slip failure. The free ends were tested on a one-point load configuration. In both specimens bond failure were observed at loads approximately 90% of the computed flexural capacity. These results pointed toward a development length in the vicinity of 40".

The strand used on series UF6 was retested on series UF7. Test results for series UF7 confirmed the findings of series UF6 to the effect of a development length in the vicinity of 40". Flexural capacity was achieved with an embedment length of 40", while Flexural/Slip failure was achieved at 38". A one-point load test at 39", resulted in bond failure at 86% of the computed flexural capacity.

4.4.5 Flexural Bond Tests Results: Phase III

3/8" Indented Wire Grade 270 Strand. Specimens casted on bed #1 on series UF8, UF9, UF10 and UF12 were reinforced with 3/8" indented wire strand. These specimens were loaded symmetrically. The computed flexural capacity was achieved at embedment a length of 36", provided the section contained shear reinforcement. This embedment length equals 65% of the development length computed with the ACI expression. The absence of shear reinforcement on the cut end of specimen UF8-1-3/8-270 allowed the formation of a longitudinal crack along the strand at transfer. This crack affected the specimens load carrying capacity, reducing it to 56% of the computed flexural capacity.

3/8" Smooth Wire Grade 270 Strand. Specimens casted on bed #2 on series UF8, UF9, UF10 and UF12 were reinforced with 3/8" smooth wire strand. These specimens were loaded symmetrically. The computed flexural capacity was achieved at embedment a length of 40", provided the section contained shear reinforcement, or 72% of the development length computed with the ACI expression. No bond failures were observed, other than strand slippage occurring in conjunction to shear failures.

Shear failures were observed on specimens that did not have shear reinforcement on one end. Figure 4.7 shows one of such failures. Specimen UF 9-2-3/8-270 (Cut End) had an explosive shear failure. Flexural compression failure had already occurred and loading was continued in an attempt to reach the computed flexural capacity. The section achieved over 90% of the computed capacity, and compression failure had been identified prior to the formation of the crack depicted in the picture. As such, the failure was classified as flexure.

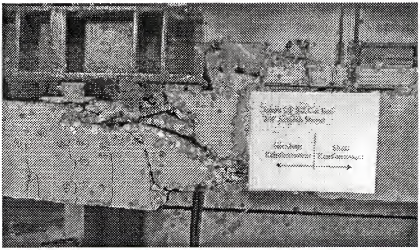

Figure 4-7 Shear Crack on Specimen UF 9-2-3/8-270

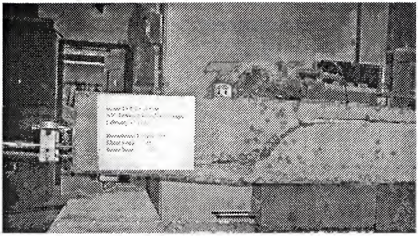

Figure 4-8 Shear Crack on Specimen 8-2

Figure 4.8 shows a picture of a shear failure observed on Specimen UF 8-1-3/8i-270. A splitting crack appeared on cut end of Specimen UF 8-1-3/8i-270 at transfer. The cut ends were not reinforced for shear.

1/2" Special Grade 270 Strand. Specimens on series UF11, reinforced with 1/2" special strands, were loaded symmetrically. Ductile behavior was observed for specimens loaded with embedment length of 55", or 75% of the development length computed with the ACI expression. The computed flexural capacity was achieved at embedment lengths of 59", or 79.8% of ACI development length. Since no bond failures were observed, the range where the development length exists cannot be stated from the data.

During the flexural bond tests on the cut ends on both specimens of series UF11, shear cracks appeared early in the loading process. This crack did not appear to affect the bond performance of the strands, yet the load carrying capacity of the specimens was affected. Both specimens achieved a ductile failure at a fraction of the computed flexural capacity. Figure 4.9 shows a picture of these cracks (The cracks were hairline cracks. They were marked with ink for the picture),

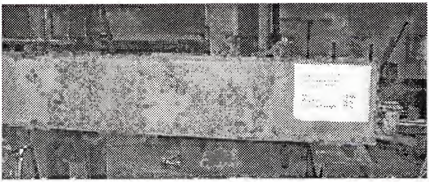

Figure 4-9 Shear Cracks within the Transfer Region on Specimen UF 11-1-1/2s-270

6/10" Grade 270 Strand. Specimens reinforced with 6/10" strand were able to develop the computed flexural capacity when loaded with embedment lengths of 71", or 79% of the development length computed with the ACI expression. No bond failure was observed, for this reason no information as to the lower limit of the development length is available, other than it is certainly shorter than 71".

7/10" Grade 270 Strand. Specimens on series UF14 were reinforced with 7/10" Grade 270 strand. These specimens were loaded symmetrically at embedment lengths shorter than 80% of the development length computed with the ACI expression. The computed flexural capacity was achieved on specimens loaded at embedment lengths as short as 74", or 69% of the development length estimated with the ACI expression. A specimen tested at an embedment length of 48", or 45% of the ACI development length, developed 80% of the specimens computed flexural capacity before failing. The failure was sudden and explosive. It was classified as a Shear/Bond failure.

4.4.6 Flexural Bond Tests Results: Phase IV

3/8" Smooth Wire Grade 270 Strand. Loaded symmetrically, flexural capacities were attained at embedment lengths as short as 32", or 59% of the development length computed with the ACI expression. This result helped clarify the situation presented with the 3/8' smooth wire strand tested on Phase III, where a lower limit on the development length of the 3/8" strand could not be established.

In specimens tested during Phase III flexural capacities were attained at embedment lengths as short as 40". Phase IV results demonstrated that flexural capacity could be achieved at embedment lengths as short as 32". Again, a low limit could not be established since no bond type of failures were observed, thus leaving open the possibility of development lengths shorter than 32".

1/2" Grade 300 Strand. The computed flexural capacity was achieved at an embedment length of 66", or 80.3% of the ACI development length. Ductile behavior was observed at embedment lengths of 65" having developed 87% of the computed flexural capacity of the section. Shear/Bond failures were observed at embedment lengths of 56" and 62", having developed in excess of 88% of the computed flexural capacity. It can be established that the development length exists in the 62" to 65" range, or 75% to 80% of the development length computed per ACI expression.

3/8" Grade 300 Strand. The computed flexural capacity was achieved at an embedment length of 74% of the ACI development length estimate, or 44". Shear/Bond failure was observed at embedment lengths of 40", or 67% of the development length estimated with the ACI expression. This specimen developed 100% of the computed flexural capacity, yet it did not exhibit a ductile behavior. It can be established that the development length exists in the 40" to 44" range, or 65% to 74% of the development length estimated with the ACI expression.

1/2" Special Grade 290 Strand. The computed flexural capacity of the section was attained in specimens loaded with embedment lengths as short as 62", or 74% of the ACI development length expression estimate. Three specimens were loaded at embedment lengths near the 80% of the development length estimated with the ACI expression. Two of this specimens, loaded at embedment lengths of 68" and 66", exhibited ductile behavior, while attaining 93% and 98% of the computed flexural capacity, respectively. The third specimen, UF18-1-1/2s-290 cut end, was loaded at 66" and developed 91% of the computed flexural capacity, yet Shear/Bond type of failure was observed.

Table 4-3.a Summary Flexural Test and Development Length Data (Phase I)

Specimen ID	End	Span (in.)	Development Length (in.)			Cracking Moment (kip-in)	Nominal Capacity[10] (kip-in)	Maximum Moment (kip-in)	Flexural Capacity Ratio	Failure Mode
			ACI [11]	Embedment	% ACI					
UF 1-1-1/2-270	Cut End	144	80.0	66.0	82.5 %	441	705	798	113 %	Flexure
UF 1-2-1/2-270	Cut End	144	78.2	62.0	79.3 %	452	707	787	111 %	Flexure
UF 1-3-1/2-270	Cut End	144	79.5	58.0	72.9 %	452	708	778	110 %	Flexure
UF 1-4-1/2-270	Cut End	144	80.0	66.0	82.5 %	441	705	768	109 %	Flexure
UF 1-5-1/2-270	Cut End	144	78.3	66.0	84.3 %	452	707	780	110 %	Flexure
UF 1-6-1/2-270	Cut End	144	79.6	56.0	70.3 %	452	708	802	113 %	Flexure

Table 4-3.b Summary Flexural Test and Development Length Data (Phase II)

Specimen ID	End	Span (in.)	Development Length (in.)			Cracking Moment (kip-in)	Nominal Capacity (kip-in)	Maximum Moment (kip-in)	Flexural Capacity Ratio	Failure Mode
			ACI	Embedment	% ACI					

---

[10] The Cracking Moments and Nominal Capacity were computed using a MathCAD template. A sample of which is presented in Appendix III. Tacking Moments were computed using transformed sections and the nominal capacity using stress-strain compatibility.

[11] The development length was computed using the effective prestress level estimated following the procedure outlined by Zia, Preston, Scott and Workman [81]. When computed using the estimated prestress level at the time of testing the computed development length was 72.5" for UF1-1 and UF1-4, and 70.8" for the other specimens.

Specimen ID	End	Span (in.)	Development Length (in.)			Cracking Moment (kip-in)	Nominal Capacity (kip-in)	Maximum Moment (kip-in)	Flexural Capacity Ratio	Failure Mode
			ACI	Embedment	% ACI					
UF 2-1-1/2-270	Cut End	144	72.8	45.0	62.8 %	442	709	755	107 %	Flexure
	Free End	144	72.8	36.0	49.4 %	445	720	815	113 %	Flexure
UF 2-2-1/2-270	Cut End	144	72.8	37.0	50.8 %	442	709	786	111 %	Flexure
	Free End	144	72.8	28.0	38.5 %	445	720	887	123 %	Flexure
UF 3-1-1/2-270	Cut End	144	73.6	26.0	35.3 %	448	725	751	104 %	Flexure
	Free End	144	73.6	44.0	59.8 %	448	725	779	107 %	Flexure
UF 3-2-1/2-270	Cut End	144	73.6	36.0	48.9 %	448	725	872	120 %	Flexure
	Free End	144	73.6	46.0	62.5 %	448	725	537	74 %	Shear
UF 4-1-1/2-270	Cut End	144	72.0	40.0	55.6 %	444	706	820	114 %	Flexure
	Free End	144	72.0	30.0	41.7 %	444	706	777	110 %	Flexure
UF 4-2-1/2-270	Cut End	144	72.0	50.0	69.4 %	444	706	747	106 %	Flexure
	Free End	144	72.0	40.0	55.6 %	444	706	795	113 %	Flexure/Slip
UF 5-1-1/2-270	Cut End	144	72.2	40.0	55.4 %	440	701	736	105 %	Flexure/Slip
	Free End	96	72.2	40.0	55.4 %	440	701	623	89 %	Bond[12]
UF 5-2-1/2-270	Cut End	144	72.2	34.0	47.1 %	440	701	799	114 %	Flexure
	Free End	84	72.2	34.0	47.1 %	440	701	349	50 %	Shear[13]
UF 6-1-1/2-270	Cut End	144	72.3	38.0	52.6 %	445	709	703	99 %	Flexure/Slip

---

[12] Flexural concrete compression failure was observed at 98%

[13] Failure was sudden. A large crack formed from the support to the point load.

Specimen ID	End	Span (in.)	Development Length (in.)			Cracking Moment (kip-in)	Nominal Capacity (kip-in)	Maximum Moment (kip-in)	Flexural Capacity Ratio	Failure Mode
			ACI	Embedment	% ACI					
	Free End	144	72.3	38.0	52.6 %	445	709	646	91 %	Bond[14]
UF 6-2-1/2-270	Cut End	144	72.4	38.0	52.6 %	445	709	860	121 %	Flexure/Slip
	Free End	144	72.4	38.0	52.6 %	445	709	620	87 %	Bond[15]
UF 7-1-1/2-270	Cut End	144	72.0	50.0	69.4 %	449	701	780	111 %	Flexure
	Free End	144	72.0	40.0	55.6 %	449	701	832	119 %	Flexure
UF 7-2-1/2-270	Cut End	144	72.0	38.0	52.8 %	449	701	725	103 %	Bond
	Free End	144	72.0	39.0	54.2 %	449	701	606	86 %	Bond[16]

Table 4-3.c Summary Flexural Test and Development Length Data (Phase III)

Specimen ID	End	Span (in.)	Development Length (in.)			Cracking Moment (kip-in)	Nominal Capacity (kip-in)	Maximum Moment (kip-in)	Flexural Capacity Ratio	Failure Mode
			ACI	Embedment	% ACI					
UF 8-1-3/8i-270	Free End	106	56.5	45.0	79.6 %	196	295	326	111 %	Flexure
	Cut End	106	56.5	45.0	79.6 %	196	295	164	56 %	Shear
UF 8-2-1/2-270	Free End	106	56.5	45.0	79.6 %	196	295	332	113 %	Flexure

---

[14] Loaded with one point load.

[15] Loaded with one point load.

[16] Loaded with one point load.

Specimen ID	End	Span (in.)	Development Length (in.)			Cracking Moment (kip-in)	Nominal Capacity (kip-in)	Maximum Moment (kip-in)	Flexural Capacity Ratio	Failure Mode
			ACI	Embedment	% ACI					
	Cut End	106	56.5	45.0	79.6 %	196	295	267	90 %	Flexure
UF 9-1-3/8i-270	Free End	104	55.5	44.0	79.3 %	198	295	328	111 %	Flexure
	Cut End	104	55.5	44.0	79.3 %	198	295	330	112 %	Shear
UF 9-2-3/8-270	Free End	104	55.5	44.0	79.3 %	198	295	276	94 %	Flexure
	Cut End	104	55.5	44.0	79.3 %	198	295	266	90 %	Flexure
UF 10-1-3/8i-270	Free End	88	55.3	36.0	65.1 %	198	295	275	93 %	Flexure
	Cut End	104	55.3	44.0	79.6 %	198	295	326	111 %	Flexure
UF 10-2-3/8-270	Free End	96	55.3	40.0	72.3 %	198	295	266	90 %	Flexure
	Cut End	104	55.3	44.0	79.6 %	198	295	254	86 %	Shear
UF 11-1-1/2s-270	Free End	134	73.9	59.0	79.8 %	521	788	797	101 %	Flexure
	Cut End	126	73.9	55.0	74.3 %	521	788	499	63 %	See Note[17]
UF 11-2-1/2s-270	Free End	134	73.9	59.0	79.8 %	521	788	777	99 %	Flexure
	Cut End	134	73.9	59.0	79.8 %	521	788	764	97 %	Flexure
UF 12-1-3/8i-270	Free End	102	53.7	43.0	80.0 %	246	344	435	126 %	Flexure
	Cut End	102	53.7	43.0	80.0 %	246	344	409	119 %	Flexure
UF 12-2-3/8-270	Free End	102	53.7	43.0	80.0 %	246	344	444	129 %	Flexure
	Cut End	102	53.7	43.0	80.0 %	246	344	409	119 %	Flexure

---

[17] Shear cracks appeared in the shear span being tested. No slip was recorded. Load-deflection chart demonstrated a marked loss of stiffness and ductile behavior. The Deflection-Span ratio was 1%, the test was stopped.

Specimen ID	End	Span (in.)	Development Length (in.)			Cracking Moment (kip-in)	Nominal Capacity (kip-in)	Maximum Moment (kip-in)	Flexural Capacity Ratio	Failure Mode
			ACI	Embedment	% ACI					
UF 13-1-6/10-270	Free End	134	90.1	71.0	78.8 %	830	1287	1204	94 %	Flexure
	Cut End	134	90.1	71.0	78.8 %	830	1287	1231	96 %	Flexure
UF 13-2-6/10-270	Free End	134	90.1	71.0	78.8 %	830	1287	1176	91 %	Flexure
	Cut End	134	90.1	71.0	78.8 %	830	1287	1242	97 %	Flexure
UF 14-1-7/10-270	Free End	140	106.9	74.0	69.2 %	1309	2077	2169	104 %	Flexure
	Cut End	112	106.9	48.0	44.9 %	1309	2077	1663	80 %	Shear/Bond
UF 14-2-7/10-270	Free End	140	106.9	84.0	78.6 %	1309	2077	2125	102 %	Flexure
	Cut	156	106.9	80.0	74.8 %	1309	2077	1867	90 %	Flexure

Table 4-3.d Summary Flexural Test and Development Length Data (Phase IV)

Specimen ID	End	Span (in.)	Development Length (in.)			Cracking Moment (kip-in)	Nominal Capacity (kip-in)	Maximum Moment (kip-in)	Flexural Capacity Ratio	Failure Mode
			ACI	Embedment	% ACI					
UF 15-1-3/8-270	Cut End	102	53.8	43.0	80.0 %	250	370	357	97 %	Flexure
	Free End	102	53.8	43.0	80.0 %	250	370	377	102 %	Flexure
UF 15-2-3/8-270	Cut End	88	53.8	36.0	66.7 %	252	373	352	94 %	Flexure
	Free End	80	53.8	32.0	59.3 %	252	373	356	95 %	Flexure
UF 16-1-1/2-300	Cut End	140	82.2	62.0	75.4 %	519	788	696	88 %	Bond[18]

---

[18] Flexural concrete compression failure observed after test was completed.

Specimen ID	End	Span (in.)	Development Length (in.)			Cracking Moment (kip-in)	Nominal Capacity (kip-in)	Maximum Moment (kip-in)	Flexural Capacity Ratio	Failure Mode
			ACI	Embedment	% ACI					
	Free End	126	82.2	56.0	68.1 %	519	788	698	89 %	Bond
UF 16-2-1/2-300	Cut End	146	82.2	65.0	79.1 %	519	786	686	87 %	Flexure
	Free End	148	82.2	66.0	80.3 %	519	786	776	99 %	Flexure
UF 17-1-3/8-300	Cut End	112	59.4	48.0	80.8 %	259	392	392	100 %	Flexure
	Free End	110	59.4	47.0	79.1 %	259	392	388	99 %	Flexure
UF 17-2-3/8-300	Cut End	104	59.4	44.0	74.1 %	259	392	418	107 %	Flexure
	Free End	96	59.4	40.0	67.3 %	259	392	392	100 %	Flex/Slip
UF 18-1-1/2s-290	Cut End	148	83.0	66.0	79.5 %	540	811	741	91 %	Bond
	Free End	152	83.0	68.0	81.9 %	540	811	758	93 %	Flexure
UF 18-2-1/2s-290	Cut End	148	83.0	66.0	79.5 %	540	811	797	98 %	Flexure
	Free End	140	83.0	62.0	74.7 %	540	811	720	89 %	Flexure

CHAPTER 5

DISCUSSION OF EXPERIMENTAL TESTS RESULTS

5.1 Introduction

The results obtained during the experimental phases of this program will be discussed in this chapter. Measured transfer lengths, end slips and flexural test results will be analyzed and discussed in light of results obtained by published research programs.

First, the effect of variables, such as concrete strength at transfer and initial prestress in the strand transfer length will be individually investigated. These individual investigations are not unit-consistent or dimensionally correct, as such the information obtained is indicative of the variables qualitative influence on bond, rather than quantitative. This section will be followed by a dimensional, or unit consistent, analysis of the data. Information and relationships obtained through a dimensional analysis of the data is also of qualitative nature, yet, combined with experimental procedures adequate predictor equations can be obtained.

5.1.1 Dimensional Analysis and Buckingham's Pi-Theorem

Dimensional analysis, attributed to Buckingham [56], is based on the logic that a general relationship between two quantities can only be established if these quantities have the same dimensions[1]. In addition, the magnitude of the ratio of the two quantities must be independent of the units in which the quantities are measured. That is, the ratio of the height to the length of a table remains constant whether it is measured in feet, inches or meters, a direct product of the linearity of our system of measurements.

Dimensional analysis differs from other types of analysis in that only their dimensions, and not so-called natural laws such as Newton's Law of Motion, govern the relation between variables. Relationships obtained with this procedure, by itself, are qualitative rather than quantitative. Yet, accurate prediction equations can be obtained when combined with experimental procedures.

The derivation of such equations, or determining the relationship amongst variables, is not always possible, or evident, from an analytical perspective. This type of analysis provides a technique to investigate and determine relationships among variables by experimental means. The likelihood of obtaining a correlation amongst the variables been studied, if such correlation exist, is enhanced by the dimensional analysis technique.

The dimensional analysis performed in this paper will take advantage of Buckingham's Pi Theorem. Buckingham's theorem states the minimum number of dimensionless groups, or π-terms, required to express a relationship amongst variables. This minimum number of π-terms equals the number of independent quantities minus the number of dimensions involved in the problem. The expression that describes the phenomenon under study can take the form of the sum, the product, or a combination of sum and product, of π-terms.

---

[1] Dimensions are parameters such as time (T), mass (M), and length (L). For the purpose of our discussion a dimension of force (F = Mass * Acceleration = ML/T^2), which is a combination of the basic dimensions, will be used.

The only restriction for a π-term is that it has to be dimensionless and independent. For example the ratio of the transfer length to the strand diameter is a π-term. Since both parameters have units of length, their ratio is dimensionless. Similarly, the initial strain in the strand, the ratio of the pre-compression in the concrete to the concrete compressive strength at transfer and the ratio of the prestress in the strand to the concrete strength at transfer are also non-dimensional, hence, possible π-terms.

5.2 Transfer Length Data

5.2.1 Transfer Length Database

A transfer length database was created using MS Excel software. The entries were obtained from the available literature, including publications by Cousins et al. [16-18], Kaar et al. [36], Russell and Burns [68], Mitchell et al. [55], Deatherage et al. [19] and Rose and Russell [66, 67]. The database contains of 401 entries, with 385 transfer length measurements and other related information such as: strand diameter, end on which the transfer length is measured, end slip, concrete strength at transfer of the prestressing force and the initial prestress in the strand.

5.2.2 Effect of Method Used to Determine Transfer Length

As discussed on Chapter 4, there are several methods that can be used to determine the transfer length from strain profiles. Recently, for most practical purposes, the Federal Highway Administration endorsed the 95% Average Maximum Strain

Method, devised at the University of Texas at Austin by Russell and Burns, over the Slope Intercept Methods.

In light of this endorsement and the fact that the data obtained during the experimental program at the University of Florida had been analyzed following the Slope Intercept Method, with intercept at 95% of the maximum average strain, the data obtained at the University of Florida was re-analyzed following the procedure endorsed by the Federal Highway Administration. The strain profiles were re-evaluated following the 95% Average Maximum Strain procedure and with the slope intercept method with intercept at 100% of the average maximum strain. A descriptive statistical analysis was performed on the data, totaling 65 measured transfer lengths. The transfer lengths were normalized with respect to the strand diameter. The results of this analysis are presented on Table 5.1.

Table 5-1 Descriptive Statistical Analysis of Transfer Length Determination Methods

Parameters in Terms of Number of Strand Diameters	95% Slope Intercept	100% Slope Intercept	95% Average Maximum Strain
Mean Transfer Length	46.8	49.3	50.0
Median Transfer Length	47.5	50.0	52.0
Standard Deviation	10.1	10.6	11.0
Range of Transfer Lengths	26.2 – 69.2	27.6 – 72.8	27.6 – 76.9
95% Confidence Interval	43.9 – 49.8	46.3 – 52.8	47.0 - 53.0

On average, the transfer lengths estimated following the procedure endorsed by the FHWA were 6.8% longer than those determined with the slope –intercept method, with intercepts at 95% the maximum average strain. The mean of these transfer lengths was also longer, by 1.4%, than those estimated by the slope intercept method with intercept at 100% of the average maximum strain. The transfer lengths estimated with the slope intercept method, with intercept at 100% of the maximum average strain, were 5.3% longer than those estimated with the intercept at 95% of the average maximum strain.

The coefficients of variation for the transfer lengths estimated following the slope intercept methods were 21.6% and 21.5% for intercepts at 95% and 100% of the average maximum strain, respectively. The coefficient of variation for the transfer lengths estimated following the 95% Average Maximum Strain Method was 22%. Figure 5-1 presents a graph of the transfer lengths estimated using the three different methods described before.

The Slope Intercept method with intercept at 95% of the average maximum strain and the 95% Average Maximum Strain Method yielded the upper and lower bound mean transfer length values. Best-fit lines, or trendlines, for the transfer lengths estimated with these two methods are included on Figure 5-1. The slope of these lines, which were not forced through the origin, differs by less than half-percent, 0.5%. Hence, these lines are essentially parallel with the intercept of the lines shifted by 1.8 strand diameters, or about 3.6%. Had the intercept of these lines been forced through the origin, the slope of these lines would have differed by less than 7%.

The variation in the transfer lengths, as estimated by each of these methods, is more than three times the maximum difference of the mean transfer lengths when estimated following the different procedures. This large scatter in the data relative to the small difference in the transfer lengths determined by the different methods indicates that concerns over which method is used when determining the transfer length are not warranted.

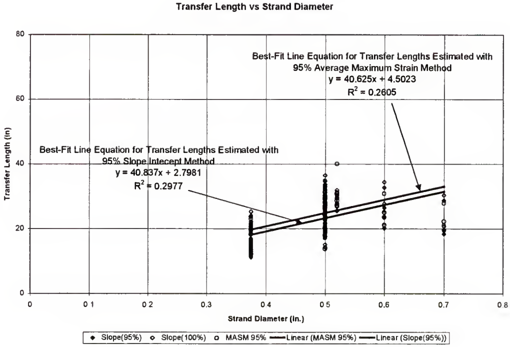

Figure 5-1 Comparison of Method Used for Determining The Transfer Length

5.2.3 Effect of Concrete Strength at Transfer

The predictor equations presented by AASHTO and ACI for transfer length does not consider the effect of the concrete strength at transfer. Research programs conducted by Sozen and Stoker [75] and, most recently, by Mitchell et al. [55] have found that the concrete strength does affect the strand bond behavior.

Figure 5-2 shows a graph of the transfer length, normalized with respect to the strand diameter, versus the concrete strength at transfer. From visual inspection, the transfer length appears to be independent of the strength of the concrete at time the prestressing force is transferred from the strand to the concrete section. A linear regression analysis of the data indicated that this is not so. The regression analysis yielded a negative sloped line. The negative slope obtained from this analysis indicates that the transfer length is reduced as the concrete strength at transfer increases.

In an extensive research program in the later part of the 1960's, Stoker and Sozen [75] studied various parameters affecting bond, including concrete strength. The experimental program consisted of short-embedment pull-out tests. From these studies, the researchers concluded that the bond strength increased approximately 10% for every 1000-psi increase in concrete strength.

Mitchell et al. [55] concluded that the transfer length is reduced by the squared root of the ratio of a benchmark concrete strength of 3-ksi to the concrete strength at transfer. That is, for a 1000- psi increase in concrete strength, f'ci = 4000 psi, results in a reduction of 15.5% transfer length when compared to a concrete strength at transfer of 3000 psi.

The transfer of the prestressing force at the University of Florida occurred at concrete strengths in the 3500 psi to 4300 psi range. For this range of concrete strengths, the transfer length measured at the University of Florida decreased approximately 4.2% per 1000-psi increase in concrete strength at transfer. Figure 5-2 shows a graph of the measured transfer lengths, normalized with respect to the respective diameter of the strand, versus the concrete strength at transfer.

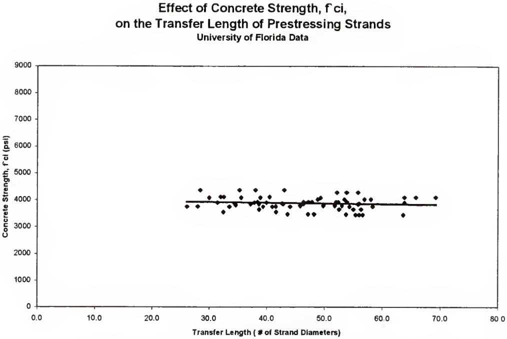

Figure 5-2 Effect of Concrete Strength on Transfer Length (University of Florida Data)

Two regression analyzes, similar to the analysis performed on the transfer lengths measured at the University of Florida, were performed. One of these analyses was performed on the entire population included on the transfer length database. The second regression analysis was done on a population that excluded the data reported by Cousins et al. [16-18]. Both regression analyses yielded results similar to those observed at the University of Florida. In both instances, a reduction of 5.1% in the transfer length could be expected for a 1000-psi increase in concrete strength at transfer. The coefficient of determination, R^{2}[2], improved when the transfer lengths reported by Cousins et al. were excluded. See Figure 5-3.

---

[2] R^2 is an indicator of the adequacy of a regression model. An R^2 of, for example, 0.87 means that the model accounts for 87% of the variability in the data. An R^2 of 1 indicates a "perfect fit". Yet, this

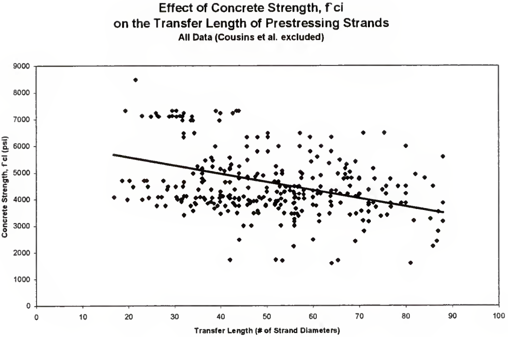

Figure 5-3 Effect of Concrete Strength on Transfer Length (Cousins et al. [16-18] excluded)

It should be noted that most of the entries, 78%, on the database are for small diameter strands, that is, strand diameters smaller than 6/10". As we shall see later in Figure 5-9, the effect of the compressive strength of the concrete appears to have an increased influence in the transfer length of strands with diameters larger than 6/10".

5.2.4 Effect of the Initial Prestress

The current code philosophy, with respect to the effect the stress in the strand has on transfer length, assumes the transfer length to be linearly proportional to the effective

---

indicator should be used with caution. An R^2 of unity can be achieved by increasing the order of the polynomial of the model, but this does not means that this is a good model.

stress in the strand. Recently, several researchers have proposed the transfer length to be proportional to the initial stress in the strand, f_{pi}.

Attempting to correlate the transfer length to the initial stress in the strand seems reasonable for two reasons. First, the initial stress in the strand is always higher than the effective prestress, ensuring that the correlation obtained is for the worst-case scenario. Second, most of the reported transfer lengths were measured soon after transfer of the prestressing force took place, as is the case of the project conducted at the University of Florida. The stress in the strand at this point is the initial prestress minus the elastic shortening loss, since losses due to creep, shrinkage and strand relaxation have not yet taken place. The initial prestress – transfer lengths pairs, measured at the University of Florida, are plotted on Figure 5-4.

A regression analysis demonstrated an increase in initial stress in the strand, f_{pi}, was corresponded by an increase in transfer length. Transfer lengths increased 1.6% per one ksi increase in stress in the strand, when evaluated in a range of initial prestress of 190 ksi to 220 ksi.

Similarly, the initial prestress- transfer length pairs reported in the literature, and included in the database were plotted. A linear regression analysis was performed on the data. The best-fit line obtained from this analysis had a negative slope, indicating a reduction in transfer length corresponding to an increase in the initial stress in the strand. This behavior is contrary to what theoretical developments indicate.

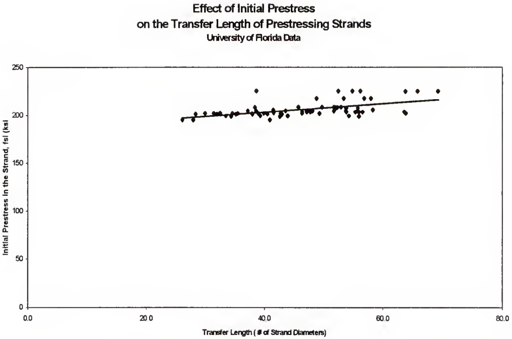

Figure 5-4 Effect of Initial Prestress on Transfer Length (University of Florida Data)

The transfer length – initial prestress pairs reported by North Carolina State University, the University of Oklahoma and those reported by Karr et al. [36] were removed from the analysis. The pairs reported by the University of Oklahoma were removed because the initial stress states reported are the target initial prestress. No reference is made to the actual initial prestress values. The transfer lengths reported by North Carolina State University were excluded from this analysis because they does not seem to be representative of the transfer length population[3].

---

[3] The researcher, Michael Simmons, in his PhD dissertation found some of the transfer lengths measured at NCSU not to be representative of the transfer length population. These transfer lengths were removed from the analysis of the data.

The transfer lengths reported by Kaar et al. [36] appear to increase proportional to an increase in strand stress until a critical stress, 160 ksi, is reached, after which the transfer length decreases as the initial stress in the strand increases. It should be kept in mind that the researchers were studying the effect of concrete strength at transfer. To achieve different concrete strengths with the same concrete mix, the transfer occurred at different time intervals. Introducing variables, such as curing time of the concrete, for which we still do not have a complete understanding of the effect they may have on the transfer length.

Figure 5-5 presents a plot of the transfer length – initial prestress pairs reported by the University of Texas [66, 67, the University of Tennessee, McGill University, Hanson and the University of Florida. A linear regression analysis yielded a positively sloped line, indicating an increase in transfer length following an increase in the initial prestress. The increase in transfer length was in the order of a quarter of a percent (0.25%) per ksi increase in stress in the strand.

The difficulty in attempting to determine the effect of the initial prestress on the transfer length is stems from the fact that most data transfer lengths were measured on specimens where the initial prestress lie in a relatively narrow range, 190 ksi to 205 ksi. The narrow range of initial prestress can be attributed to two reasons.

First, most research programs worked with a single grade of strand. Second, most researchers have assumed that a higher initial stress in the strands yields a worst-case scenario for the transfer length. As such, the strands are stressed to a target initial prestress equal to 75% of the guaranteed strength of the strand. Deviations from the target initial prestress are to be expected, but this are mostly due to the difficulty in achieving an exact predetermined stress in the strand during the jacking operation.

Figure 5-4 shows a clear trend where an increase in the initial stress is corresponded by an increase in transfer length. This trend is not clear in Figure 5-5. Furthermore, had all the data in the database been included this trend would have been reversed. Such divergence could be attributed to the fact that the research at the University of Florida systematically investigated the effect of initial prestress. Meanwhile, for most research programs, by setting a constant target initial prestress level and using a single grade of strand, the range for the initial prestress for any particular research program is relatively narrow and statistically insignificant.

By using three different grades of strands, the researchers at the University of Florida were able to obtain three distinct initial prestress levels, 202 ksi, 218 ksi and 225 ksi. This was done, while variables such as concrete strength, section size and shape, specimen age and other variables identified as affecting transfer length and bond performance were kept constant. By doing so, the effect of the initial prestress on the transfer length was isolated.

Future research programs should consider predetermined variations in the level of initial prestress. For the available data, the initial stress in the strand appears to have no independent effect on transfer length. The effect of this parameter needs to be studied in light of a dimensional analysis.

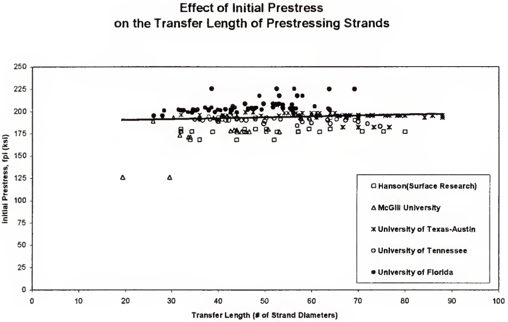

Figure 5-5 Effect of Initial Prestress on Transfer Length

5.2.5 Effect of Strand Diameter

5.2.5.1 Normalized transfer lengths histograms

Section 11.4.3 of the ACI 318-99 allows the estimate of the transfer length as fifty-strand diameters and the assumption of linear transfer of prestress for shear design considerations. The transfer length estimates are particularly critical for shear design. The shear capacity of the section is directly influenced by prestress level on the section. As such, underestimating the transfer length leads to un-conservative shear designs.

The following paragraphs will discuss the validity, or appropriateness, of ACI 318 Section 11.4.3 by means of histograms of the measured transfer length normalized with respect to strand diameter. Figure 5-6 shows the results obtained at the University of Florida. Figure 5-7 shows the histogram for all the entries on the database. Transfer lengths reported by Cousins et al. [16-18] were substantially longer than those obtained at the University of Florida. In general, the transfer lengths reported by Cousins et al. were also longer than those reported by others researchers. Figure 5-8 is similar to Figure 5-7, but the results reported by Cousins et al. have been excluded from the analysis.

University of Florida Transfer Length Data. The histogram of the transfer lengths measured at the University of Florida showed a normal distribution around 47.7 strand diameters with a mean of 48.5 strand diameters, See Figure 5-6. Ninety-two percent of the transfer lengths measured at the University of Florida were less than sixty-strand diameters ($60d_b$), while 97% were less than sixty-five strand diameters, ($65d_b$).

The longest transfer lengths measured at the University of Florida were 65.8 and 69.2 strand diameters. It should be noted that these were measured on a 1/2" Grade 300 strand. The transfer lengths for Grade 300 strands, in terms of strand diameters, were consistently longer than those of Grade 270 strands. This will be discussed further in following sections.

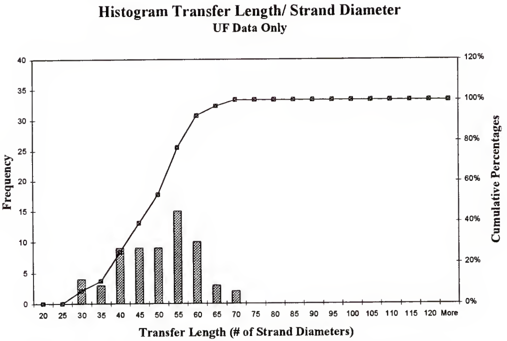

Figure 5-6 Histogram of Transfer Length to Strand Diameter

An analysis of the data gathered on Grade 270 Strands showed that ninety-six (96%) of the data had transfer lengths shorter than sixty strand diameters ($60d_b$). No transfer length measured more than sixty-five strand diameters. The sample had a mean of $45.4d_b$ and a median of 46.1.

Database Transfer Length Data. The histogram for all the entries in the database, again, showed a normal distribution. The median had shifted from forty-eight strand diameters ($48d_b$) to fifty-two strand diameters ($52d_b$), in comparison with the data gathered at the University of Florida. The high frequency region was skewed away from the high transfer length-strand diameter ratios. Only 65% of the entries have transfer lengths shorter than sixty strand diameters ($60d_b$) when all the entries in the database are considered. An inclusion of 95% of the entries is not achieved until entries with transfer lengths as long as a hundred strand diameters ($100d_b$) are included. Transfer lengths in excess of one hundred-twenty strand diameters ($120d_b$) were found. See Figure 5-7.

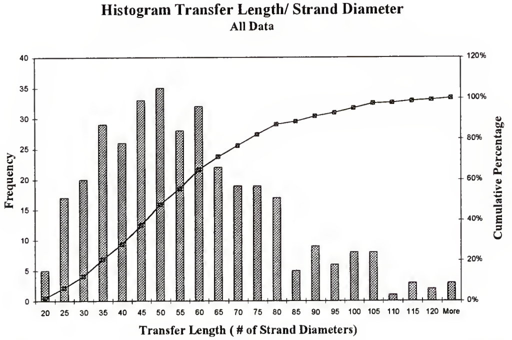

Figure 5-7 Histogram of Transfer Length to Strand Diameter Ratio (ALL)

An inspection of the entries in the database revealed that most of these large transfer length-strand diameter ratios were reported by Cousins et al. [16-18], the same report that prompted the FHWA Memorandum in 1988.

Database Transfer Length Data with Cousins et al. Data Excluded. A histogram where the data reported by Cousins et al. has been excluded is presented on Figure 5-8. The transfer length – strand diameters distributed normally. The median was forty-eight strand diameters ($48d_b$). Fifty percent of the entries had transfer lengths between thirty-five ($35d_b$) and sixty ($60d_b$) strand diameters. The longest transfer length reported, when the data reported by Cousins et al. is excluded, is less than ninety-strand diameters ($90d_b$). Seventy-five percent of the entries had transfer length-strand diameter ratios smaller than sixty strand diameters, ($60d_b$). Ninety-two and ninety-six percent inclusions were achieved at transfer lengths shorter than seventy-five, ($75d_b$) and eighty strand diameters ($80d_b$), respectively.

The data indicates that ACI 318-99 Section 11.4.3 transfer length estimate of fifty strand diameters ($50d_b$) is a good predictor of the average transfer length for Grade 250 and Grade 270 strands. While an average value of the transfer length is desirable for the verification of the stresses in the section at transfer and the service condition, it may lead to unconservative shear designs. If a ninety-five percent confidence of the estimate is desired, an eighty-strand diameters ($80d_b$) transfer length should be used.

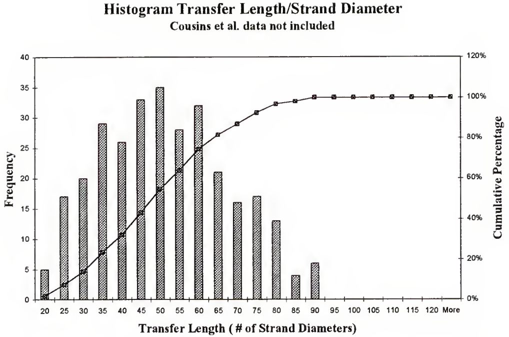

Figure 5-8 Histogram of the Transfer Length to Strand Diameter Ratio

5.2.5.2 Effect of strand diameter on transfer length

As presented in the background discussion on Chapter 2, current code philosophy on bond and transfer length of prestressing strands assumes a linearly proportional relation with the strand diameter. Transfer lengths measured on large diameter strands at the University of Florida did not conform to this philosophy.

As other researchers found before, the author found the smaller diameter strands to follow this linear-proportionality philosophy. Transfer lengths for strand diameters up to the 1/2" special strand, with a nominal strand diameter of 0.52”, appeared to be proportional to the strand diameter. The transfer lengths for 6/10” and 7/10” diameter strand did not followed this trend.

The measured transfer lengths for the 6/10” and 7/10” strands averaged 25.7” and 22.2 inches, respectively. These transfer lengths are comparable to those measured on

1/2" Grade 270 strands during Phase I and Phase II of this research project (Lt = 24.0"). The transfer lengths measured on Grade 270 – smooth wire strands at the University of Florida are presented on Figure 5-9.

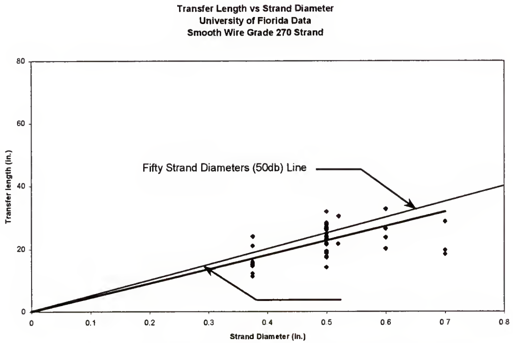

Figure 5-9 Transfer Length versus Strand Diameter Chart (Smooth Wire Grade 270 Strand tested at the University of Florida)

Transfer lengths measured on indented wire strand and higher grade, i.e. Grade 290 and Grade 300, strands were not included, so the only variable affecting the transfer lengths present is the strand diameter. We should recall that the initial stress in the strand and the concrete strength at transfer were kept relatively constant. The initial prestress is approximately 75% of the strand guaranteed strength and the concrete strength is in the 3700 psi to 4300 psi range.

A review of the literature revealed that Kaar, LaFraugh and Mass [36] observed a similar behavior. They disregarded this observation because the 6/10" strand tested was slightly rusted. Yet, the rust in the strand, by itself, cannot explain the difference in bond and transfer length behavior. Figure 5-10 depicts a graph of the transfer lengths measured by Karr, LaFraugh and Mass.

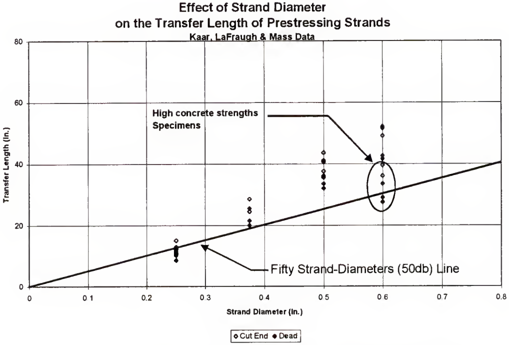

Figure 5-10 Transfer Length Data (Kaar et al.)[36]

Transfer lengths measured on the cut ends of specimens with low concrete strength at transfer followed the linear proportionality trend of the smaller diameter strands for all strand diameters. Yet, on the free ends of these specimens, an improved transfer length performance was observed. It appears that due to the impact at transfer and the low concrete strength the mechanical interlocking was destroyed, reducing the transfer mechanism to mostly frictional.

A marked improvement in transfer length performance was observed for transfer lengths measured on specimens with high concrete compressive strengths at transfer. This improvement in transfer length, performance points toward an enhanced mechanical bonding capability that is independent of the strand surface condition, but dependent on the diameter of the strand and the concrete strength at transfer.

In the late 1980's, Deatherage et al. [19] reported that transfer lengths measured on specimens reinforced with 6/10" strand did not followed this trend. Their results indicated that, although the transfer lengths had increased relative to those of smaller diameter strands, the increase in transfer length was not linearly proportional to the increase in strand diameter. Figure 5-11 presents a chart of the transfer length versus the strand diameter for the data gathered by Deatherage, Burdette and Chew.

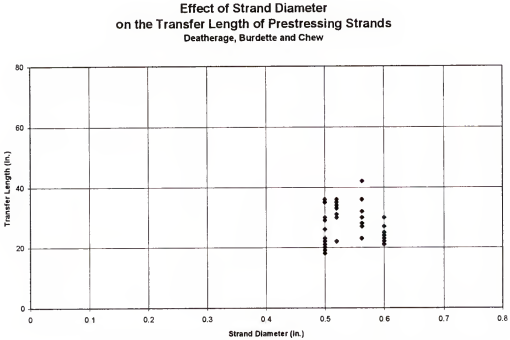

Figure 5-11 Transfer Length Data (Deatherage et al.)[19]

Russell and Burns later found transfer length to be exponentially related the strand diameter, in a relation in the form of Equation 5.1.

$$L_t = Kd_b^x \qquad \text{Equation 5.1}$$

The data gathered by Russell and Burns [68] was limited to 1/2" and 6/10" diameter Grade 270 strands. In their conclusions, the authors recommended a linear relationship.

Figure 5-12 presents a transfer length versus strand diameter chart for all the entries in the database. Figure 5-13 depicts the same graph, but the data obtained by Cousins et al. has been excluded.

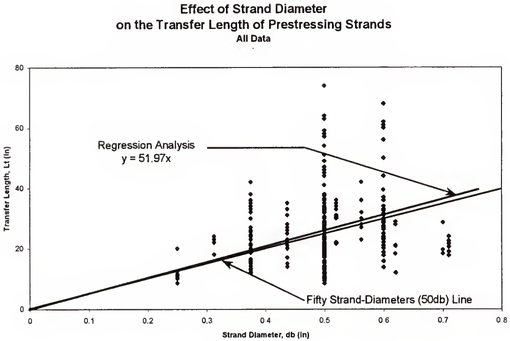

Figure 5-12 Transfer Length versus Strand Diameter Chart
(All entries on the Database)

The disproportionate distribution in the population of transfer lengths forces any regression type analysis to describe the behavior of the smaller diameter strands. Since, currently the industry standard is 1/2" Grade 270 strand, nearly half the entries on the database correspond to this size of strands. Yet, a clear trend can be observed for the larger diameter strands. All the transfer lengths reported for strands with strand diameter in excess of 6/10" fall below the regression analysis line and the ACI 50d$_b$ line. Further research is desirable to increase the population of transfer lengths measured on large diameter of strands, before the development of empirical equations is attempted.

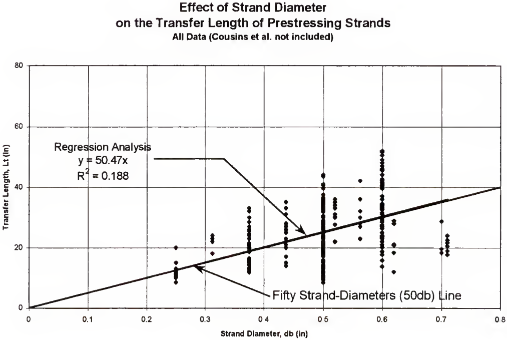

Figure 5-13 Transfer Length versus Strand Diameter Chart
(Cousins et al. excluded)

Mayfield et al. [52] reported the transfer lengths reported for 0.71" strand. These transfer lengths were reported in a chart format. The values in the database were estimated from the charts published by Mayfield et al. The strand tested was a 19 wire strands. As such, a direct comparison of these results to the others included in the database should not be attempted.

5.2.6 End Slip – Transfer Length Relationship

The end-slip, or draw-in, is the distance the strand slips into the concrete section when the prestressing force is transferred. The draw-in occurs under the same bond conditions as the prestressing force is transferred, that is, the same initial prestress in the strand, strand surface condition and concrete strength at transfer, among other variables identified as affecting bond. As such, the measurement of end-slip has been proposed as an *in-situ* bond indicator.

As discussed in Chapter 2, several equations have been derived to correlate the transfer length to the end-slip, known as slip-theory. Currently two slip-theory based transfer length expressions are generally accepted. In the United States, the generally accepted expression assumes a linear profile, Equation 2.18. One proposed by the International Federation of Concrete, FIP, assumes a parabolic strain profile, Equation 2.19.

$$Lt = \lambda * \frac{Les}{\varepsilon pi} \qquad \text{Equation 2.17}$$

$$Lt = 2 * \frac{Les}{\varepsilon pi} \qquad \text{Equation 2.18}$$

$$Lt = 3 * \frac{Les}{\varepsilon pi} \qquad \text{Equation 2.19}$$

Polish researchers found λ to be 2.86. De Uijl, through simulations, found that the value of λ to lie between 2.4 and 2.7 with an average of 2.56.

The research project at the University of Florida measured end-slips. These end-slip measurements helped verify the transfer lengths measured by means of surface strain measurements. Measurements on the cut ends were often lost due to the impact received by the instrumentation at transfer. Most of the research projects included in the database did not measured end-slip at transfer. A graph of the transfer length - end slip pair measured at the University of Florida is presented on Figure 5-13.

Equations 2.18 and 2.19 have been consistently proven by research work done in various laboratories. Equation 2.18 coincides with the average of the available data, while Equation 2.19 envelops 90% of the data points. Eighty-percent (75%) of the pairs measured at the University of Florida are enveloped by Equation 2.17 with a coefficient λ equal to 2.6. Yet, if the end slips measured on the higher strength strands are excluded then Equation 2.19 and Equation 2.17 envelops 95% and 90% of the data points, respectively. This does not means that Equation 2.17, Equation 2.18 and Equation 2.19 do not apply to the higher grade strands. It is simply that the lines drawn on Figure 5-14 were computed for an initial prestress, f_{si}, of 202.5 ksi.

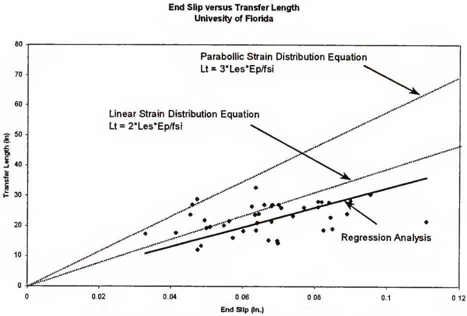

Figure 5-14 End Slip versus Transfer Length Chart (University of Florida Data)

Figure 5-15 presents a chart of the end-slip computed transfer lengths – transfer length pairs reported by researchers at the University of Texas Austin[68] and University of Oklahoma [66], in addition to those reported by the University of Florida. Again, Equation 2.18 coincided with the linear regression line and Equation 2.19 enveloped over 90% of the data points. Equation 2.17, with λ=2.6, enveloped 80% of the pairs.

The use of end-slip, first presented by Anderson and Anderson, as a bond quality control tool, not only seems appropriate for the prestressed/precast concrete producers, but also for design engineers. The design engineer by limiting the amount of slip allowable can obtain a better estimate of the upper bound value of the transfer length. As discussed before under-estimates of the transfer length can lead to over-estimating the shear capacity of the section within the transfer zone. These are typically the critical sections in the design for shear. (Prestressed concrete is typically used as simple supports structures, hence the high shear zones are at the ends of the elements.)

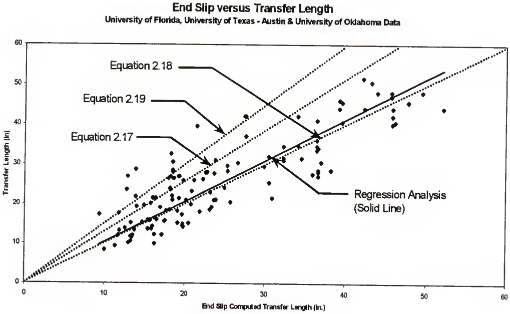

Figure 5-15 End Slip versus Transfer Length Chart
University of Florida, University of Texas & University of Oklahoma

5.3 Development Length

As mentioned before, the development length of a strand cannot be directly measured. As such, the best we can do is to estimate a range where the development length exists by performing flexural tests at different embedment lengths. The development length is then said to exist in a range bounded by the longest embedment length at which a bond type of failure was observed and the shortest embedment length at which a flexural type of failure was observed.

Two flexural tests were performed on each specimen, one on each end. A total of four tests were performed on each series, except on Phase I which consisted of one-six specimen series and where only the cut ends were tested.

The determination of the range within which the development length exists was not always possible, because bond failures were not observed. For this reason, the most we can say, with some degree of certainty, is that flexural capacity was developed at such embedment lengths and that the development length could be shorter than those embedment lengths, but is not possible to estimate how much shorter.

In some instances, it was possible to determine the range where the development lengths exist, as in the case for some series reinforced with half inch strands. For example on series UF16, reinforced with 1/2" Grade 300, a definite range was established between 56" and 65" and a test at 62" exhibited a hybrid failure, the failure was determined as bond type of failure but flexural concrete crushing was identified immediately after the loading was stopped.

Yet on Phase II, specimens reinforced with 1/2" strands were able to attain full flexural capacity at embedment lengths as short as 26" while bond failures were observed at embedment lengths as long as 40". Two factors can be identified as the culprits of such paradox: the loading configuration and transfer length.

The spans used in some of Phase II specimens were set at 144". By doing so the intended constant moment region was negated and the section of maximum moment was shifted from the leading point load, the point load closer to the end being tested, to the trailing load. Since the flexural bond distribution is not known, the critical section[4] could not be established. As such, in the case of the strand that developed in 26" it is not possible to determine whether bond failure would have been observed, or not, had the point of maximum moment had coincided with the embedment length. An schematic of the loading configurations and the resulting shear and moment diagrams are presented in Figure 5-16.

In series UF5, UF6 and UF7, the loading error was corrected by loading either symmetrically or with one point load. This allowed for the intended constant moment region in the case of symmetric loading and, in both types of loading, for the maximum moment section to coincide with the embedment length. In those series, specimens that had attained flexural capacity when loaded at certain embedment length with 144" spans, failed in bond when loaded symmetrically with the same embedment length or with one point load.

---

[4] The critical section should be considered as the point where the ratio of the anchorage demand to the anchorage capacity is at a maximum. The ACI defines it as the point of maximum moment.

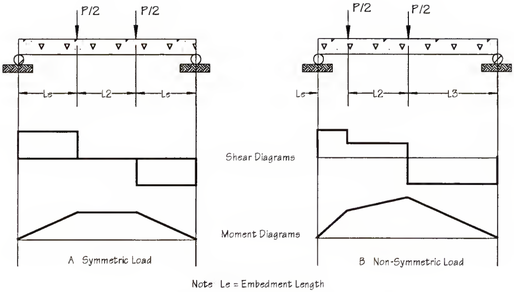

Figure 5-16 Schematic of loading types and resulting shear and moment diagrams. A. Shear and Moment Diagram for a beam loaded symmetrically. B. Shear and Moment diagram for a beam loaded non-symmetrically. Note: The span remains constant. The effect of the beam selfweight has been neglected.

With reference to the transfer length, it was noted that strands where flexural capacity was achieved with short embedment lengths also had short transfer lengths. Several researchers have proposed development length equations linearly proportional to the transfer lengths [9, 68, 72]. Equation 5.1, proposed by Brooks, Grestle and Logan [9], states that the development length is related to the transfer length by a constant that equals the ratio of the stress in the strand at the limit state to the effective stress in the strand.

$$L_d = \frac{f_{ps}}{f_{pe}} * L_t \qquad \text{Equation 5.1}$$

Researchers at the University of Oklahoma [72] have proposed a crack control criteria by defining the constant as the ratio of the section nominal capacity to the moment that causes cracking.

A review of the literature revealed that researchers at Lehigh University [8] found that bond failure occurred when the stress in the strand within the transfer zone exceeded the effective prestress. Janney before them had also found that bond failure occurred when a high bond stress progressed toward the end of the beam and overlapped the transfer zone.

The researchers at University of Oklahoma [72] recognized that the stress in the strand increases at the cracks and the stress wave is directly related to the formation of cracks. The rationale is that by inhibiting the formation of cracks within the transfer region then the increase in strand stresses is negligible and bond failures are precluded.

The researchers at the University of Florida also believe the development length to be linearly related to the transfer length. Yet it is our belief that the constant should be the ratio of the strain in the strand at the limit state to the strain due to the effective prestress.

The stress waves described by Janney [34], and the researchers at Lehigh [8], were measured with strain gauges. Hence, these stress waves are actually strain waves. A simple correlation was attempted using Equation 5.2 with the data gathered at the University of Florida.

$$L_d = \frac{\varepsilon_{ps}}{\varepsilon_{pe}} * L_t \qquad \text{Equation 5.2}$$

where, ε_{ps} is the strain in the strand at the limit state
ε_{pe} is the strain in the strand due to the effective prestress

The results of this correlation are presented on Figure 5-16. Figure 5-16 presents a chart of the embedment lengths versus the estimated development lengths, using Equation 5.2.

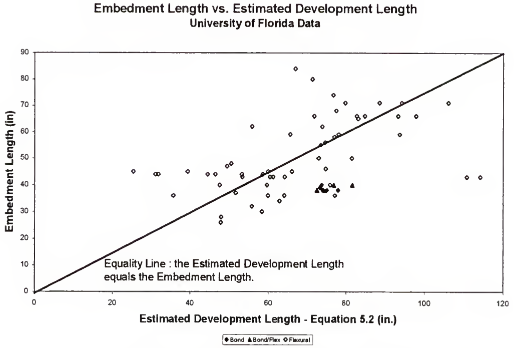

Figure 5-16 Embedment Length versus Predicted development Length Comparison Chart

Due to the nature of the flexural bond tests, where a range of values is determined through a trial and error process, meaningful descriptive statistical analysis could not be performed on the results obtained from Equation 5.2. The results were evaluated graphically in Figure 5-16.

Figure 5-16 shows an interesting trend where the bond type failures form a lower boundary, parallel to the Equality Line. Data points below the equality line are expected to have some type of bond failure. A similar type of analysis was done for data reported by other researchers, but the trend shown on Figure 5-16 could not be reproduced.

Further investigation is required to determine the adequacy of Equation 5.2. Equation 5.2 is simple, yet powerful. The strain in the strand at the limit state due to flexural action is determined from compatibility equations. The steel stresses required for the computation of flexural capacity are computed from this strain. The effect of shear – moment interaction can be accounted for by using modified compression field theory, MCFT, to estimate the strain in the strand, accounting for the shear contribution to the stress in the strand. Response2000, a Windows™-based software developed at the University of Toronto, consider MCFT for the computation of strains and stresses.

CHAPTER 6

TRANSFER LENGTH PREDICTOR EQUATION

6.1 Introduction

A design equation to estimate the transfer length is developed, tested and presented in this chapter. The knowledge and understanding of the nature of bond acquired through the analysis of the data presented in Chapter 5 was applied to the development of the transfer length predictor equation.

The aforementioned analysis of the data provided the author with a better understanding of the nature of bond and how it is influenced by parameters such as, concrete strength and strand diameter. The parameters targeted for study in this program included the effect of strand diameter and initial prestress. The exploration of the effect parameters such as concrete cover and concrete strength may have on bond was possible through a review of the published literature.

6.2 Nature of Bond

Regarding the effect the diameter of the strand may have on the strand's bond performance, transfer lengths were found to be proportional to the strand diameter for small diameter strands, $d_b < 6/10"$. For larger strands, transfer lengths are no longer proportional to the diameter of the strand. The departure from linear proportionality to the diameter of the strand observed in the transfer lengths measured on large diameter strands had already been reported in the literature.

Deatherage et al. [19] first reported that the transfer lengths measured on large diameter strands did not followed the trend of linear proportionality to the strand diameter seen in small diameter strands. The authors of an earlier publication found a similar trend. Yet, the authors credited the improved bond performance to rust in the 6/10" diameter strand [36].

Had, as reported by the authors, the corrosion in the strand been responsible for the reduction in the measured transfer lengths for 6/10" strands, this improved bond performance should have also been reflected on the transfer lengths measured on the cut ends of low concrete strength specimens. This improved bond performance was not reflected in the transfer lengths measured on those specimens. The improved bond performance was only observed on high concrete strength specimens and on the free ends of low concrete strength specimens. For this reason, it can be concluded that mechanical interlocking played an important role in the improved bond performance and the mechanical interlocking on the cut ends of low concrete strength specimens was destroyed at transfer, explaining the absence of an improved bond performance on this specimens.

Although the range of concrete strengths at transfer explored at the University of Florida was limited, transfer lengths were found to decrease as the concrete strength increases. Researchers at McGill University [55], which explored a substantially larger range of concrete strengths at transfer, proposed a correction factor that accounted for the strength of the concrete, see Equation 2.9.

The concrete cover was found to be effective for concrete covers of two-and-a-half strand diameters (2½ d_b) or smaller. Reductions in concrete cover carries increases in transfer lengths, while increases in concrete cover do not affect the bond performance of the strands.

The analysis of the data gathered at the University of Florida also revealed transfer length increases proportional to the initial prestress. This finding could not be corroborated with the data available in the literature.

6.3 Transfer Length Predictor Equation

The bond phenomena will be treated as a plane stress, concentric, thick walled elastic cylinder problem. The derivations for friction bond strength will not depart from the work done by Janney [34] and Dinsmore et al. [23]. Recently, Abrishami [1,2] did some developments where the cylinder material was described as series of layers: a cracked layer, a partially cracked layer and an isotropic, un-cracked layer. Bearing in mind that the ultimate goal is to obtain a design equation that adequately predicts transfer length, the material of the cylinder is assumed to be isotropic.

6.3.1 Transfer Length Equation Limitation and Assumptions

The development of an expression for the estimation of the transfer lengths required that some assumptions be made. The first assumption is regarding to the stresses in the concrete. The second assumption is regarding mechanical interlocking.

Concerning the concrete stresses, although the circumferential and radial stresses at the concrete-steel interface are of the same order of magnitude as the compressive strength of the concrete, stresses of such magnitude are limited to the region in immediate vicinity to the concrete – steel interface and diminish rapidly as the distance from the center of the cylinder increases [1, 2].

Figure 6-1 present a schematic of the circumferential stresses induced due to the swelling of the strand. These stresses are tensile. The distribution of the radial stresses is similar in shape and magnitude, but the stresses are compressive[1].

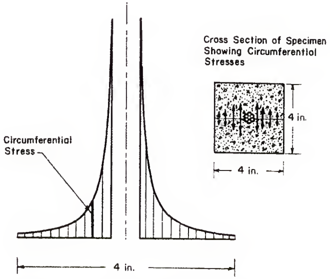

Figure 6-1 Schematic of Theoretical Distribution of Circumferential Stresses. Source: Reference 75

Research has found the mechanical properties of confined concrete to exceed those of unconfined concrete [6]. Rehm reported shear strengths in the order of ten times the concrete compressive strength for confined concrete [48].

The concrete cover affects transfer length only for concrete covers of two and a half strand diameters ($2.5d_b$) and smaller [21]. For concrete covers of less than three strand diameters the transfer length increases almost linearly. Concrete cover over two-

---

[1] For more information related to the stresses induced due to the swelling of the strand and/or due to the shrinkage of the concrete, please refer to References 1 and 75..

and-a-half strand diameters precludes the formation of splitting cracks and additional cover does not improve bond performance.

Assumption #1: Sufficient concrete cover is provided such that splitting cracks are precluded.

Assumption #2 The concrete in the immediate vicinity of the concrete – steel interface is well confined.

The research done by Mayfield [52], comparing the bond behavior of Dyform strands with that of regular strands, indicated that compacting the strand affected, in detriment, the bond performance of the strand. Proving the added bond capability due to mechanical interlocking. Figure 6-2 presents a schematic of the compacted, or Dyform, strand

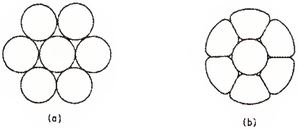

Figure 6-2 Schematic of the strand geometry. (a) Regular strand. (b) Compacted strand (Dyform) Source: Hurst's Prestress Concrete Design textbook

In the 1950s Rehm [65] found that the effectiveness of the concrete shear keys formed between the deformations in deformed reinforcing bars was a function of the size and shape of the deformations. These concepts appear to be true for strands also.

Using the bond performance of small diameter strands as a benchmark , Figure 5.9 show a marked improvement in bond performance for high concrete strength specimens reinforced with 6/10" strand. No difference in bond performance is observed for low-concrete strength specimens reinforced with 6/10" strand, or the cut ends. It must be concluded that the interstices of the larger diameter strands are large enough for the concrete in fluid form to fill them and be effective shear keys.

Mechanical interlocking is produced by the reaction of the strand outer wires against matching concrete shear keys as the strand tries to slip without twisting. The matching concrete shear keys are formed when the concrete is poured in fluid form and fills the interstices of the strand. The strength of the shear keys depends on the concrete strength and the geometry of the shear keys [65].

Assumption #3 Mechanical Interlocking is a function of the strand geometry and the concrete strength. For the mechanical interlocking, the interstices of the strand need certain dimensions that allow for the concrete, in fluid form, to fill them and harden as effective shear keys. The dimensions of the interstices of the 6/10" diameter strands, and larger, are such that allow for the mechanical interlocking to become effective.

6.3.2 Mechanical Interlocking Bond Strength

Figure 6.3 shows a schematic of the geometry of a strand. The center wire of the strand is a little larger, about 4%, than the outer wires to prevent the center wire from slipping. For the purpose of our discussion, the diameter of the center wire is assumed to be equal to that of the outer wires. The diameter of the individual wires, d_i, is equal to one-third the strands nominal diameter[2], d_b.

---

[2] ASTM defines the nominal diameter as the crown to crown distance, db.

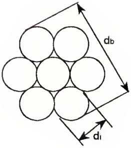

Figure 6-2 Strand Geometry

An enlargement of a section of the strand is presented on Figure 6.4. For clarity only two of the outer wires are presented. The mechanical interlocking bond strength was defined as the shear strength developed over the length "x_i", as defined in Figure 6.4. A right triangle and two outer wires define the length "x_i". Two corners of the right triangle, each with a 45° internal angle, coincide with the center of each wire. The length "x_i" is the distance between the two points where the legs of the triangle intersect the outer wires.

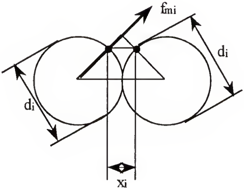

Figure 6-3 Schematic of the derivation of the Mechanical Interlocking Bond Strength

Recognizing that d_i equals one-third d_b, Equation 6.1 defines the distance x_i as:

$$x_i = {}^{d_b}\!/_{3} * (1 - \sin 45^\circ) \qquad \text{Equation 6.1}$$

Strands have six interstices. The shear strength acts over a unit distance equal to one over the cosine of the pitch. Figure 6-4 shows a schematic of the strand and the pitch.

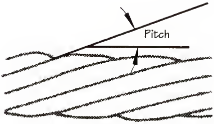

Figure 6-4 Schematic of the strand.

As such, Equation 6.2 defines the unit shear strength developed over the length "x_i". Equation 6.2 is simplified in Equation 6.3.

$$f_{mi} = 2\sqrt{f_{ci}}\,\frac{\left[6\left({}^{d_b}\!/_{3}\,(1-\sin 45^\circ)\right)\right]}{\cos\Phi} \qquad \text{Equation 6.2}$$

where Φ is the pitch of the strand

f_{ci} is the strength of the concrete at transfer

$$f_{mi} = 4\sqrt{f_{ci}}\,\frac{d_b(1-\sin 45^\circ)}{\cos\Phi} \qquad \text{Equation 6.3}$$

6.3.3 Frictional Bond Strength

6.3.3.1 Radial pressure at the concrete – steel interface

The friction bond strength is function of the radial stress on the concrete –steel interface and the friction coefficient. The radial stress at the interface is a function of the distance from the free end. The solution for the circumferential and radial stress in a thick-walled cylinder, obtained from Timonshenko and Goodier's book, *Theory of Elasticity,* is presented in Equation 6.4 [78].

$$\sigma_\theta = \frac{a^2 p_i}{b^2 - a^2}\left(1 + \frac{b^2}{r^2}\right) \qquad \text{Equation 6.4}$$

$$\sigma_r = -\frac{a^2 p_i}{b^2 - a^2}\left(1 - \frac{b^2}{r^2}\right)$$

where σ_r is the radial stress

σ_θ is the tangential, circumferential, stress

a is the inner radius of the cylinder

b is the outer radius of the cylinder

r is the distance from the center of the cylinder

p_i is the internal pressure on the cylinder

For the stresses at the interface, Equation 6.4 is evaluated at $r = a$. Equation 6.4 can be further simplified, see Equation 6.5, if the outer radii is assumed to be much larger than the inner radii, that is $b >> a$.

$$\sigma_\theta = p_i$$

$$\sigma_r = -p_i \qquad \text{Equation 6.5}$$

The internal pressure, p_i, is obtained from strain compatibility at the concrete – steel interface. Equation 6.6 gives the radial stain of a wire.

$$\varepsilon_r = \frac{\Delta r}{r} = \frac{\sigma_\theta - \upsilon(\sigma_z + \sigma_r)}{E} \qquad \text{Equation 6.6}$$

For the special case where the wire is free to expand, that is the radial and circumferential stresses are zero ($\sigma_r = \sigma_\theta = 0$) and the wire is prestressed, the radial strain on the wire is given by Equation 6.7.

$$\varepsilon_r = \frac{\upsilon_s \Delta\sigma_z}{E_s} = \frac{\upsilon_s(f_{si} - f_s)}{E_s} \qquad \text{Equation 6.7}$$

where f_{si} is the initial prestress

f_s is the transferred prestress at a given section

E_s the Young's Modulus of the wire

υ_s is the Poisson Ratio of the steel

At the concrete steel interface, Equation 6.8 gives the strain in the concrete cylinder. Equation 6.8 is a special case of Equation 6.6. The fact that the radial and tangential stresses have the same magnitude at the concrete – steel interface is recognized, see Equation 6.5.

$$\varepsilon_{rc} = \frac{\sigma_r(1 + \upsilon_s) + \sigma_z \upsilon_c}{E_c} \qquad \text{Equation 6.8}$$

The concrete axial compression, σ_z, can be expressed as the stress in the concrete cross section due to the transferred prestress at a given section, $f_s * \rho$. The radial stress can then be found from strain compatibility. The radial stress equals the difference between the strain on the unrestrained wire as the prestress decreases and the concrete restrain, times the Elastic Modulus of the steel. Equation 6.9 summarizes the strain compatibility relation.

$$\sigma_r = (\varepsilon_\theta - \varepsilon_{\theta_c})\, E_s \qquad \text{Equation 6.9}$$

Equation 6.10, a complete expression for the radial stress, σ_r, is obtained by substituting Equation 6.7 and 6.8 into Equation 6.9.

$$\sigma_r = \frac{(f_{si} - f_s)\, \upsilon_s - \rho\, f_s \upsilon_c\, n}{1 + (1 + \upsilon_c)\, n} \qquad \text{Equation 6.10}$$

6.4 Friction and Mechanical Bond

It can easily be shown that the change in force[3] on the strand equals the bond strength[4], μ, times the differential area over which the bond strength is acting. The differential area over which bond act is the perimeter of the wire times a differential length of wire. The relationship between bond and longitudinal stress in the wire is presented in Equation 6.11.

$$\mu = \frac{A_p}{\Sigma_o} \frac{df}{dx} \qquad \text{Equation 6.11}$$

where Ap is the area of the wire/strand

Σo is the perimeter of the wire/strand

$\frac{df}{dx}$ is the change in stress with distance

---

[3] The change in force is the cross sectional area, A_p, times the change in stress, df.

[4] The bond strength is a force per area.

The proposed bond stress includes frictional and mechanical interlocking components. The mechanical interlocking component is given by Equation 6.3 for large diameter strands, $d_b \geq 6/10"$. For strand diameters smaller than 6/10", the mechanical interlocking component is equaled to zero. Equation 6.12 presents the proposed bond stress equation.

$$\mu = \varphi\,(\sigma_r + f_{mi}\cos 45^\circ) + f_{mi}\sin 45^\circ \qquad \text{Equation 6.12}$$

where ϕ is the steel/concrete friction coefficient, $\phi \approx 0.3$ [75].

Equating Equation 6.11 and Equation 6.12 yields a first order, non-homogeneous differential equation. Equation 6.13 presents the solved differential equation.

$$\frac{df}{dx} + k_1 f_s = k_2$$

$$\therefore f_s = A\,e^{-k_1 z} + \frac{k_2}{k_1}$$

Boundary Condition $\rightarrow f_s = 0 \text{ @ } z = o$

$$\therefore A = -\frac{k_2}{k_1}$$

where

$$k_1 = k_3(\upsilon_s + n\,\rho\,\upsilon_c)$$

$$k_2 = k_3\,\upsilon_s\,f_{si} \quad + \frac{\Sigma_o}{A_p}\text{fmi}\,(\varphi\cos 45^\circ + \sin 45^\circ)$$

$$k_3 = \frac{\varphi \Sigma_o}{k_4 A_p}$$

$$k_4 = 1 + (1 + \upsilon_c)\, n$$

Equation 6.13

$$\therefore f_s = \frac{k_1}{k_2}(1 - e^{-k_1 z})$$

where z is the distance from the end of the specimen to the section under consideration,

n is the modular ratio and the remaining terms are as defined in previous sections of this chapter.

6.5 Transfer Length Predictor Equation

As presented in Chapter 2, the transfer length is the distance over which the prestressing force in the strand is transferred to the surrounding concrete. As such the stress in the strand at the end of the transfer length is, approximately, equal to the initial prestress. Equation 6.13 is evaluated for the boundary condition where $z = L_t$ and solved for the transfer length, Equation 6.14.

$$L_t = -\frac{1}{k_1}\ln(1 - \frac{k_2}{k_1} f_{si}) \qquad \text{Equation 6.14}$$

Again, bearing in mind that the ultimate goal is to present a simple design equation in a format similar to the present code equation format, Equation 6.13 was expanded into a series and evaluated for the boundary condition, $z = L_t$.

$$f_{si} = k_2 L_t - \frac{1}{2} k_1 k_2 L_t^2 + \ldots \qquad \text{Equation 6.15}$$

The higher order terms were dropped from Equation 6.15 and the equation solved for the transfer length, Equation 6.16.

$$L_t = \frac{f_{si}}{k_2} = f_{si}\frac{A_p}{\Sigma_o}\left[\frac{1}{\dfrac{\varphi\, \upsilon_s\, f_{si}}{1+(1+\upsilon_c)n} + f_{mi}\,(\varphi \text{ cosine } 45^\circ + \text{sine } 45^\circ)}\right] \qquad \text{Equation 6.16}$$

6.5.1 Measured Transfer Lengths versus Predicted Transfer Lengths: University of Florida Data

Transfer lengths were computed, using Equation 6.16, with the parameters gathered at the University of Florida and compared to the measured transfer lengths. The computed transfer lengths showed a good correlation to the measured transfer lengths, $R^2 \approx 45\%$, considering the scatter of the data seen in Chapter 5.

A linear regression analysis showed that the computed transfer lengths were about one-half the measured transfer length. An expected shortfall since Equation 6.16 was obtained by truncating Equation 6.15. Equation 6.16 had to be modified such that the computed transfer lengths were increased by a factor of two (2).

Previous researchers have demonstrated the effect the surface condition has on the measured transfer lengths. To account for the different surface conditions of the strands, correction factors were applied to the computed transfer lengths. Transfer lengths computed for rusted strands were reduced by 25%[5], i.e. multiplied by a factor of 0.8. The computed transfer lengths for indented or deformed wires were multiplied by a factor of

---

[5] Reductions of 20% to 40% in transfer length, due to rusting of the strand, have been reported. The average improvement that can be expected is about 25%.

0.7, or a 42% reduction[6]. The transfer lengths measured at the University of Florida were compared to the corresponding estimations of the transfer lengths.

Figure 6-5 presents the graph of the measured transfer lengths, measured at the University of Florida, versus the corresponding transfer lengths estimates. By accounting for the different surface conditions the Coefficient of Determination, R^2, improved from, approximately, 45% to 69%. With a coefficient of variation of about 0.14.

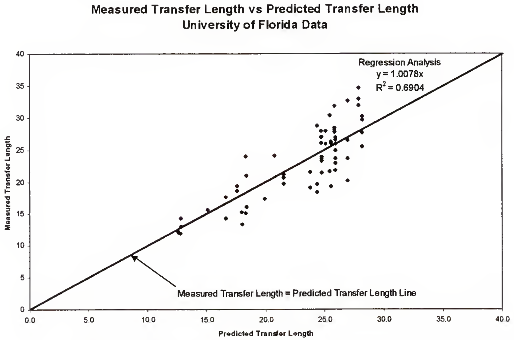

Figure 6-5 Measured Transfer Length versus Predicted Transfer Length Comparison. (UF Data Only)

6.5.2 Recent Research Projects Database

A database containing the transfer lengths reported by the most recent projects only was developed. The data reported by Mayfield [52], the University of Texas [68] and the University of Oklahoma [67], McGill University [55], Deatherage at the University of Tennessee – Knoxville [19] and the University of Florida were included. Although the data reported by Mayfield cannot be considered recent, inclusion of this data on the database was deemed necessary since, aside from the transfer lengths reported by the University of Florida, Mayfield is the only other researcher to report transfer lengths for 7/10" diameter strands, albeit the strand tested were 19-wire strands. A total of 229 data points were included in the database.

---

[6] Ratio of the transfer lengths measured on 3/8" indented wire strands to those measured on 3/8" smooth wire strands.

Transfer length reported by McGill University for specimens, 16/89-975 and 16/89-675, as well as University of Texas series FC5, FCT5, FC6 and FCT6 were expunged from the database. The researchers at McGill University reported having problems during the stressing operation for these two specimens. The initial prestress levels of the strands on these two specimens were substantially low, 126 ksi, and are not considered typical of prestress concrete applications.

The specimens belonging to the University of Texas series FC5, FCT5, FC6 and FCT6 were 5" by 13" specimens reinforced with five (5) strands. The pre-compression levels on these specimens were of the order of 2250 psi and 3000 psi, for 1/2" and 6/10" diameter strands, respectively. The magnitude of the stresses to which these specimens were subjected appears to have adversely affected the bond performance of the strands. The transfer lengths reported for these series were, on average, 25% to 30% longer than those reported for their companion AASHTO type sections.

6.5.3 Test for Systematic Errors

The ratios of the measured transfer lengths to the predicted transfer lengths were computed. These ratios were plotted against parameters such as concrete strength or strand diameter. This type of graph permitted the identification of systematic errors on the predictor equation.

The coefficient of variation of the ratio of the measured to predicted transfer length for the database population was 0.24, compared to 14% for the data gathered at the University of Florida. Such difference is expected due to the variations in test procedures and materials used in the different research programs.

Systematic errors in the effect of the initial prestress and the compressive strength of the concrete at transfer were identified. Transfer lengths for the Grade 290 and Grade 300 strands underestimated, that is measured to predicted transfer length ratios greater than 1.0. The effect of high concrete strengths, f`c > 6000 psi, on transfer length was overestimated, i.e. measured to predicted transfer length ratios smaller than 1.0, see Figure 6-6.

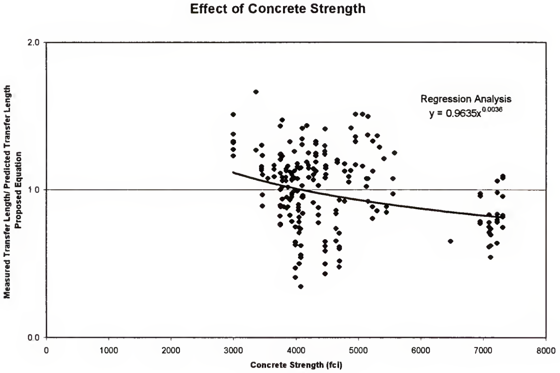

Figure 6-6 Effect of Concrete Strength (un-corrected)

Two correction factors were introduced to account for the higher Grades of strand and the concrete strength. The transfer length predictor equation was simplified[7] in Equation 6.17.

$$L_t = \alpha_1\,\alpha_2\,\alpha_3\,2\,f_{si}\,\frac{A_p}{\Sigma_o}\left[\frac{1}{\dfrac{\varphi\,\upsilon_s\,f_{si}}{1+(1+\upsilon_c)n}+f_{mi}}\right] \qquad \text{Equation 6.17}$$

where f_{mi} is the mechanical interlocking bond strength, zero for $d_b < 6/10"$ and $2\sqrt{f_{ci}}$ for $d_b \geq 6/10"$.

α_1 is the strand surface condition correction factor, 1.0, 0.8 and 0.7, for shiny, rusted and deformed strands, respectively

α_2 initial prestress correction factor, $\left[\dfrac{f_{pi}}{202.5\text{ ksi}}\right]^{\frac{4}{3}}$

α_3 concrete strength correction factor, $\sqrt[3]{\dfrac{4000\text{ psi}}{f_{ci}}}$

A correction factor to account for the strength of the concrete at transfer, similar to α_3 but in terms of the squared root of the concrete strength, has already been proposed by researchers at McGill University, see Equation 2.9. Recently, Darwin, while working on high rib area reinforcing bars, found good correlations for the development length of reinforcing bars with the fourth root of the concrete strength. The correction factor α_3, as presented, minimized the coefficient of variation of the transfer lengths ratio and removed the systematic error from the predictor equation.

---

[7] The "ϕ cos(45) + sin (45)" term was dropped because the value of this term is approximately 1.0. A factor of two, obtained from a linear regression analysis of the data gathered at the University of Florida, was applied to Equation 6.16.

Figure 6.7 presents a graph of the ratios of the measured transfer length to the predicted transfer length versus the strand diameter. Incorporating the correction factors that account for the strand surface condition, the initial prestress in the strand and the compressive strength of the concrete at transfer resulted in a horizontal trendline with an average value of 1.0. The power of the equation approaches zero, 0.032, indicating an insignificant deviation from the mean value with changes in the strand diameter[8].

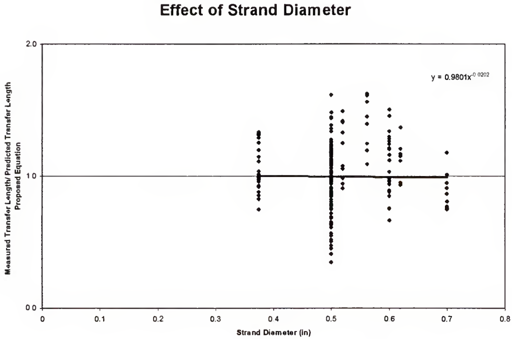

Figure 6-7 Effect of Strand Diameter on the Measured -Predicted Transfer Length Ratios

Figure 6.8 and 6.9 presents graphs similar to the graph depicted in Figure 6.7. Figure 6.8 presents the effect of initial prestress on the ratio of the measured to predicted transfer length. Figure 6.9 presents the effect of the compressive strength of the concrete, at the time the prestressing force is transferred from the strand to the concrete section, on the measured to predicted transfer length ratio. Again, incorporating the correction factors produced a horizontal trendline with mean values of 1.0, and slight deviations from the mean with over the range of values for initial prestress and concrete compressive strength at transfer.

---

[8] Any number raised to a power of 0 equals 1, $x^0=1$.

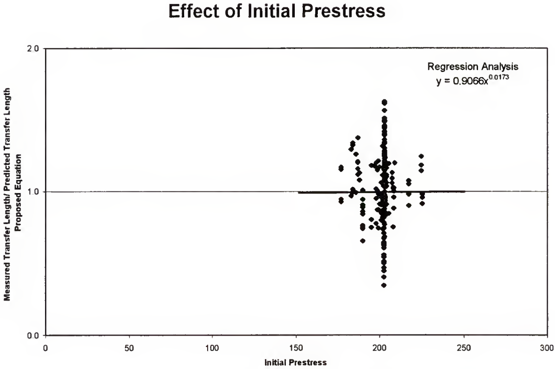

Figure 6-8 Effect of Initial Prestress on Proposed Predictor Equation

Similar graphs were prepared for the transfer length predictor equation proposed in the ACI 318 Commentary, Zia and Mostafa (presented in Nilson's textbook) [57] and Equation 2.9. Other transfer length predictor equations have been proposed. Most of these equations are variations of the equation presented on the Commentary of ACI 318, where the estimate of the transfer length is increased by certain factor. Some of the proposed equations relate the transfer length to the initial prestress, instead of the effective prestress as the equation in the Commentary to ACI 318.

The equations used in the following investigation depart, to some degree, from the equation presented on the Commentary to ACI 318 in their description of the transfer length phenomena.

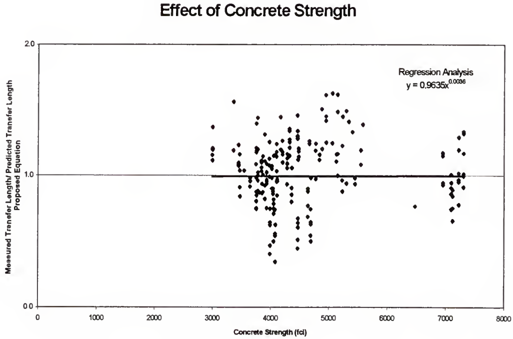

Figure 6-9 Effect of Concrete Strength on Proposed Predictor Equation (Corrected)

Most of the proposed equations assume a linear relationship between the tranfer length and the diameter of the strand. The equations under study differ in that, aside from the equation presented on the Commentary to ACI 318, the transfer length is related to the initial prestress and attempt to include the effect of the strength of the concrete at transfer into the description of the transfer length behavior. The equation presented by Zia & Mostafa is the first, reported, attempt to account for the effect of the concrete strength. Equation 6.9, proposed by researchers at McGill University, describe the effect of the concrete strength in terms of the squared root of the ratio of a benchmarck concrete strength (3 ksi) to the concrete strength at transfer.

As mentioned before, the three equations under investigation assume a linear relationship between the transfer length and the strand diameter. As such, the response of any of these equation over the range of strand diameter is similar to that of the other two. Figure 6.10 shows the variation in measured to predicted transfer length ratio over the range of strand diameters. A regression analysis of the ratios of the measured to predicted transfer length yielded a negatively sloped line, indicating that the predictor equation tend to overestimate the effect of strand diameter for large diameter strands.

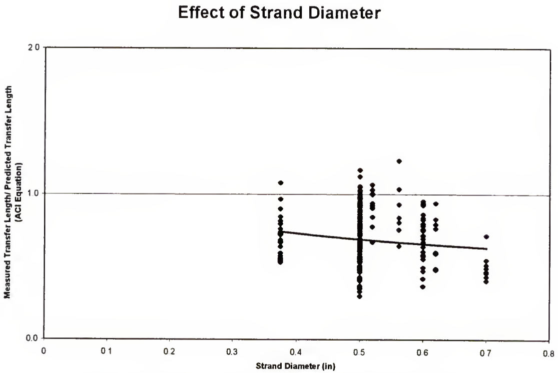

Figure 6-10 Effect of Strand Diameter on ACI Predictor Equation

Figure 6-11 and Figure 6-12 present the effect of the initial prestress and the strength of the concrete at transfer on the ACI Commentary equation, respectively. As seen in Figure 6-11 and Figure 6-12, the transfer length predictor equation proposed in the Commentary of ACI 318 does not adequately describe the effect of the initial prestress nor that of the strength of the concrete at transfer on transfer length.

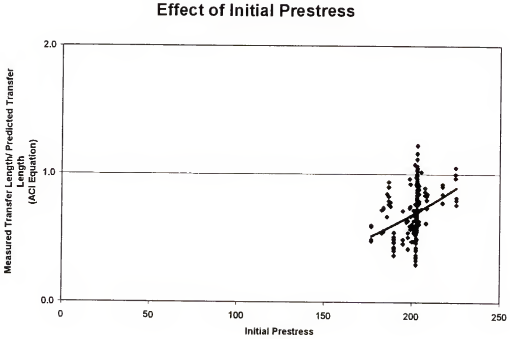

Figure 6-11 Effect of Initial Prestress on ACI Commentary Predictor Equation

The transfer length predictor equation proposed by Zia and Mostafa, Equation 2.7, relates the transfer length as inversely, linearly, proportional to the concrete strength at transfer. As seen previously, the transfer length – concrete strength relationship, although inversely proportional, is not linear.

Figure 6-13 presents the effect of the concrete strength on the Zia & Mostafa transfer length predictor equation. Figure 6-14 depicts the effect of the concrete strength on Equation 2.9. Equation 2.7 and Equation 2.9 describe the effect of the initial prestress similar to the equation presented in the Commentary of ACI 318. The systematic errors observed on these two equations, Equation 2.7 and Equation 2.9, over the range of initial prestress are similar to those observed on Figure 6.11.

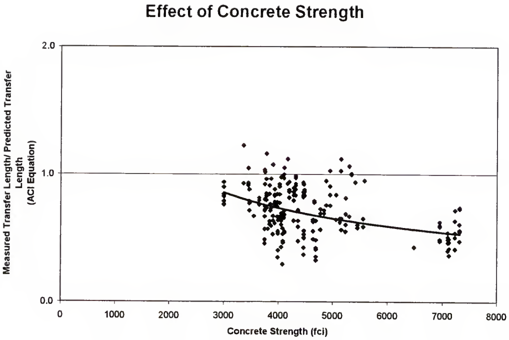

Figure 6-12 Effect of Concrete Strength on ACI Commentary Predictor Equation

The equation proposed by Zia & Mostafa did not adequately describe the effect of the concrete strength at transfer on the transfer length. Equation 2.9 description of the effect of the concrete strength is substantially better than that of the ACI Commentary or Zia & Mostafa equations. Yet, Equation 2.9 did not adequately describe the effect of the initial prestress on the transfer length.

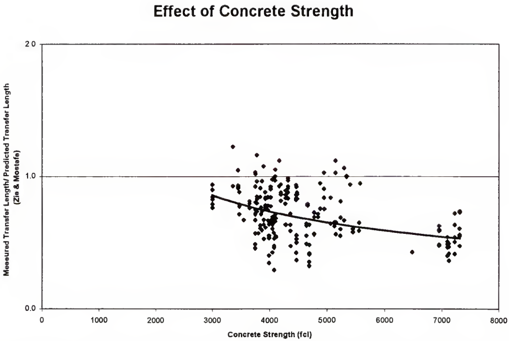

Figure 6-13 Effect of Concrete Strength on Zia & Mostafa Predictor Equation

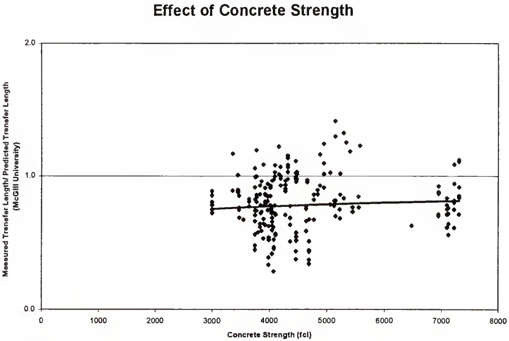

Figure 6-14 Effect of Concrete Strength on McGill University Predictor Equation.

6.6 Transfer Length Design Equation

The mean and the standard deviation of the measured transfer length to predicted transfer length ratios was computed for the data gathered at the University of Florida and all the data included in the recent research projects database. The coefficient of variations, COV[9], for measured to predicted transfer length for the University of Florida data was 13.2%. The coefficient of variation for all the data in the database was 24.0%. The third column identified as "UF Design" represents Equation 6.18, presented later in this text, using $\alpha_4 = 3.3$.

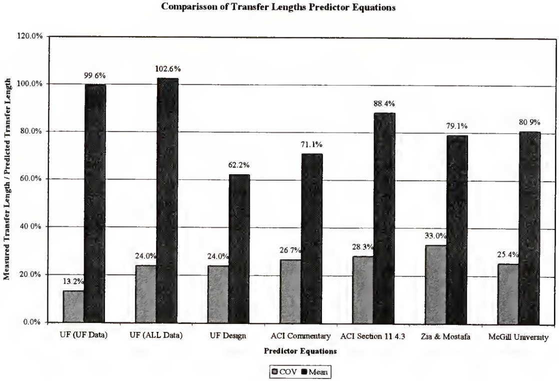

Figure 6-15 Comparison of Proposed Transfer Length Predictor Equations

---

[9] COV = standard deviation/mean

These represent 10% and 6% improvements over those obtained for the equations proposed by the ACI Commentary and McGill University, respectively. The improvement over the Zia & Mostafa and the ACI Section 11.4.3 are more significant, in the order of 37.5% and 18%, respectively.

For clarity Equation 6.17 is rewritten in the form of Equation 6.18.

$$Lt = \alpha_1 \alpha_2 \alpha_3 \alpha_4 f_{si} \frac{A_p}{\Sigma_o} \left[\frac{1}{\dfrac{\varphi \upsilon_s f_{si}}{1+(1+\upsilon_c)n} + f_{mi}} \right] \qquad \text{Equation 6.18}$$

The factor α_4 has been introduced to facilitate the development of a design equation (The factor α_4 had a value of two (2) in Equation 6.17.). For a design equation it is desirable to obtain a value that envelopes, at least, 95% of the experimentally measured transfer lengths. To that end the bond strength, that is the term in the bracket of equation 6.18, is reduced by a strength reduction factor, given by Equation 6.19. Mathematically this operation is identical to increasing the factor α_4, by the inverse of Equation 6.19.

$$\varphi = (1 - k\,COV) \qquad \text{Equation 6.19}$$

where k = 1.64 for an infinite number of observations and 2.0 for forty (40) observations
COV is the Coefficient of Variation

Since the database contained over 220 observation, a k=1.64 will be used and substituting the computed Coefficient of Variation, COV =24.0%, into Equation 6.20, ϕ = 0.6064. Multiplying the factor α_4 by the inverse of ϕ, a design value for α_4 is obtained, $\alpha_4 = 3.3$.

Figure 6-16 presents a graph of the effect of the strand diameter on the ratio of the measured to predicted transfer lengths, with $\alpha_4 = 2$. The line identified as 95% Fractile Analysis Line represents the shift in the average ratio caused by the reduction factor, ϕ. Since the systematic errors have been removed from Equation 6.18, similar graphs can be constructed for the effect of concrete strength and initial prestress, f_{pi}.

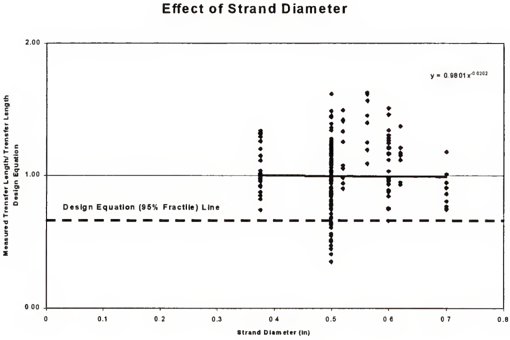

Figure 6-16 Design Transfer Length Equation (95% Fractile) Equation 6.18 with α_4=3.3

CHAPTER 7

CONCLUSIONS AND DESIGN RECOMMENDATIONS

7.1 Introduction

The purpose of this investigation was to obtain fundamental information regarding the effect of strand diameter and initial prestress on the transfer and development length performance of prestressing strands. The efficient use of high strength concrete demands an increase in prestressing force. As mentioned before, the increase in prestressing force demands either additional strands, for which sections have been developed to provide additional space to accommodate the additional strands, or by increasing the per strand force. The later is achieved by increasing the area of individual strands, increasing the strand's breaking strength or a combination of both.

The effect of the strand diameter and the initial prestress on transfer and development length was explored experimentally. An attempt was made to analytically explain the behavior observed in the effect of large diameter strands on transfer length.

7.2 Transfer Length

7.2.1 Experimental Program

Transfer lengths were measured experimentally by means of concrete surface deformation measurements and end-slip measurements. Concrete surface profiles were constructed and transfer lengths estimated following the procedures presented in Chapter

4, that is the Slope-Intercept method and the 95% Average Maximum Strain method. Transfer lengths were also estimated from end-slip measurements assuming a linear strain profile.

7.2.2 Conclusions

Transfer lengths measured on specimens reinforced with small diameter strands, i.e. strand diameters smaller than 6/10", were proportional to the strand diameter. The transfer lengths measured on specimens with large diameter strands, that is $d_b \geq 6/10"$, were not proportional to the strand diameter.

The transfer length provisions presented in the Commentary to ACI 318 adequately predicted the mean transfer length for small diameter strands. For large diameter strands, the Commentary on ACI 318 transfer length provisions overestimated the transfer lengths. ACI 318 Section 11.4.3, $L_t = 50d_b$, also provided a good estimate of the mean transfer length. Inclusion of 95% of the data required 75 to 80 strand diameters.

Transfer lengths were found to be inversely proportional to the compressive strength of the concrete at transfer, f'_{ci}, and directly proportional to the initial prestress, f_{pi}. That is, the transfer lengths decreased as the concrete strength increased and increased as the initial prestress in the strand increased.

As previously reported in the literature, a good correlation was found between the transfer lengths estimated from end-slip measurements and the transfer lengths estimated from measured deformations. A best-fit analysis of the data coincided with the transfer lengths estimated assuming a linear strain profile. The transfer lengths estimated, from end-slip measurements, assuming a parabolic strain profile enveloped most of the data, about 90%.

A fifty percent (50%) improvement in the transfer lengths estimated from measured deformations was observed on the 3/8" Grade 270 indented wire strand compared to the 3/8' Grade 270 smooth wire strand. The improved bond performance of the indented wire was corroborated by the measured end-slips. Simple pullout tests, Moustafa type test, could not reproduce the improved bond performance of the indented wire strand.

7.3 Development Length

7.3.1 Experimental Program

The specimens were cured for 28 days and tested in a two-point load configuration. The two-point configuration provided a constant moment region, neglecting the effect of the specimen's weight, which allowed for the loading of the specimen at the critical anchorage section. Strand slippage and deflections were continuously recorded and the cracks patterns marked at discrete intervals.

7.3.2 Conclusions

All the specimens loaded at embedment lengths in excess of 80% of the ACI 318 development length estimate, where adequate shear reinforcement was provided, were able to achieve ductile, flexure type, failures.

As presented in the literature, the formation of cracks crossing the level of the strand within the transfer region led to bond failures. In addition, the results seen on series UF17, 1/2" Special Grade 290 strand, where bond and flexural type failures were observed at identical embedment lengths on ends with different transfer lengths, indicated that the development length appears to be proportional to the transfer length. Yet, it is not possible to reach a conclusion, with some degree of certainty, because the data available is insufficient.

7.4 Design Recommendations

A transfer lengths predictor equation was successfully developed. The predictor equation is based on the thick-walled hollow cylinder solution presented by Timoshenko. Frictional and mechanical interlocking bond mechanisms are present in the transfer bond mechanism of large diameter strands, while the transfer bond mechanism for small diameter strand is, predominantly, frictional.

Equation 7.1 reasonably predicts the measured transfer lengths.

$$L_t = \alpha_{rm}\alpha_1\alpha_2\alpha_3\alpha_4 f_{si}\frac{A_p}{\Sigma_o}\left[\frac{1}{\dfrac{\varphi\,\upsilon_s f_{si}}{1+(1+\upsilon_c)n}+f_{mi}}\right] \qquad \text{Equation 7.1}$$

where f_{si} is the initial prestress in the strand

A_p is the strand nominal area

Σ_o is the perimeter of the strand, $1.33\,\pi\,d_b$

n is the modular ratio, Eps/Ec

φ is the friction coefficient of the steel, 0.3.

ν_s and ν_c are the Poisson ratios for the steel and concrete, respectively.

f_{mi} is the mechanical interlocking bond strength, zero for $d_b < 6/10"$ and $2\sqrt{f_{ci}}$ [1] for $d_b \geq 6/10"$.

α_{rm} is the release method correction factor, 1.0 for gradual release and 1.3 for flame-cut, or sudden release.

---

[1] f'_{ci} has unit of pound per square inches, psi.

α_1 is the strand surface condition correction factor, 1.0, 0.8 and 0.7, for shiny, rusted and deformed strands, respectively

α_2 initial prestress correction factor, $\left[\frac{f_{pi}}{202.5\,\text{ksi}}\right]^{\frac{4}{3}}$

α_3 concrete strength correction factor, $\sqrt[3]{\frac{4000\,\text{psi}}{f'_{ci}}}$

α_4 a constant that assume a value of 2 for stress verification and 3.3 for shear and moment strength verification.[2]

The adequacy of Equation 7.1 is limited to elements where sufficient concrete cover and confinement steel is provided to preclude the formation of splitting cracks, that is concrete cover greater than four strand diameters, concrete compressive strengths in a 3500 psi to 8000 psi range and initial prestress in a 190 ksi to 225 ksi range. Equation 7.1 is valid for strand diameters ranging from 3/8" to 7/10".

7.5 Future Research

Over the course of this study several questions were raised that could not be answered. An understanding of the nature of bond cannot be complete without those questions being satisfactorily answered. Further experimental studies need to be done to answer the following questions.

- Effect of partial prestressing.
- Effect of aggregate type, gravel versus limestone.

---

[2] Simmons, in his PhD Dissertation, demonstrate that underestimating the transfer length leads to unsafe shear designs. Yet, a short estimate of the transfer length yields a worst-case scenario for allowable stress verification. This provision is similar to that found on the CEB-FIP Model Code 1990.

- Additional measured transfer lengths for large diameter strands, such that empirical analysis of the data is not dominated by the behavior of the small diameter strands.

APPENDIX I

CONCRETE STRAIN PROFILES

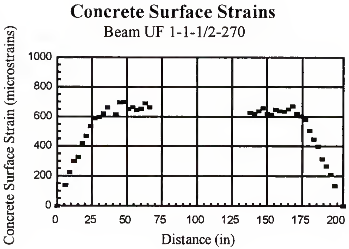

Figure I-1 Concrete Surface Strain: Beam UF 1-1-1/2-270

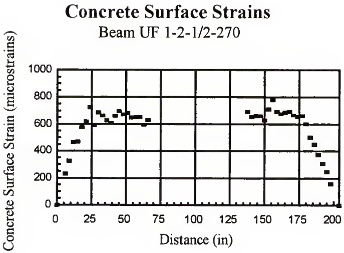

Figure I-2 Concrete Surface Strain: Beam UF 1-2-1/2-270

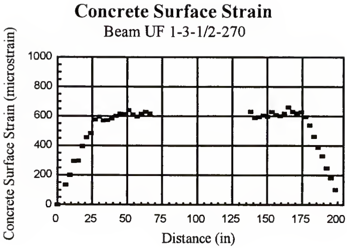

Figure I-3 Concrete Surface Strain: Beam UF 1-3-1/2-270

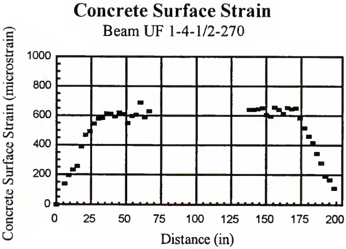

Figure I-4 Concrete Surface Strain: Beam UF 1-4-1/2-270

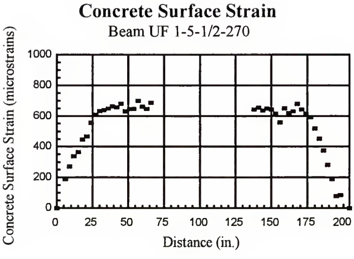

Figure I-5 Concrete Surface Strain: Beam UF 1-5-1/2-270

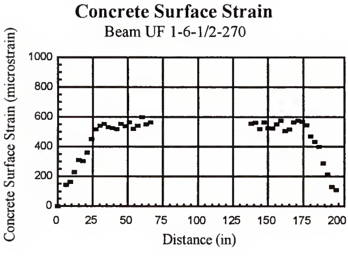

Figure I-6 Concrete Surface Strain: Beam UF 1-6-1/2-270

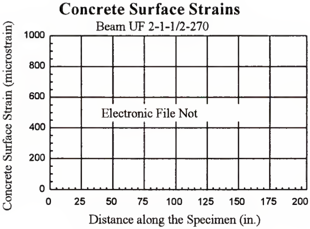

Figure I-7 Concrete Surface Strain Beam UF 2-1-2/1-270

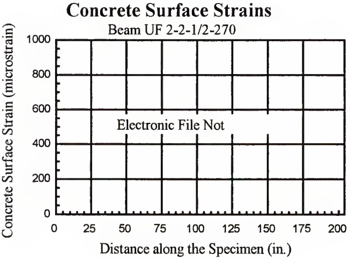

Figure I-8 Concrete Surface Strain Beam UF 2-2-2/1-270

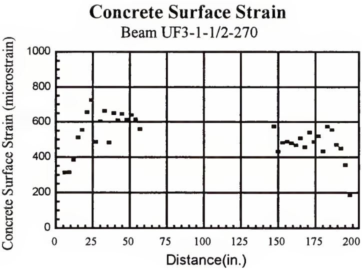

Figure I-9 Concrete Surface Strain: Beam UF 3-1-1/2-270

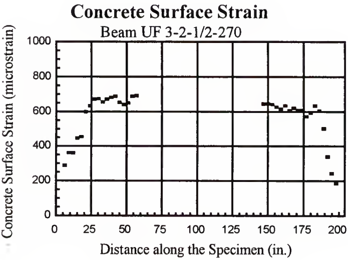

Figure I-10 Concrete Surface Strain: Beam UF 3-2-1/2-270

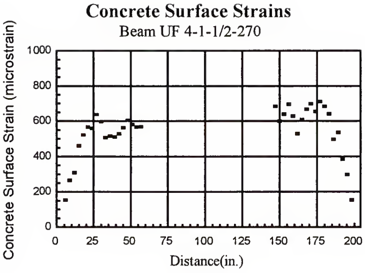

Figure I-11 Concrete Surface Strain: Beam UF 4-1-1/2-270

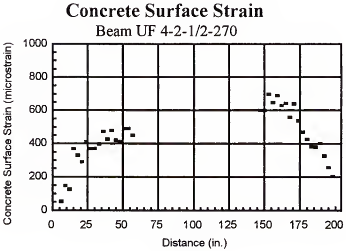

Figure I-12 Concrete Surface Strain: Beam UF 4-2-1/2-270

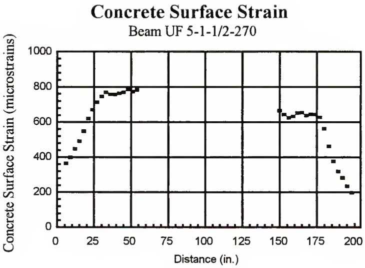

Figure I-13 Concrete Surface Strain: Beam UF 5-1-1/2-270

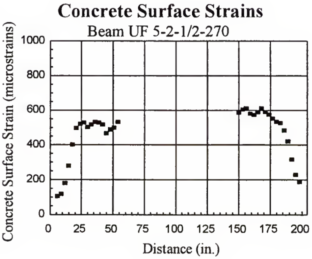

Figure I-14 Concrete Surface Strain: Beam UF 5-2-1/2-270

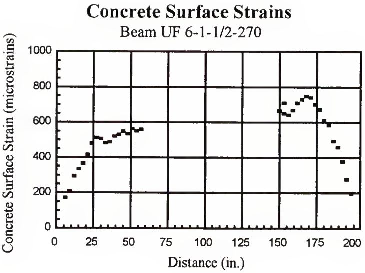

Figure I-15 Concrete Surface Strain: Beam UF 6-1-1/2-270

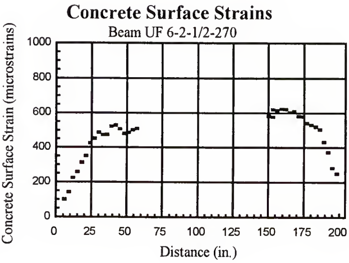

Figure I-16 Concrete Surface Strain: Beam UF 6-2-1/2-270

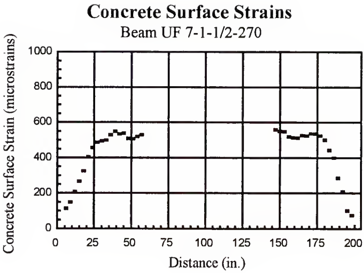

Figure I-17 Concrete Surface Strain: Beam UF 7-1-1/2-270

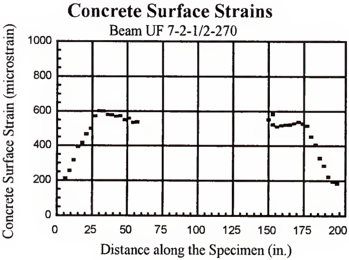

Figure I-18 Concrete Surface Strain: Beam UF 7-2-1/2-270

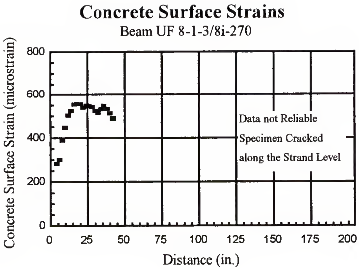

Figure I-19 Concrete Surface Strain: Beam UF 8-1-3/8i-270

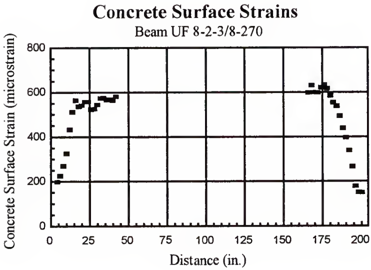

Figure I-20 Concrete Surface Strain: Beam UF 8-2-3/8-270

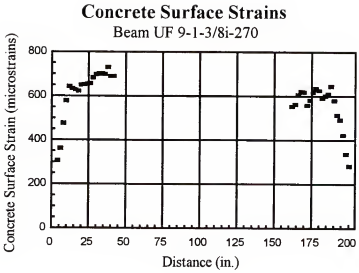

Figure I-21 Concrete Surface Strain: Beam UF 9-1-3/8i-270

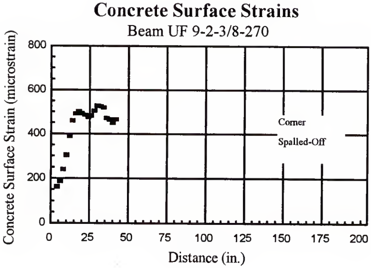

Figure I-22 Concrete Surface Strain: Beam UF 9-2-3/8-270

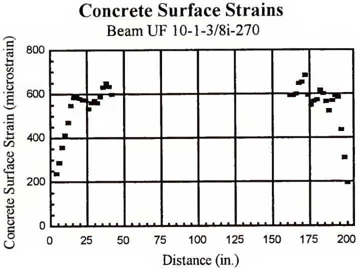

Figure I-23 Concrete Surface Strain: Beam UF 10-1-3/8i-270

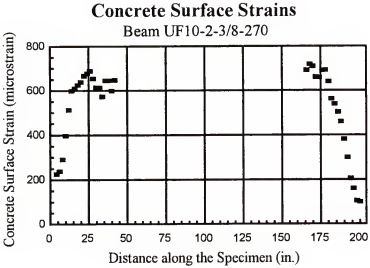

Figure I-24 Concrete Surface Strain: Beam UF 10-2-3/8-270

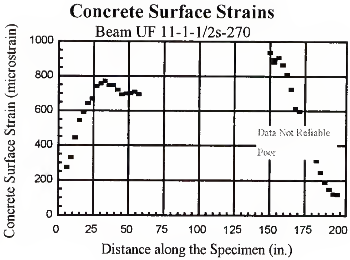

Figure I-25 Concrete Surface Strain: Beam UF 11-1-1/2s-270

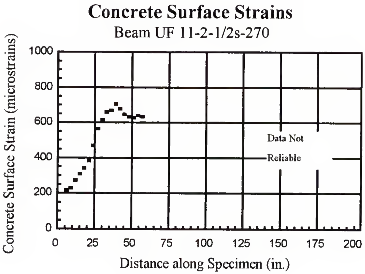

Figure I-26 Concrete Surface Strain: Beam UF 11-2-1/2s-270

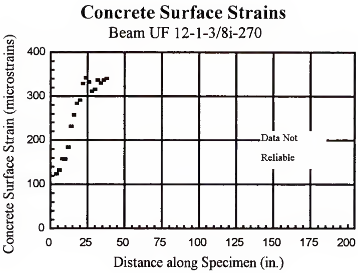

Figure I-27 Concrete Surface Strain: Beam UF 12-1-3/8i-270

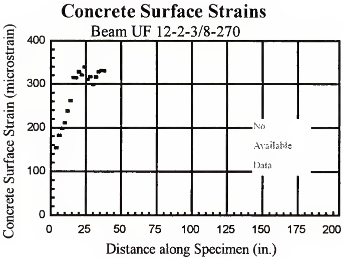

Figure I-28 Concrete Surface Strain: Beam UF 12-2-3/8-270

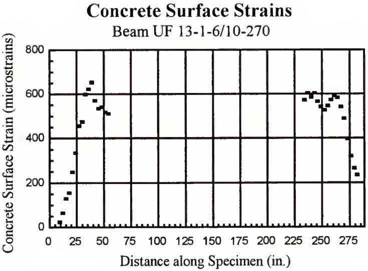

Figure I-29 Concrete Surface Strain: Beam UF 13-1-6/10-270

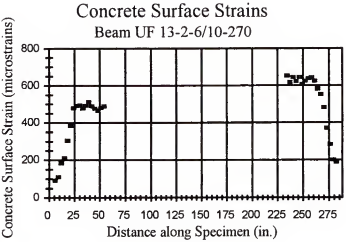

Figure I-30 Concrete Surface Strain: Beam UF 13-2-6/10-270

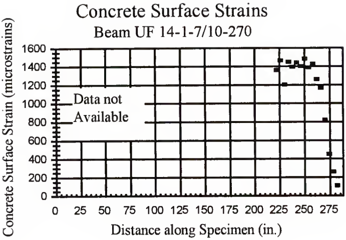

Figure I-31 Concrete Surface Strain: Beam UF 14-1-7/10-270

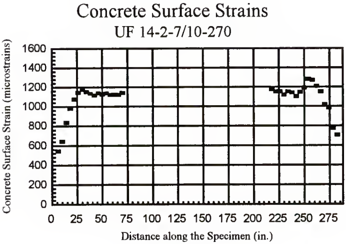

Figure I-32 Concrete Surface Strain: Beam UF 14-2-7/10-270

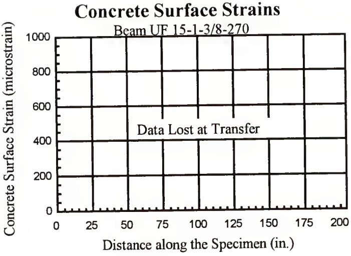

Figure I-33 Concrete Surface Strain Beam UF 15-1-3/8-270

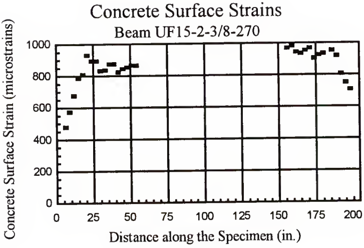

Figure I-34 Concrete Surface Strain: Beam UF 15-2-3/8-270

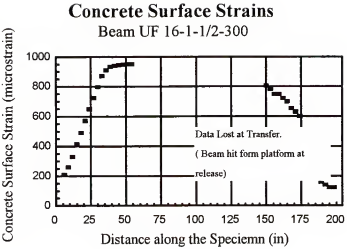

Figure I-35 Concrete Surface Strain: Beam UF 16-1-1/2-300

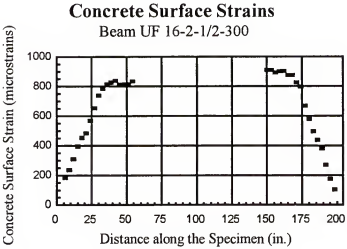

Figure I-36 Concrete Surface Strain: Beam UF 16-2-1/2-300

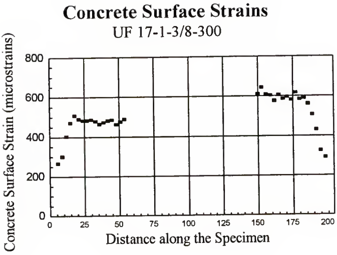

Figure I-37 Concrete Surface Strain: Beam UF 17-1-3/8-300

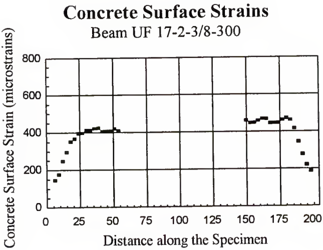

Figure I-38 Concrete Surface Strain: Beam UF 17-2-3/8-300

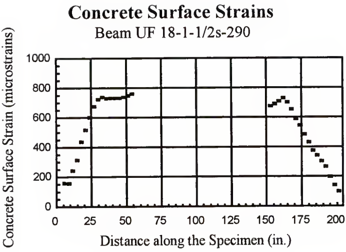

Figure I-39 Concrete Surface Strain: Beam UF 18-1-1/2s-290

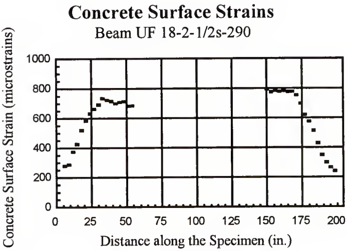

Figure I-40 Concrete Surface Strain: Beam UF 18-2-1/2s-290

APPENDIX II

LOAD DISPLACEMENTS CHARTS

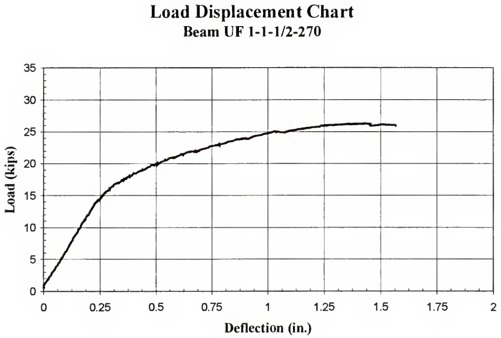

Figure II-1 Load Displacement Diagram Beam UF 1-1-1/2-270

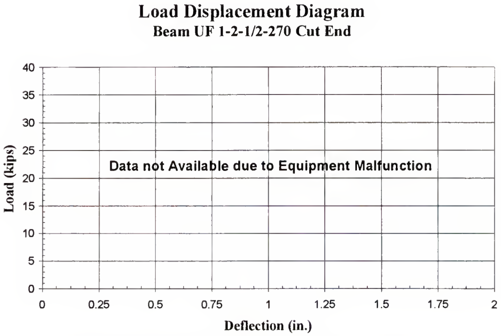

Figure II-2 Load Displacement Diagram Beam UF 1-2-1/2-270

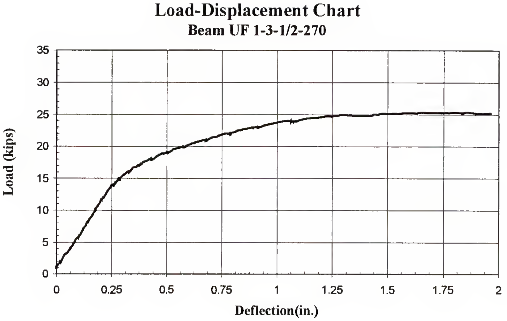

Figure II-3 Load Displacement Diagram Beam UF 1-3-1/2-270

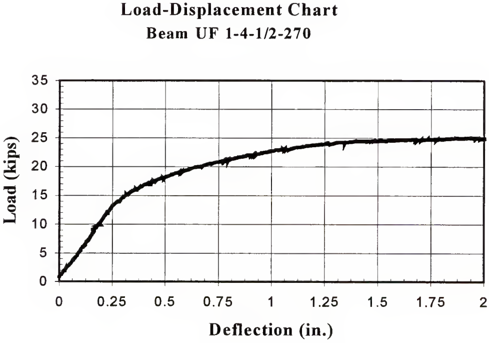

Figure II-4 Load Displacement Diagram Beam UF 1-4-1/2-270

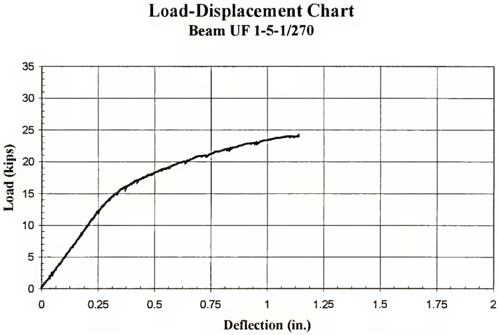

Figure II-5 Load Displacement Diagram Beam UF 1-5-1/2-270

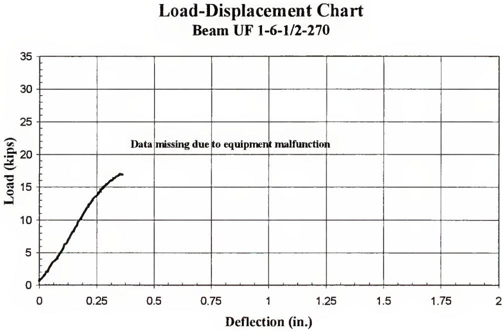

Figure II-6 Load Displacement Diagram Beam UF 1-6-1/2-270

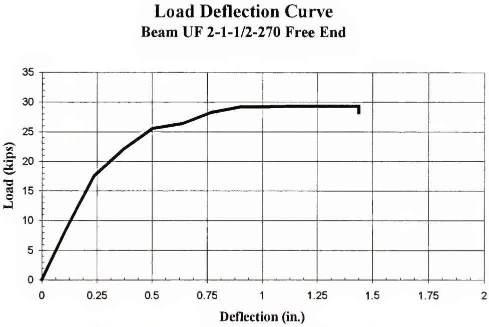

Figure II-7 Load Displacement Diagram Beam UF 2-1-1/2-270 Free End

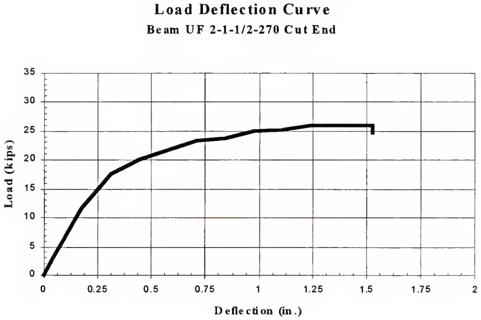

Figure II-8 Load Displacement Diagram Beam UF 2-1-1/2-270 Cut End

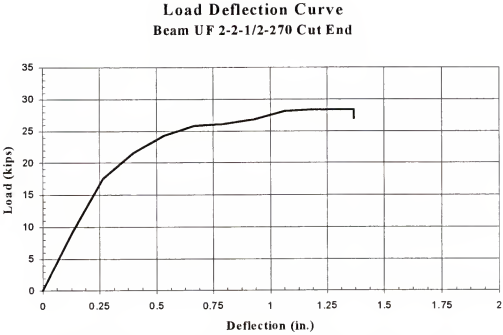

Figure II-9 Load Displacement Diagram Beam UF 2-2-1/2-270 Cut End

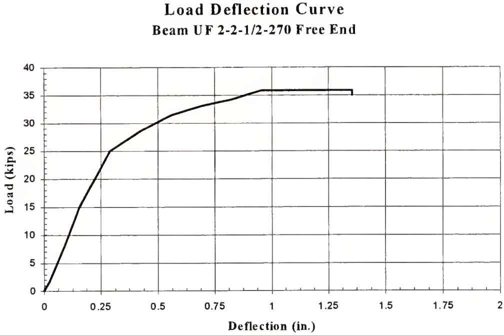

Figure II-10 Load Displacement Diagram Beam UF 2-2-1/2-270 Free End

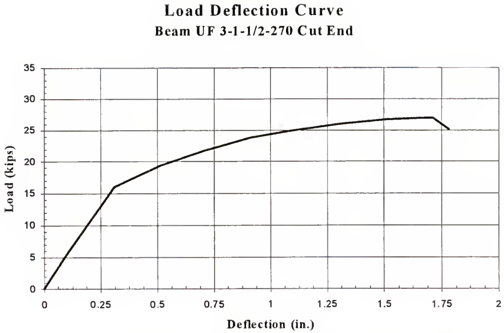

Figure II-11 Load Displacement Diagram Beam UF 3-1-1/2-270 Cut End

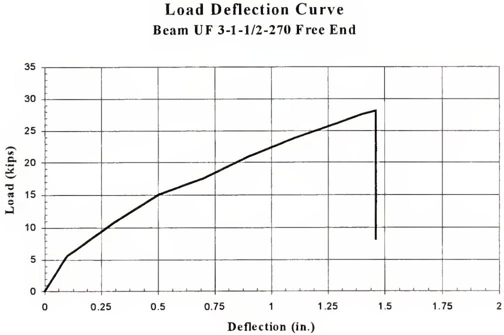

Figure II-12 Load Displacement Diagram Beam UF 3-1-1/2-270 Free End

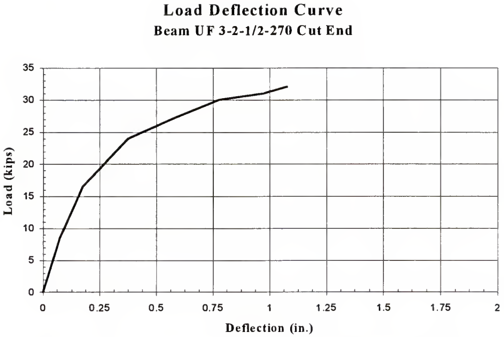

Figure II-13 Load Displacement Diagram Beam UF 3-2-1/2-270 Cut End

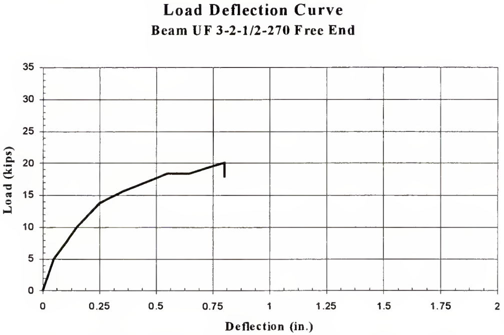

Figure II-14 Load Displacement Diagram Beam UF 3-2-1/2-270 Free End

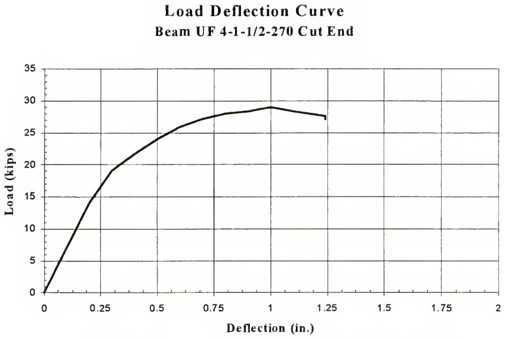

Figure II-15 Load Displacement Diagram Beam UF 4-1-1/2-270 Cut End

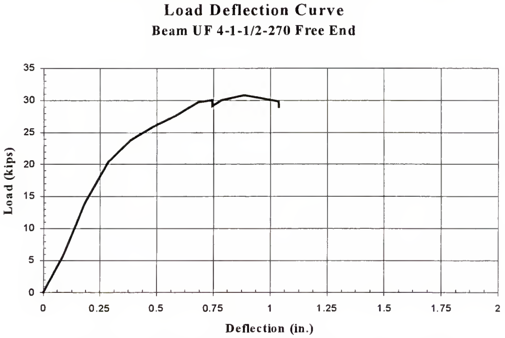

Figure II-16 Load Displacement Diagram Beam UF 4-1-1/2-270 Free End

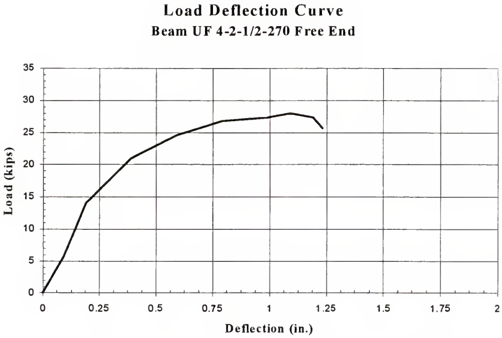

Figure II-17 Load Displacement Diagram Beam UF 4-2-1/2-270 Free End

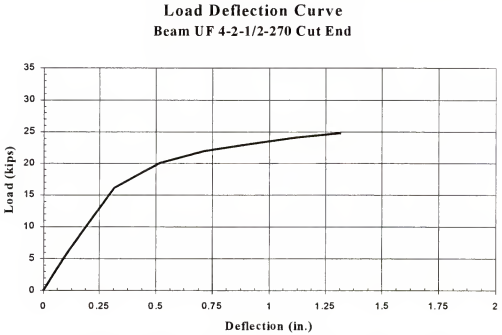

Figure II-18 Load Displacement Diagram Beam UF 4-2-1/2-270 Cut End

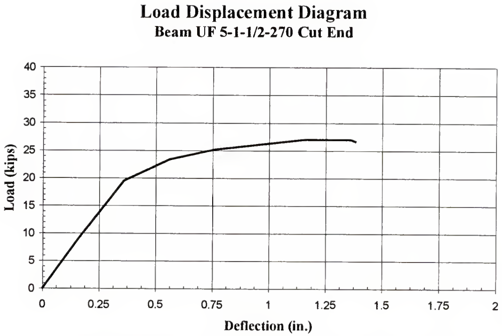

Figure II-19 Load Displacement Diagram Beam UF 5-1-1/2-270 Cut End

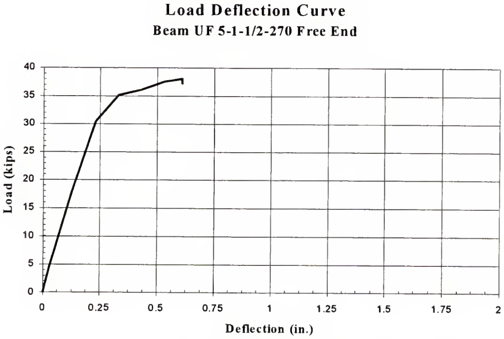

Figure II-20 Load Displacement Diagram Beam UF 5-1-1/2-270 Free End

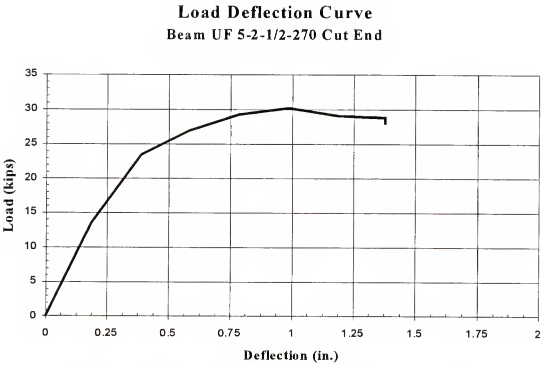

Figure II-21 Load Displacement Diagram Beam UF 5-2-1/2-270 Cut End

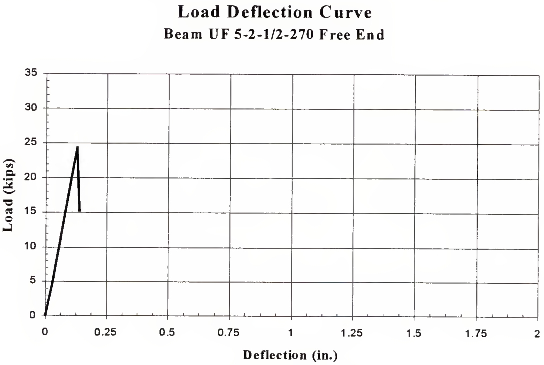

Figure II-22 Load Displacement Diagram Beam UF 5-2-1/2-270 Free End

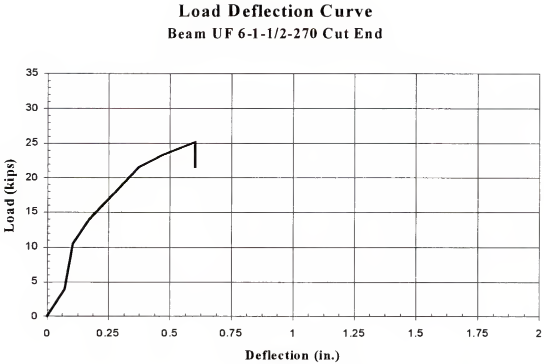

Figure II-23 Load Displacement Diagram Beam UF 6-1-1/2-270 Cut End

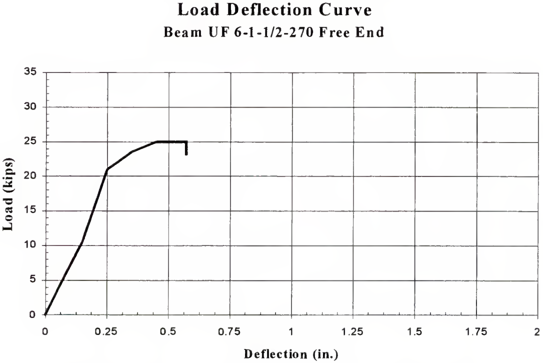

Figure II-24 Load Displacement Diagram Beam UF 6-1-1/2-270 Free End

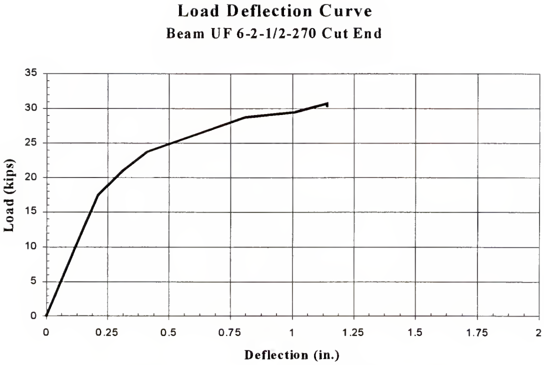

Figure II-25 Load Displacement Diagram Beam UF 6-2-1/2-270 Cut End

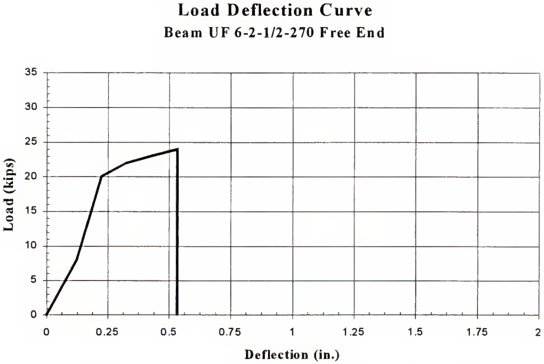

Figure II-26 Load Displacement Diagram Beam UF 6-2-1/2-270 Free End

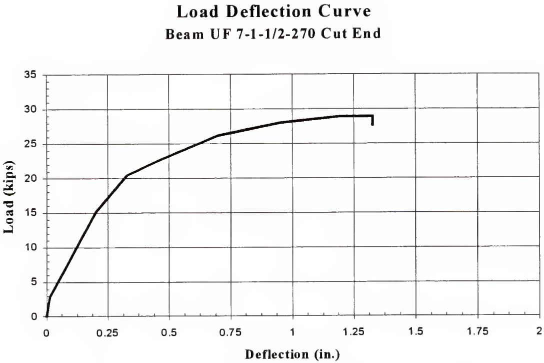

Figure II-27 Load Displacement Diagram Beam UF 7-1-1/2-270 Cut End

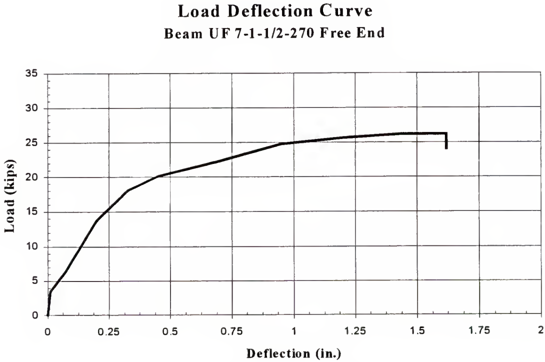

Figure II-28 Load Displacement Diagram Beam UF 7-1-1/2-270 Free End

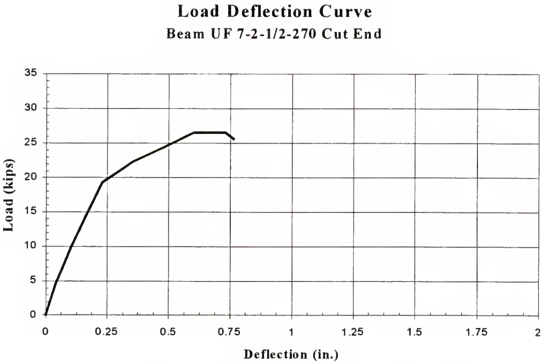

Figure II-29 Load Displacement Diagram Beam UF 7-2-1/2-270 Cut End

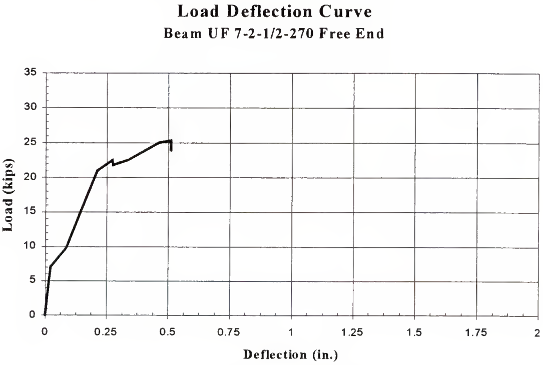

Figure II-30 Load Displacement Diagram Beam UF 7-2-1/2-270 Free End

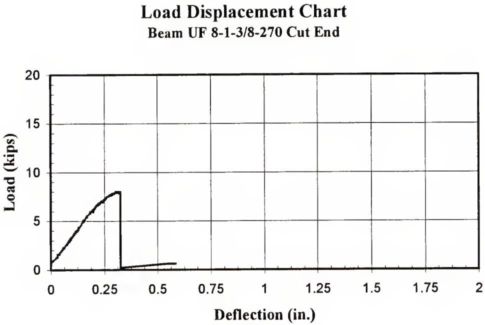

Figure II-31 Load Displacement Diagram Beam UF 8-1-3/8i-270 Cut End

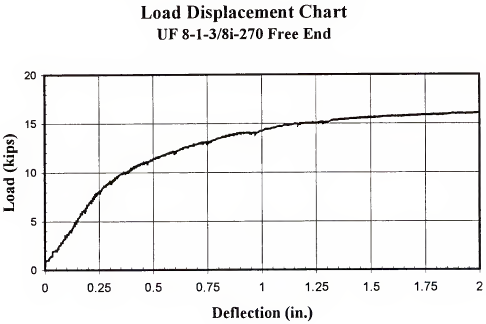

Figure II-32 Load Displacement Diagram Beam UF 8-1-3/8i-270 Free End

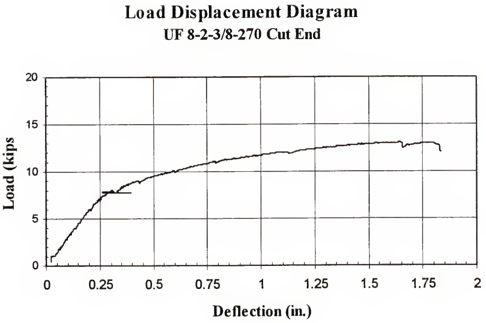

Figure II-33 Load Displacement Diagram Beam UF 8-2-3/8-270 Cut End

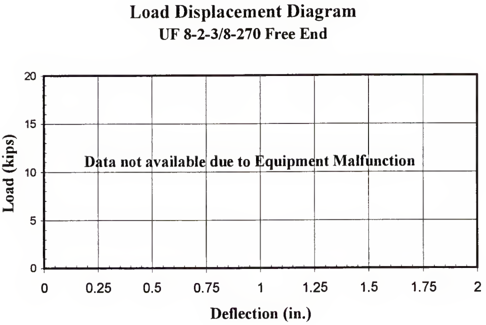

Figure II-34 Load Displacement Diagram Beam UF 8-2-3/8-270 Free End

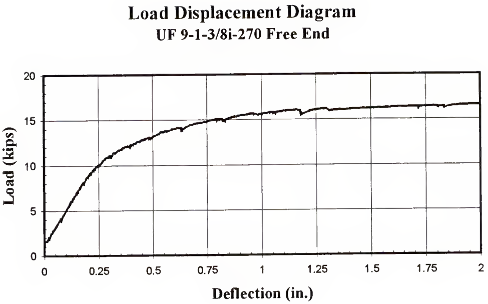

Figure II-35 Load Displacement Diagram Beam UF 9-1-3/8i-270 Free End

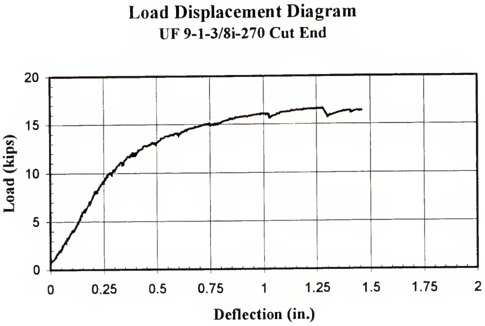

Figure II-36 Load Displacement Diagram Beam UF 9-1-3/8i-270 Cut End

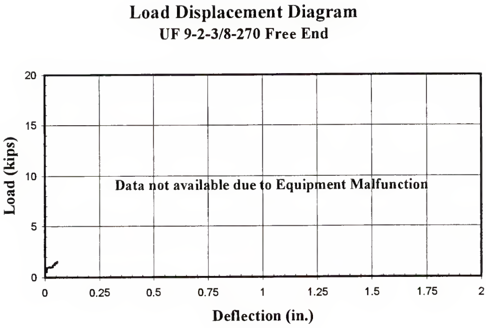

Figure II-37 Load Displacement Diagram Beam UF 9-2-3/8-270 Free End

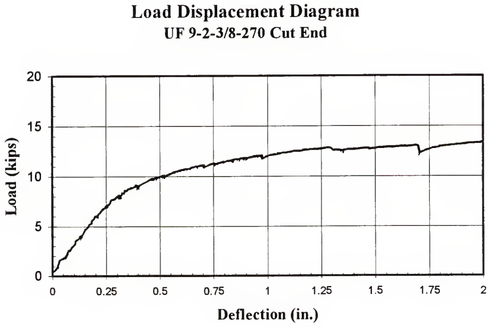

Figure II-38 Load Displacement Diagram Beam UF 9-2-3/8-270 Cut End

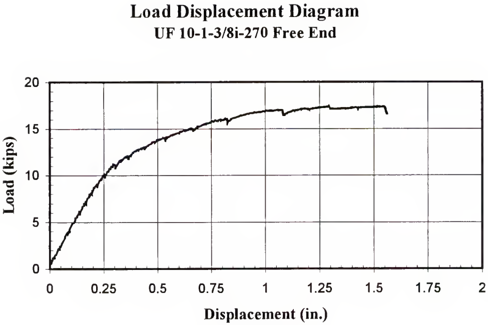

Figure II-39 Load Displacement Diagram Beam UF10-1-3/8i Free End

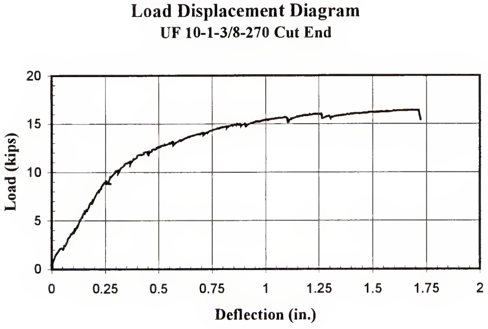

Figure II-40 Load Displacement Diagram Beam UF10-1-3/8i Cut End

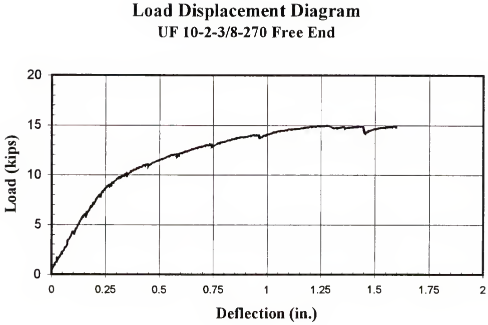

Figure II-41 Load Displacement Diagram Beam UF10-2-3/8-270 Free End

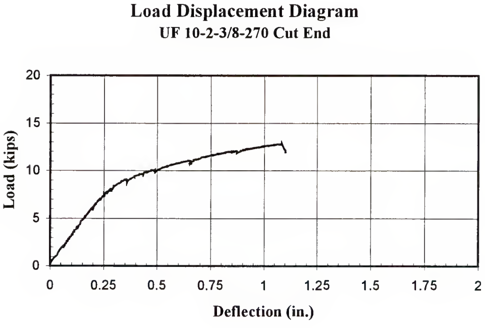

Figure II-42 Load Displacement Diagram Beam UF10-2-3/8-270 Cut End

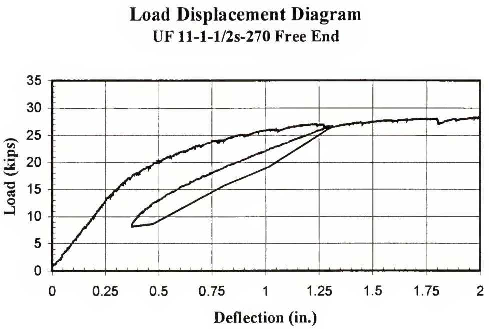

Figure II-43 Load Displacement Diagram Beam UF 11-1-1/2s-270 Free End

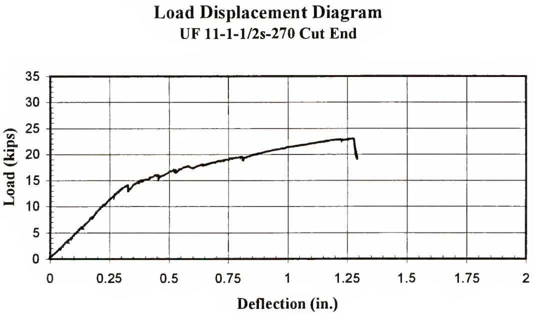

Figure II-44 Load Displacement Diagram Beam UF 11-1-1/2s-270 Cut End

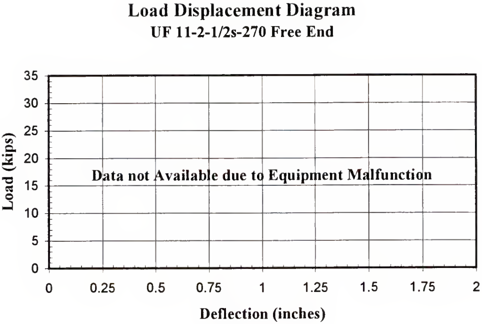

Figure II-45 Load Displacement Diagram Beam UF 112-1/2s-270 Free end

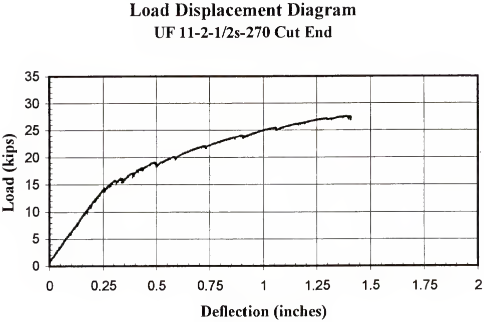

Figure II-46 Load Displacement Diagram Beam UF 11-2-1/2s-270 Free End

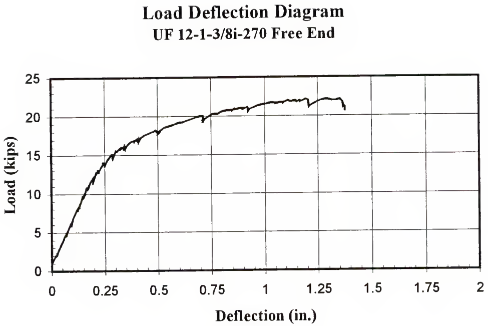

Figure II-47 Load Displacement Diagram Beam UF 12-1-3/8i Free End

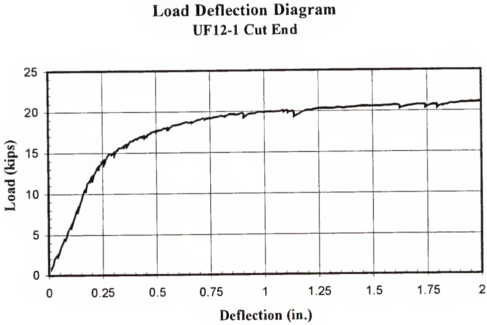

Figure II-48 Load Displacement Diagram Beam UF 12-1-3/8i-270 Cut End

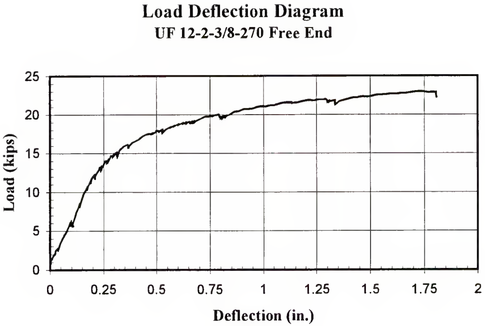

Figure II-49 Load Displacement Diagram Beam UF 12-2-3/8 Free End

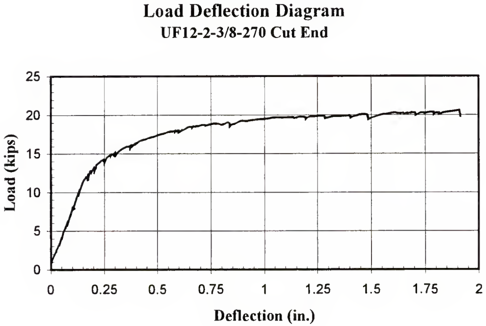

Figure II-50 Load Displacement Diagram Beam UF 12-2-3/8-270 Cut End

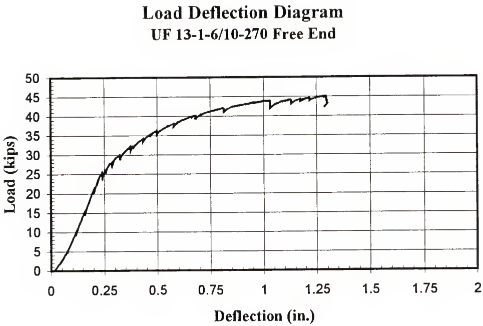

Figure II-51 Load Displacement Diagram Beam UF 13-1-6/10-270 Free End

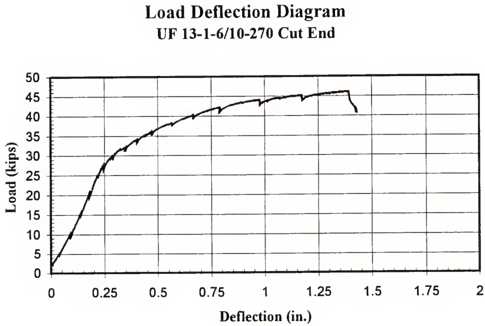

Figure II-52 Load Displacement Diagram Beam UF 13-1-6/10-270 Cut End

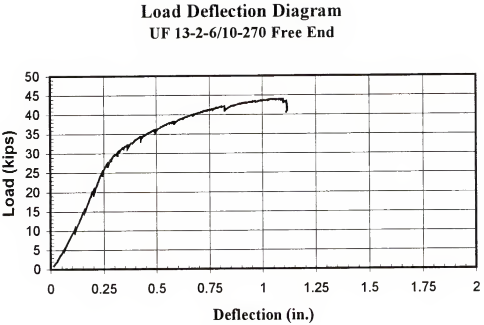

Figure II-53 Load Displacement Diagram Beam UF 13-2-6/10-270 Free End

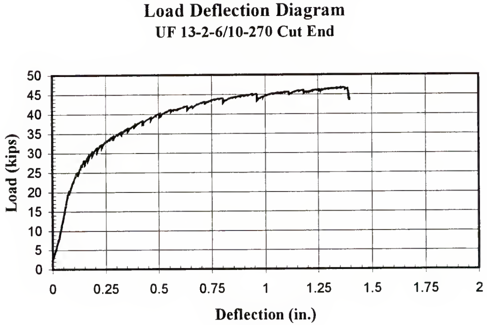

Figure II-54 Load Displacement Diagram Beam UF 13-2-6/10-270 Cut End

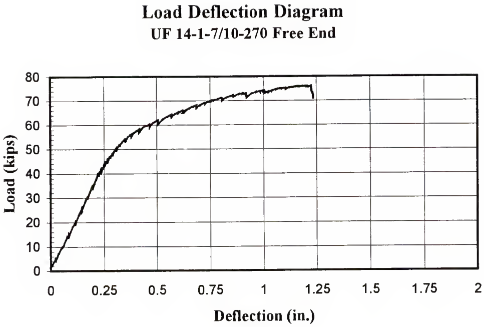

Figure II-55 Load Displacement Diagram Beam UF 14-1-7/10-270 Free End

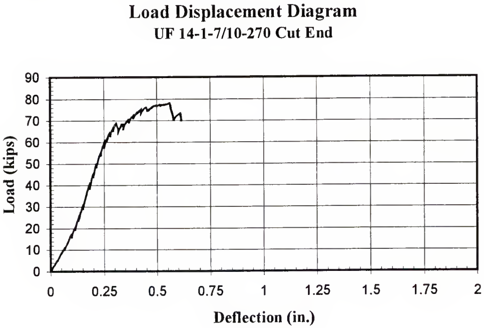

Figure II-56 Load Displacement Diagram Beam UF 14-1-7/10-270 Cut End

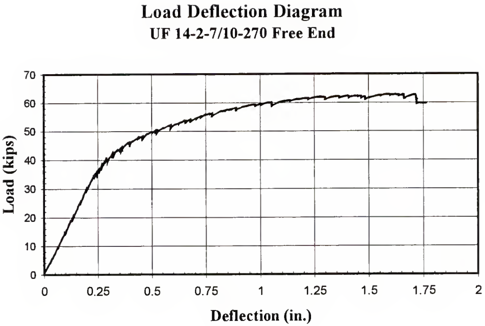

Figure II-57 Load Displacement Diagram Beam UF 14-2-7/10-270 Free End

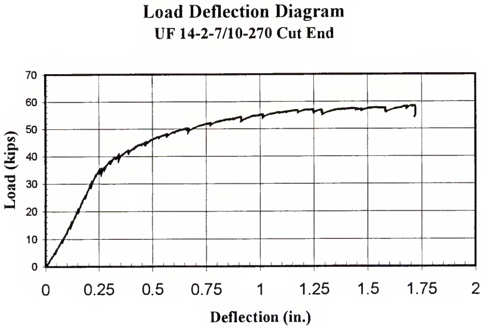

Figure II-58 Load Displacement Diagram Beam UF 14-2-7/10-270 Cut End

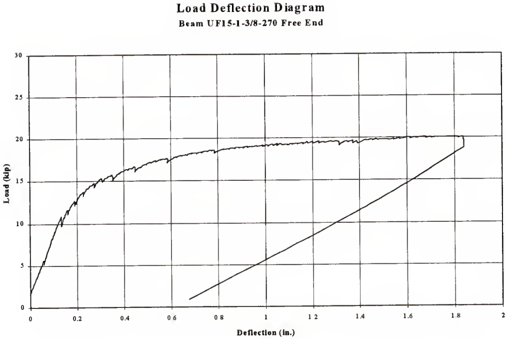

Figure II-59 Load Displacement Diagram Beam UF15-1-3/8-270 Free End

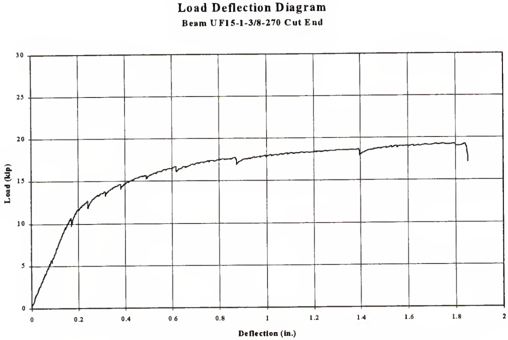

Figure II-60 Load Displacement Diagram Beam UF15-1-3/8-270 Cut End

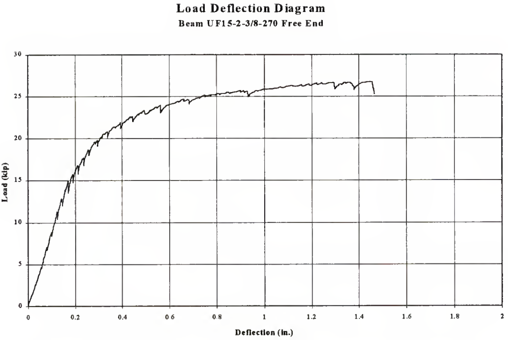

Figure II-61 Load Displacement Diagram Beam UF15-2-3/8-270 Free End

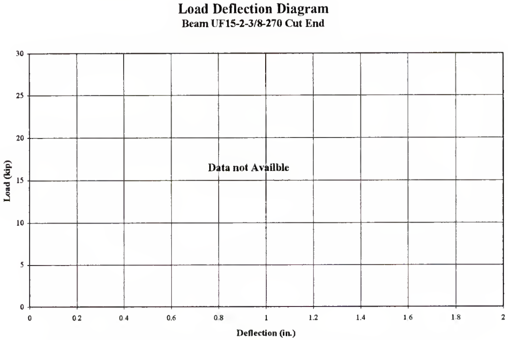

Figure II-62 Load Displacement Diagram Beam UF15-2-3/8-270 Cut End

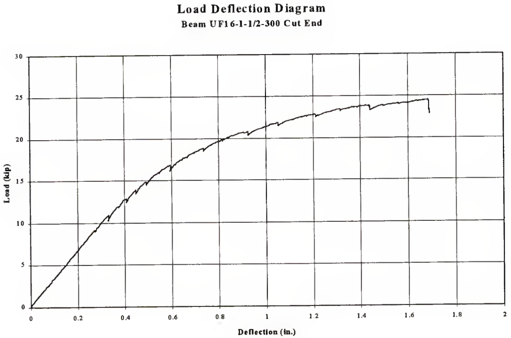

Figure II-63 Load Displacement Diagram Beam UF16-1-1/2-300 Cut End

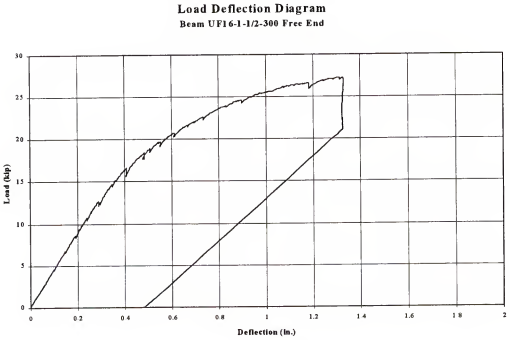

Figure II-64 Load Displacement Diagram Beam UF16-1-1/2-300 Free End

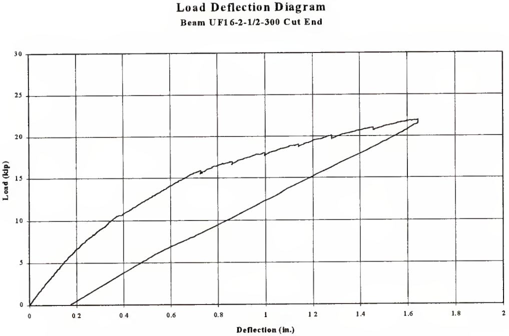
Load Deflection Diagram

Beam UF16-2-1/2-300 Cut End

Figure II-65 Load Displacement Diagram Beam UF16-1-1/2-300 Cut End

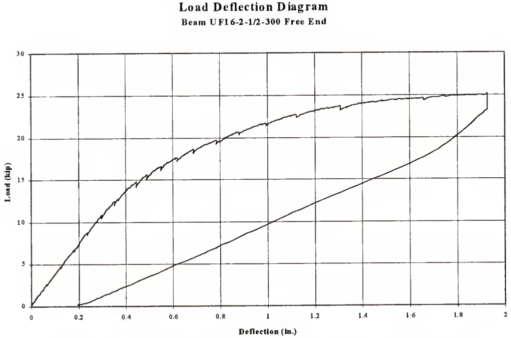
Load Deflection Diagram

Beam UF16-2-1/2-300 Free End

Figure II-66 Load Displacement Diagram Beam UF16-2-1/2-300 Free End

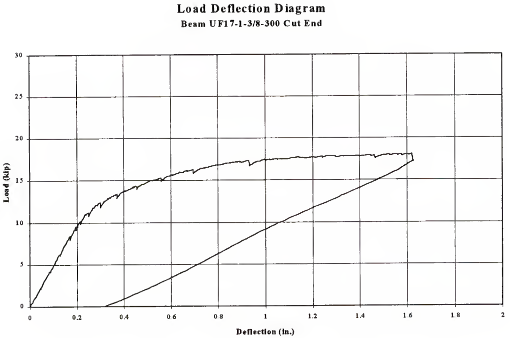

Figure II-67 Load Displacement Diagram Beam UF17-1-3/8-300 Cut End

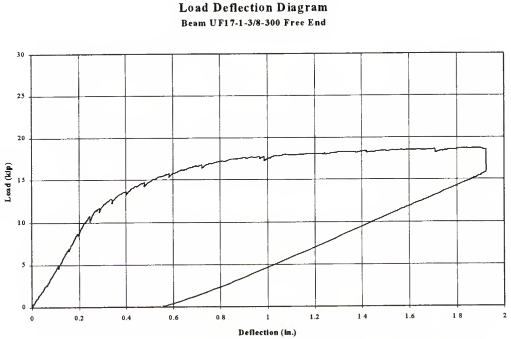

Figure II-68 Load Displacement Diagram Beam UF17-1-3/8-300 Free End

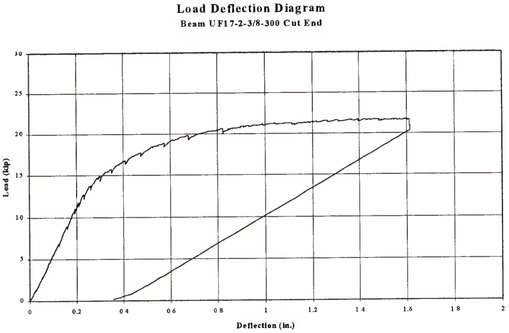

Figure II-69 Load Displacement Diagram Beam UF17-2-3/8-300 Cut End

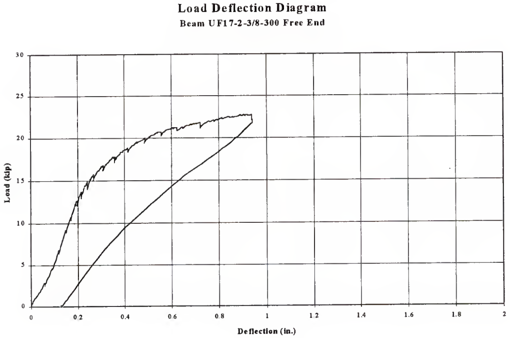

Figure II-70 Load Displacement Diagram Beam UF17-2-3/8-300 Free End

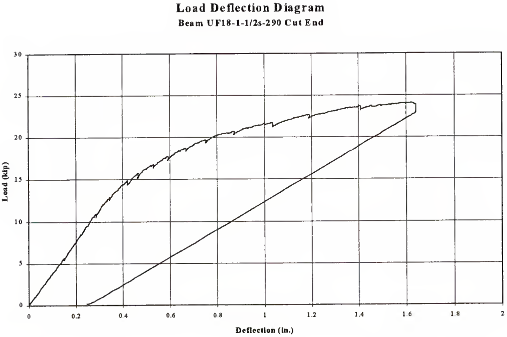

Figure II-71 Load Displacement Diagram Beam UF18-1-1/2s-290 Cut End

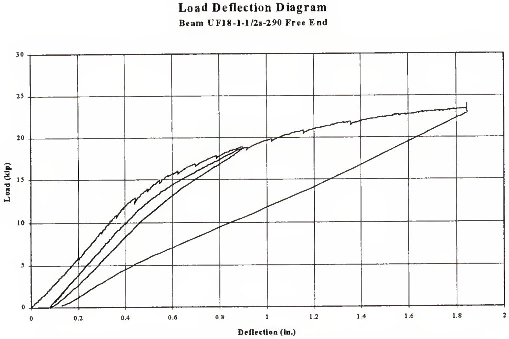

Figure II-72 Load Displacement Diagram Beam UF18-1-1/2s-290 Free End

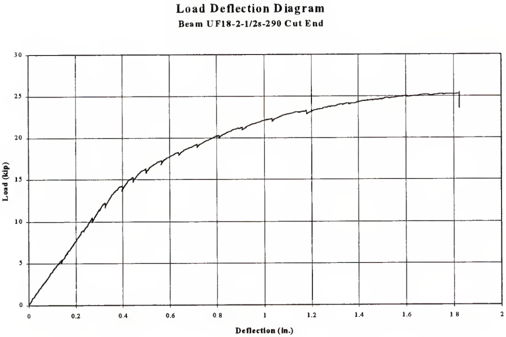

Figure II-73 Load Displacement Diagram Beam UF18-2-1/2s-290 Cut End

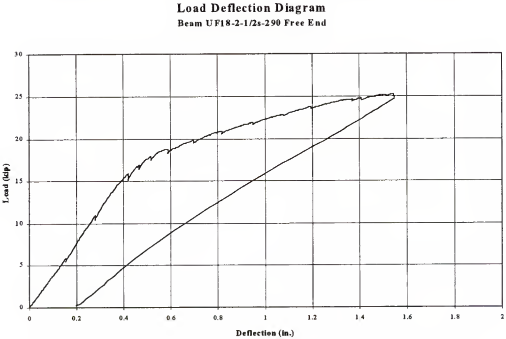

Figure II-74 Load Displacement Diagram Beam UF18-2-1/2s-290 Free End

APPENDIX III

MATHCAD TEMPLATES

Research UF

1. Preliminary Beam Calcs.

A. Defined Variables

$kip := 1000 \cdot lbf$ $\quad ksi := \frac{kip}{in^2}$ $\quad psi := \frac{lbf}{in^2}$

$minute := 60 \cdot sec$ $\quad hour := 60 \cdot minute$ $\quad day := 24 \cdot hour$ $\quad year := 365 \cdot day$

B. Data

$l := 17 \cdot ft$ $\quad b := 6 \cdot in$ $\quad h := 12 \cdot in$ $\quad f_{pu} := 270 \cdot ksi$

$A_s := 0.88 \cdot in^2$ $\quad A_{ps} := 0.306 \cdot in^2$ $\quad \gamma_c := 150 \cdot \frac{lbf}{ft^3}$ $\quad P_i := 62 \cdot kip$

$E_s := 29000 \cdot ksi$ $\quad E_{ps} := 28600 \cdot ksi$ $\quad f_y := 60000 \cdot psi$

$f'_{c2} := 3500 \cdot psi$ $\quad f'_{c1} := 5000 \cdot psi$ $\quad d_s := 1.125 \cdot in$

C. Calculations

$e := \frac{h}{2} - \frac{b}{3}$ $\quad d_{ps} := \frac{h}{2} + e$ $\quad d_c := \frac{h}{2}$ $\quad A_c := b \cdot h$

$I_c := \frac{b \cdot h^3}{12}$ $\quad c_1 := \frac{h}{2}$ $\quad c_2 := \frac{h}{2}$

$S_{bot} := \frac{I_c}{c_1}$ $\quad S_{top} := \frac{I_c}{c_2}$ $\quad r2 := \frac{I_c}{A_c}$

$w_o := \gamma_c \cdot A_c$ $\quad w_o = 0.075 \frac{kip}{ft}$

$M_o := \frac{1}{8} \cdot w_o \cdot l^2$ $\quad M_o = 32.512\, kip \cdot in$

$E_c := 57000 \cdot \sqrt{\frac{f'_{c1}}{psi}} \cdot psi$ $\quad E_c = 4.031 \times 10^6\, psi$

$f'_{ci} := f'_{c2}$

$\beta_1 := 0.85 - \frac{0.05 \cdot (f'_{c1} - 4000 \cdot psi)}{1000 \cdot psi}$ $\quad \beta_1 = 0.8$

2. Section Properties @ Flexural Test

Elastic Modulus Raitos: $n' := \dfrac{E_s}{E_c}$ $\quad n' = 7.195$

$n := \dfrac{E_{ps}}{E_c}$ $\quad n = 7.096$

Transformed Steel Areas: $A'_{tr1} := (n' - 1) \cdot A_s$ $\quad A'_{tr1} = 5.452\,\mathrm{in}^2$

$A_{tr1} := (n - 1) \cdot A_{ps}$ $\quad A_{tr1} = 1.865\,\mathrm{in}^2$

Transformed Centroid: $\Sigma A := A_c + A'_{tr1} + A_{tr1}$ $\quad \Sigma A = 79.317\,\mathrm{in}^2$

$\Sigma Ay := A_c \cdot d_c + A'_{tr1} \cdot d_s + A_{tr1} \cdot d_{ps}$ $\quad \Sigma Ay = 456.787\,\mathrm{in}^3$

$y_{top} := \dfrac{\Sigma Ay}{\Sigma A}$ $\quad y_{top} = 5.759\,\mathrm{in}$

$y_{bot} := h - y_{top}$ $\quad y_{bot} = 6.241\,\mathrm{in}$

Transformed Moment of Inertia:

	A	y	$A \cdot y^2$	I_g
Concrete	$A_c = 72\,\mathrm{in}^2$	$y1 := y_{bot} - \dfrac{h}{2}$	$Ay_{c1} := A_c \cdot y1^2$	$I_c = 864$ ir
A_s	$A'_{tr1} = 5.452\,\mathrm{in}^2$	$y2 := y_{top} - d_s$	$Ay_{s1} := A'_{tr1} \cdot y2^2$	
A_{ps}	$A_{tr1} = 1.865\,\mathrm{in}^2$	$y3 := d_{ps} - y_{top}$	$Ay_{p1} := A_{tr1} \cdot y3^2$	

$A_{tr1} := A_c + A'_{tr1} + A_{tr1}$ $\quad A_{tr1} = 79.317\,\mathrm{in}^2$

$I_{tr1} := I_c + Ay_{c1} + Ay_{s1} + Ay_{p1}$ $\quad I_{tr1} = 1.019 \times 10^3\,\mathrm{in}^4$

$S_{top1} := \dfrac{I_{tr1}}{y_{top}}$ $\quad S_{top1} = 176.906\,\mathrm{in}^3$

$S_{bot1} := \dfrac{I_{tr1}}{y_{bot}}$ $\quad S_{bot1} = 163.243\,\mathrm{in}^3$

$e_{tr1} := y_{bot} - \dfrac{b}{3}$ $\quad e_{tr1} = 4.241\,\mathrm{in}$

$r2_{tr1} := \dfrac{I_{tr1}}{A_{tr1}}$ $\quad r2_{tr1} = 12.845\,\mathrm{in}^2$

3. Section Properties @ Release

$E_c := 57000 \cdot \sqrt{\dfrac{f_{c2}}{psi}} \cdot psi$ $\qquad E_c = 3.372 \times 10^6\,psi$

Elastic Modulus Raitos: $n' := \dfrac{E_s}{E_c}$ $\qquad n' = 8.6$

$n := \dfrac{E_{ps}}{E_c}$ $\qquad n = 8.481$

Transformed Steel Areas: $A'_{tr2} := (n' - 1) \cdot A_s$ $\qquad A'_{tr2} = 6.688\,in^2$

$A_{tr2} := (n - 1) \cdot A_{ps}$ $\qquad A_{tr2} = 2.289\,in^2$

Transformed Centroid: $\Sigma A := A_c + A'_{tr2} + A_{tr2}$ $\qquad \Sigma A = 80.977\,in^2$

$\Sigma Ay := A_c \cdot d_c + A'_{tr2} \cdot d_s + A_{tr2} \cdot d_{ps}$ $\qquad \Sigma Ay = 462.416\,in^3$

$y_{top} := \dfrac{\Sigma Ay}{\Sigma A}$ $\qquad y_{top} = 5.759\,in$

$y_{bot} := h - y_{top}$ $\qquad y_{bot} = 6.241\,in$

Transformed Moment of Inertia:

	A	y	$A \cdot y^2$	I_g
Concrete	$A_c = 72\,in^2$	$y1 := y_{bot} - \dfrac{h}{2}$	$Ay_{c2} := A_c \cdot y1^2$	$I_c = 864\,in^4$
A_s	$A'_{tr2} = 6.688\,in^2$	$y2 := y_{top} - d_s$	$Ay_{s2} := A'_{tr2} \cdot y2^2$	
A_{ps}	$A_{tr2} = 2.289\,in^2$	$y3 := d_{ps} - y_{top}$	$Ay_{p2} := A_{tr2} \cdot y3^2$	

$A_{tr2} := \Sigma A$ $\qquad A_{tr2} = 80.977\,in^2$

$I_{tr2} := I_c + Ay_{c2} + Ay_{s2} + Ay_{p2}$ $\qquad I_{tr2} = 1.053 \times 10^3\,in^4$

$S_{top2} := \dfrac{I_{tr2}}{y_{top}}$ $\qquad S_{top2} = 184.36\,in^3$

$S_{bot2} := \dfrac{I_{tr2}}{y_{bot}}$ $\qquad S_{bot2} = 167.386\,in^3$

$e_{tr2} := y_{bot} - \dfrac{b}{3}$ $\qquad e_{tr2} = 4.29\,in$

$r2_{tr2} := \dfrac{I_{tr2}}{A_{tr2}}$ $\qquad r2_{tr2} = 13.001\,in^2$

4. Effective Prestress

$f_{pi} := \frac{P_i}{A_{ps}}$ $\quad f_{pi} = 202.614\,\text{ksi}$

A. Elastic Shortening

$f'_c := f'_{c2}$ $\quad f'_c = 3.5 \times 10^3\,\text{psi}$

$K_{es} := 1.0$ $\quad K_{cir} := 0.9$ $\quad$ ** Coefficients obtained from P. Zia, K. Preston & N.Scott Paper

$E_{ps} = 2.86 \times 10^4\,\text{ksi}$ $\quad E_{ci} := 57000 \cdot \sqrt{\frac{f'_c}{\text{psi}}} \cdot \text{psi}$ $\quad E_{ci} = 3.372 \times 10^6\,\text{psi}$

$P_i := A_{ps} \cdot f_{pi}$ $\quad P_i = 62\,\text{kip}$

$M_g := M_o$ $\quad M_g = 32.512\,\text{kip} \cdot \text{in}$

$$f_{cir} := K_{cir} \cdot \left(\frac{P_i}{A_c} + \frac{P_i \cdot e^2}{I_c} \right) - \frac{M_g \cdot e}{I_c} \qquad f_{cir} = 1.658\,\text{ksi}$$

$$ES := K_{es} \cdot E_{ps} \cdot \frac{f_{cir}}{E_{ci}} \qquad ES = 14.06\,\text{ksi}$$

B. Creep

$\text{day} := 24 \cdot 60 \cdot 60 \cdot \text{sec}$ $\quad \text{year} := 365 \cdot \text{day}$ $\quad t := 28 \cdot \text{day}$

$K_{cru} := 2.0$ $\quad RH := 0.75$ $\quad K_{cr} := K_{cru} \cdot (1.27 - 0.0067 \cdot RH \cdot 100) \cdot \frac{\left(\frac{t}{\text{day}}\right)^{0.6}}{10 + \left(\frac{t}{\text{day}}\right)^{0.6}}$

$f'_c := f'_{c1}$ $\quad f'_c = 5 \times 10^3\,\text{psi}$

$E_c := 57000 \cdot \sqrt{\frac{f'_c}{\text{psi}}} \cdot \text{psi}$ $\quad E_c = 4.031 \times 10^6\,\text{psi}$ $\quad f_{pes} := f_{pi} - ES$

$f_{cds} := \frac{M_g \cdot e}{I_c}$ $\quad f_{cs} := \frac{A_{ps} \cdot f_{pes}}{A_c} \cdot \left(1 + \frac{e^2}{r2}\right)$

$$CR := K_{cr} \cdot \frac{E_s}{E_c} \cdot (f_{cs} - f_{cds}) \qquad CR = 8.066\,\text{ksi}$$

C. Shrinkage

$K_{sh} := 1.0$ $e_{shu} := 8.0 \cdot 10^{-6}$ $e_{sh} := \dfrac{t}{35 \cdot day + t} \cdot e_{shu}$

$A := \dfrac{A_c}{in}$ $P := 2 \cdot b + 2 \cdot h$ $\dfrac{A}{P} = 2$

$SH := e_{sh} \cdot K_{sh} \cdot E_s \cdot \left[1 - 0.06 \cdot \left(\dfrac{A}{P} \right) \right] \cdot (1.4 - RH)$ $SH = 0.059\,ksi$

D. Relaxation

$K_{re} := 5.0 \cdot ksi$ $J := 0.04$

$\dfrac{f_{pi}}{f_{pu}} = 0.75$ Therefore $C := 1.0$

$RE := \left[K_{re} - J \cdot (SH + CR + ES) \right] \cdot C$ $RE = 4.113\,ksi$

E. Total Losses

$TL := ES + CR + SH + RE$ $TL = 26.298\,ksi$

F. Effective Prestress

$f_{se} := f_{pi} - TL$ $f_{se} = 176.317\,ksi$

5. Initial Stresses

$f_r := 7.5 \cdot \sqrt{\dfrac{f'_c}{psi}} \cdot psi$ $f_r = 530.33\,psi$

$P_{si} := A_{ps} \cdot f_{pi}$ $P_{si} = 62\,kip$

$f_{ci} := -P_{si} \cdot \left(\dfrac{1}{A_{tr2}} + \dfrac{e_{tr2}^{\,2}}{I_{tr2}} \right)$ $f_{ci} = -1.849\,ksi$

$f_{top} := -P_{si} \cdot \left(\dfrac{1}{A_{tr2}} - \dfrac{e_{tr2}}{S_{top2}} \right)$ $f_{top} = 0.677\,ksi$

$f_{bot} := -P_{si} \cdot \left(\dfrac{1}{A_{tr2}} + \dfrac{e_{tr2}}{S_{bot2}} \right)$ $f_{bot} = -2.355\,ksi$

6. Cracking Moment

$S_{bot1} = 163.243\,in^3$ $\quad S_{top1} = 176.906\,in^3$

$I_{tr1} = 1.019 \times 10^3\,in^4$

$f'_{c1} = 5 \times 10^3\,psi$ $\quad E_c := 57000 \cdot \sqrt{\frac{f'_{c1}}{psi}} \cdot psi$ $\quad E_c = 4.031 \times 10^3\,ksi$

$M_{cr} := S_{bot1} \cdot (f_r - f_{bot})$ $\quad M_{cr} = 470.929\,kip \cdot in$

7. Nominal Flexural Strength

A. Calculation of concrete compression block:

By trial and error:

Assume: $c := 2.073 \cdot in$

$\varepsilon_{so} := \frac{0.5 \cdot f'_{c1}}{E_c}$ $\quad \varepsilon_{so} = 6.203 \times 10^{-4}$ $\quad \varepsilon_{cu} := 0.003$

$\varepsilon_o := 3.414 \cdot \varepsilon_{so}$ $\quad \varepsilon_o = 2.1176 \times 10^{-3}$

Concrete:

$$C_c := c \cdot b \cdot f'_{c1} \cdot \left(\frac{\varepsilon_{cu}}{\varepsilon_o} - \frac{\varepsilon_{cu}^2}{3 \cdot \varepsilon_o^2} \right) \qquad C_c = 46.499\,kip$$

Compression Steel:

$\varepsilon'_s := \frac{c - d_s}{c} \cdot \varepsilon_{cu}$ $\quad \varepsilon'_s = 1.371925 \times 10^{-3}$

$f'_s := E_s \cdot \varepsilon'_s$ $\quad f'_s = 39.786\,ksi$

$C_s := f'_s \cdot A_s$ $\quad C_s = 35.012\,kip$

Prestressing Steel:

$$\varepsilon_s := \frac{d_{ps} - c}{c} \cdot \varepsilon_{cu} \qquad \varepsilon_s = 0.011472$$

$$\varepsilon_{ce} := \frac{f_{se} \cdot A_{ps}}{E_c \cdot A_c} \cdot \left(1 + \frac{e^2}{r2}\right)$$

$$\varepsilon_{se} := \frac{f_{se}}{E_{ps}}$$

$$\varepsilon_{ps} := \varepsilon_s + \varepsilon_{se} + \varepsilon_{ce} \qquad \varepsilon_{ps} = 0.018071$$

$$f_{ps1} := E_{ps} \cdot \varepsilon_{ps}$$

$$f_{ps2} := \left(270 - \frac{0.04}{\varepsilon_{ps} - 0.007}\right) \cdot \text{ksi}$$

*Ref. PCI Design Handbook - 1996

$$f_{ps} := \text{if}\left(\varepsilon_{ps} \le 0.0086, f_{ps1}, f_{ps2}\right)$$

$$f_{ps} = 266.387\ \text{ksi}$$

Tension:

$$T := f_{ps} \cdot A_{ps} \qquad T = 81.514\ \text{kip}$$

Compression:

$$C := C_s + C_c \qquad C = 81.51\ \text{kip}$$

Tension = Compression

Therefore: Equilibrium

B. Location of concrete compression block resultant:

$$y' := \frac{b \cdot f'_{c1} \cdot \left(\frac{2}{3} \cdot \frac{\varepsilon_{cu}}{\varepsilon_o} \cdot c^2 - \frac{1}{4} \cdot \frac{\varepsilon_{cu}}{\varepsilon_o} \cdot c^2\right)}{C_c} \qquad y' = 1.637\ \text{in}$$

C. Nominal Moment and Curvature:

$$Mn := C_c \cdot \left(d_{ps} - y'\right) + C_s \cdot \left(d_{ps} - d_s\right) \qquad Mn = 699.613\ \text{kip} \cdot \text{in}$$

REFERENCES

1. Abrishami, H.H., Studies of Bond and Cracking of Structural Concrete, Ph.D. Thesis, Department of Civil Engineering and Applied Mechanics, McGill University, Montreal Canada, June 1994

2. Abrishami, H.H. & Mitchell, D., Bond Characteristics of Pretensioned Strands, ACI Materials Journal, May-June, 1993, pp. 228-235

3. AASHTO, Standard Specifications for Highway Bridges, American Association of State Highway and Transportation Officials, Washington DC, 1992

4. American Concrete Institute, Building Code Requirements for Structural Concrete (ACI 318-95) and Commentary (ACI 318R-95), Farmington Hills, Michigan, July 1995.

5. Anderson, A.R. & Anderson, R.G., Assurance Criterion for Flexural Bond in Pretensioned Hollow Core Units, Journal of the American Concrete Institute, Vol. 73 No. 8, August 1976, pp. 457-464.

6. Attard, M.M. & Setunge, S., Stress Strain relationship of Confined and Unconfined Concrete, American Concrete Institute Material Journals, Vol. 93, No. 5, September – October 1996, pp. 432 – 442.

7. Balazs, G., Transfer Length of Prestressing Strand as a Function of the Draw-in and Initial Prestress, PCI Journal, March- April, 1993, pp. 86-93

8. Badaliance, R. & VanHorn, D.A., Ultimate Flexural Bond in Beams Pretensioned with High Strength Strand, Fritz Engineering Laboratory Report No. 309.1, Lehigh University, February 1966.

9. Brooks, M.D., Gerstle, K.H. & Logan D.R., Effect of Initial Strand Slip on the Strength of Hollow Core Slab, PCI Journal Vol. 33 No. 1, January – February 1988, pp. 90-111.

10. Bruggeling, A.S.G., Description of the (Step-by-Step Release) SSR Method for the experimental Determination of the Actual Transmission Length and Relevant Parameters, Holland, July 1995.

11. Bruggeling, A.S.G., State of the Art Report: The Transmission length and the Anchorage Length, Report 150603, FIP Commission 2, Bond Behavior of Prestressing Strands Work Group, 1994.

12. Bruggeling, A.S.G., Tendon Transmission Length Under Static Conditions, Report to FIP Commission 2, Prestressing Materials and Systems, May 1992.

13. Buckner, C.D., A Review for Strand Development Length for Pretensioned Concrete Members, PCI Journal, March-April, 1995, pp. 84-105

14. Buckner, C.D., An Analysis of Transfer and Development Length for Pretensioned Concrete Members, FHWA-Report No.94-049, December 1994

15. Cousins, T.E., Badeaux, M.H. & Moustafa, Saad, Proposed Test for Determining Bond Characteristics of Prestressing Strands, PCI Journal, January-February, 1992, pp. 66-73.

16. Cousins, T.E., Johnston, D.W. & Zia, P., Development Length of Epoxy Coated Prestressing Strands, Materials Journal, American Concrete Institute, Volume 87 No. 4, July-August, 1990, pp. 309-318.

17. Cousins, T.E., Johnston, D.W. & Zia, P., Transfer and Development Length of Epoxy Coated and Uncoated Prestressing Strands, PCI Journal, July-August, 1990 pp. 92-103

18. Cousins, T.E., Johnston, D.W. & Zia, P., Transfer Length of Epoxy Coated Prestressing Strands, Materials Journal, American Concrete Institute, Volume 87 No. 3, May– June, 1990.

19. Deatherage, J.H., Burdette, E.G & Chew, C.K., Development Length and Lateral Spacing Requirements of Prestressing Strands for Prestressed Concrete Bridge Girders, PCI Journal, January-February, 1994, pp. 70-83

20. Den Uijl, J.A., Bond Modeling of Prestressing Strands, ACI Special Publication 180-7 A Tribute to Peter Gergely, pp. 145-169.

21. Den Uijl, J.A., Bond of Strands in High Performance Concrete , 4th International Symposium on the Utilization of High Strength/High Performance Concrete, May 29-31, 1996, Paris, 1175-1184.

22. Devalapura, R. & Tadros, M., Stress-Strain Modeling of 270 ksi Low-Relaxation Prestressing Strands, PCI Journal, March April 1992, pp. 100-106

23. Dinsmore, G., Nordby, G., Hanson, N. and Kaar, P., Discussion of a Paper by Norman W. Hanson and Paul H. Kaar: Flexural Bond Tests of Pretensioned Prestressed Beams, American Concrete Institute Journal, Volume 31 No. 3 September 1959, pp.1485-1492

24. Edwards, A. D. & Picard, A., Bonding Properties of ½ in. Diameter Strands, American Concrete Journal, November 1972, pp.684-689.

25. Evans, R.H. and Robinson, G.W., Bond Stresses in Pretressed Concrete from X-Ray Photographs, Proceedings, Institution of Civil Engineers, London, Part 1, 1955, pp. 212-235

26. Fagundo, F.E., Alcaraz, G., Hoffman, V. & Richardson D., Bond, Transfer and Development Length Performance of Prestressing Strands, Structures Research Laboratory Report, Civil Engineering Department, University of Florida, May 1997

27. Fagundo, F.E. & Alcaraz, G., Effect of Strand Diameter on Bond, Transfer and Development Length Performance of Prestressing Strands, Interim Report – Phase III, Civil Engineering Department, University of Florida, January 2000

28. Federation Internationale de la Precontrainte, Report on Prestressing Steel: 7.Test for the determination of tendon transmission length under static conditions, FIP, ISBN 0-907862-03-9, 1982

29. Ghosh, S.K. & Fintel, M., Development Length of Prestressing Strands, Including Debonded Strands, and Allowable Concrete Stresses in Pretensioned Members, PCISFRAD Project No. 2, PCI Journal, September- October 1986, pp.38-57

30. Hanson, N., Influence of Surface Roughness of Prestressing Strands on Bond Performance, Precast/ Pretressed Concrete Institute Journal February 1969, pp. 32-45

31. Hanson, N. and Kaar, P., Flexural Bond Tests of Pretensioned Prestressed Beams, American Concrete Institute Journal Proceedings, V. 55 No. 7 January 1959, pp. 783-803.

32. Hofstetter, G., Simo, J.C., Taylor R.L., A Modified Cap Model: Closest Point Solution, Computer and Structures, Vol. 46, No. 2, 1993, pp. 203-214.

33. Hurst, M.K., Prestressed Concrete Design, Chapman and Hall, London-New York, 1988

34. Janney, J. R., Nature of Bond in Pretensioned Prestressed Concrete, Journal of The American Concrete Institute, Proceedings Volume 50, No. 9, May 1954, pp 717-736.

35. Janney, J. R., Report of Strands Transfer length Studies on 270K Prestressing Strands, PCI Journal, Volume 8, No. 1, pp. 41-45.

36. Kaar, P., Hanson, N., LaFraugh, R.W. & Mass, M.A., Influence of Concrete Strength on Strands Transfer Length, Precast/Prestressed Concrete Institute Journal October 1963, pp. 47-67

37. Keuser, M. & Mehlhorn, G., Finite Element Models for Bond Problems, Journal of Structural Engineering, American Society of Civil Engineers, Vol. 113 No. 10, October 1987, pp. 2160-2173.

38. Keuser, M. & Mehlhorn, G., Bond Between Prestressed Steel and Concrete, Computer Analysis using ADINA, Computers and Structures, Vol. 17 No. 5-6, 1983, pp. 669-676.

39. Krishnamurthy, D., A Relationship Between Transmission Length and Diameter of Prestressing Tendons, Journal of the Institution of Engineers (India), Vol. 52 No. 9, May 1972, pp. 243-247.

40. Krishnamurthy, D., A Theory for the Transmission Length Prestressing Tendons, Indian Concrete Journal, Vol. 47 No. 2, February 1973, pp. 73-80.

41. Lane, S., New Development Length Equation for Pretensioned Strands in Bridge Beams and Piles, Turner-Fairbank Highway Research Center, Federal Highway Administration, FHWA-RD-98-116, December 1998.

42. Lane, S., Development Length of Prestressing Strands, Public Roads Volume 54 No. 2,September 1992, pp.67-71.

43. Lane, S., Transfer Length in Rectangular Prestressed Concrete Concentric Specimens, Public Roads Volume 56 No. 2,September 1990, pp.200-205.

44. Lenschow, R. J. & Sozen, M.A., Practical Analysis of the anchorage Zone problem in Prestressed Beams, Journal of the American Concrete Institute, November 1965, pp. 1421-1438

45. Logan, D.R., Acceptance Criteria for Bond Quality of Strand for Pretensioned Prestressed Concrete Applications, PCI Journal, March-April 1997, pp 52-81

46. Loov, R., A General Equation for the Steel Stress for Bonded Prestressed Concrete Members, PCI Journal, Volume 33, No. 6, November - December, 1988, pp. 108-148.

47. Lutz, L., Analysis of the Stresses in Concrete Near a Reinforcing Bar Due to Bond and Transverse Cracking, ACI Journal, October 1970,pp. 778-787

48. Lutz, L. & Gergely, P., Mechanics of Bond and Slip of Deformed Bars in Concrete, Research Report, Cornell University, 1967(Published on ACI Journal Proceedings V. 64 No. 11, November 1967, pp. 711-721)

49. Marshall, W.T. & Krishnamurthy, D., Transmission Length Prestressing Tendons from Concrete Cube Strength at Transfer, Indian Concrete Journal, July 1969, pp. 244-253.

50. Martin, L.D. & Korkosz, W.J., Strength of Prestressed Concrete Members at Sections where Strand are not Fully Developed, PCI Journal, September-October 1995, pp. 58-66.

51. Martin, L.D. & Scott, N.L., Development of Prestressing Strand in Pretensioned Members, ACI Journal, August 1976, pp. 453-456.

52. Mayfield B, Davies G, Kong F.K., Some Tests on the Transmission Length and Ultimate Strength of Pretensioned Concrete Beams Incorporating Dyform Strand, Magazine of Concrete Research, Vol. 22, No. 73, December 1970, pp. 219-226

53. Mirza, S.M. & Houde, J., Study of Bond Stress-Slip Relationships in Reinforced Concrete, ACI Journal, Proceedings V. 76 No. 1, January 1979, pp. 19-46

54. Mitchell, A., Dimensional Analysis Approach to a Correlation between Transfer Length and Diameter of Strands in Prestressed Concrete, Highest Honors Report, Civil and Coastal Engineering Department, University of Florida, July 1999

55. Mitchell, D., Cook, W.D., Khan, A.A. and Tham, T., Influence of High Strength Concrete of Transfer and Development length of Prestressing Strand, PCI Journal, pp 52-65.

56. Murphy, G., Similitude in Engineering, The Ronald Press Company, New York, 1950

57. Nilson, A., Design of Prestressed Concrete, Second Edition, John Wiley and Sons, New York, 1987

58. Nilson, A., Internal Measurement of Bond Slip, Research Report, Cornell University, 1972 (Published on ACI Journal, Proceedings V 69 No. 7, July 1972, pp. 439-441.)

59. Over, R.S. and Au, T., Prestress Transfer Bond of Pretensioned Strands in Concrete, Part 1 ACI Journal Proceedings V. 62, No. 11 November 1965 pp. 1451-1460

60. Over, R.S. and Au, T., Prestress Transfer Bond of Pretensioned Strands in Concrete, Part 2 Supplement to ACI Journal Publication No. 62-81

61. PCI, PCI Design Handbook: Precast and Prestressed Concrete, Fifth Edition, Precast/ Prestressed Concrete Institute, Chicago, Illinois, 1999.

62. Peattie, K.K. & Pope, J.A., Effect of Age of Concrete on Bond Resistance, Journal of the American Concrete Institute, Vo 27 No. 6, February 1956, Proceedings Volume 52, pp. 661-672

63. Petrou, M.F., Joiner, W.S., Hussein, A.A. & Trezos, C.G., Excessive Strand Slippage in Prestressed Piles, Report Department of Civil and Environmental Engineering, University of South Carolina. Not Dated.

64. Preston, K., Characteristics of 15% Stronger &-Wire Strand, PCI Journal, February 1963, pp. 39-41

65. Rehm, G., The Fundamental Law of Bond, RILEM Symposium on Bond and Crack Formation on Reinforced Concrete, Stockholm, 1957, pp. 491-499.

66. Rose, D.R. and Russell, B.W., Investigation of Standardized Tests to Measure the Bond Performance of Prestressing Strand, PCI Journal, July-August, 1997,pp 56-80

67. Rose, D.R. and Russell, B.W., Investigation of Standardized Tests to Measure the Bond Performance of Prestressing Strand, Research Report, Fears Structural Engineering Laboratory, School of Civil Engineering and Environmental Science, University of Oklahoma, July 1996.

68. Russell, B.W., Burns, N.H., Design Guidelines for Transfer, Development and Debonding of Large Diameter Seven wire Strands Pretensioned Concrete Girders, Center for Transportation Research, University of Texas at Austin, Report No. FHWA/TX-93+1210-5F, January 1993.

69. Russell, B.W., and Burns, N.H., Measured Transfer Lengths of 0.5 and 0.6 in. Strands in Pretensioned Concrete, PCI Journal, September-October, 1996, pp. 44-63.

70. Russell, B.W., and Burns, N.H., Measurement of Transfer Lengths on Pretensioned Concrete Elements, Journal of Structural Engineering, May 1997, pp. 541-549.

71. Russell, B.W., Burns, N.H. and ZumBrunnen, L.G., Predicting the Bond Behavior of Prestressed Concrete Beams Containing Debonded Strands, PCI Journal, September-October, 1994, pp. 60-77

72. Russell, B.W., and Paulsgrove, D.R., Fundamental Mechanisms for the Development of Prestressing Strands, Research Report, Fears Structural Engineering Laboratory, School of Civil Engineering and Environmental Science, University of Oklahoma, July 1996

73. Sason, Augusto, Evaluation of Degree of Rusting on Prestressed Concrete Strand, PCI Journal May-June 1992, pp.25-30.

74. Shahawy, M, Issa M., & Batchelor B., Strand Transfer Length in Full Scale AASHTO Prestressed Concrete Girders, PCI Journal V37 No. 3, May – June 1992, pp. 84-96

75. Stoker, M.F., & Sozen, M.A, Investigation of Prestressed Concrete for Highway Bridges: Part VI, Bond Characteristics of Prestressing Strands, University of Illinois, Structural Research Series No. 334, June 1969

76. Tabatai, H., & Dickson, T.J., The History of the Pretensioning Strand Development Length Equation, PCI Journal V. 38 no. 6, November –December 1993, pp. 64-75.

77. Thorsen, Neils, Use of Large Tendons in Pre-Tensioned Concrete, Journal of the American Concrete Institute, Volume 27 No 6, February 1956.pp. 649-659

78. Timoshenko & Goodier, Theory of Elasticity, Engineering Societies Monographs, McGraw Hill Books, New York.

79. Tulin, L G & Al-Chalabi, M.M, Bond Strength as a Function of Strand Tension and Cement Paste Content for Lightweight Aggregate Concrete, ACI Journal, October 1969, pp. 840-846.

80. Weerasekera, R, Transfer and Flexural Bond in Pretensioned Prestressed Concrete, PhD Thesis, Toronto University, 1992.

81. Zia, P. & Mostafa, T., Development of Prestressing Strands, PCI Journal September-October 1977, pp. 54-65

82. Zia, P., Preston, K., Scott, N. & Workman, Estimating Prestress Losses, Concrete International June 1979, pp. 32-38.

BIOGRAPHICAL SKETCH

Gabriel Domingo Alcaraz Emmanuelli, son of Enrique Alcaraz, Esq. and Elba Emmanuelli, Esq., was born in April 16, 1969, in Mayaguez, Commonwealth of Puerto Rico. After graduating from the Academia Inmaculada Concepcion High School in May 1997, he attended the University of Puerto Rico – Mayaguez campus. Receiving his Bachelors of Science in Civil Engineering degree in June 1995. In May 1996, the Puerto Rico's Department of State and the Puerto Rico's College of Engineers and Land Surveyors admitted him to the practice of engineering, as a Professional Engineer.

In August of 1995, he entered the Graduate School at the University of Florida and received his Masters in Engineering (Structures) in May 1997. In December 1999, he was admitted to PhD Candidacy.

He is married, since August 1995, to Idelisse (Lissie) Perez and father, since January 1997, to Gabby.

I certify that I have read this study and that in my opinion it conforms to acceptable standards of scholarly presentation and is fully adequate, in scope and quality, as a dissertation for the degree of Doctor of Philosophy.

Fernando E. Fagundo, Co-Chairman
Professor of Civil Engineering

I certify that I have read this study and that in my opinion it conforms to acceptable standards of scholarly presentation and is fully adequate, in scope and quality, as a dissertation for the degree of Doctor of Philosophy.

Ronald A. Cook, Co-Chairman
Professor of Civil Engineering

I certify that I have read this study and that in my opinion it conforms to acceptable standards of scholarly presentation and is fully adequate, in scope and quality, as a dissertation for the degree of Doctor of Philosophy.

John M. Lybas
Associate Professor of Civil Engineering

I certify that I have read this study and that in my opinion it conforms to acceptable standards of scholarly presentation and is fully adequate, in scope and quality, as a dissertation for the degree of Doctor of Philosophy.

Michael C. McVay
Professor of Civil Engineering

I certify that I have read this study and that in my opinion it conforms to acceptable standards of scholarly presentation and is fully adequate, in scope and quality, as a dissertation for the degree of Doctor of Philosophy.

Milagros Rivera-Sanchez
Associate Professor of Journalism And
Communications

This dissertation was submitted to the Graduate School of the College of Engineering and to the Graduate School and was accepted as partial fulfillment of the requirements for the degree of Doctor of Philosophy.

August 2000

M. Jack Ohanian
Dean, College of Engineering

Winfred M. Phillips
Dean, Graduate School